Alkane Synthesis in the Genus *Desulfovibrio*

Submitted by Hannah Daniels to the University of Exeter
as a thesis for the degree of
Master of Philosophy in Biological Sciences
In March, 2016

I certify that all material in this thesis which is not my own work has been identified, and that no material has been previously submitted and approved for the award of a degree by this or any other university.

Signature:

Hannah Daniels

Acknowledgements

I would like to thank both my academic supervisor John Love and industrial supervisor Rob Lee for providing the opportunity to undertake this research and their collaboration, advice and support throughout the project.

I would also like to thank Royal Dutch Shell for funding the research and the Biodomain team at Shell Technology Centre, Houston for all their help and support during the initial 12 months of the project.

Finally, I would like to thank everyone in the Mezzanine Lab at the University of Exeter for making me feel part of the team and their support and guidance throughout my research.

Abstract

Petroleum based transport fuels (PBTFs) are vital to both industrial and social prosperity. However, PTBFs are a finite resource and their combustion contributes significantly to greenhouse-gas emissions. Finding a sustainable, carbon neutral alterative to PBTFs is vital to sustain modern lifestyles and mitigate climate change. The only PBTF alternatives currently produced industrially are ethanol and fatty-acid methyl esters derived from food crops (first generation biofuels). First generation biofuels cannot be used directly in most current combustion engines and production methods threaten food sustainability. Advanced biofuels derived from synthetic biological pathways engineered into industrially tractable microorganisms would mitigate the constraints of first generation biofuels. The success of advanced biofuel research relies on identifying and characterising enzymes integral to microbial hydrocarbon production, which may be used to build optimal synthetic systems. The current study investigated alkane production in the genus *Desulfovibrio* with the aim of determining the alkane synthesis pathway and identifying critical enzymes. A screen of 21 *Desulfovibrio* strains, cultured in stable isotope labelled media, identified six alkane producing strains which synthesised mainly *n*-octadecane and *n*-eicosane. Due to the even chain length alkanes produced, a reductive pathway with full carbon conservation was hypothesised. Identification of alkanes in the cell lysate of several *Desulfovibrio* strains allowed proteins associated with alkanes to be narrowed down by fractionating cell lysate, followed by GC/MSD and protein analysis of each fraction. 2D-DIGE was employed to separate individual proteins and allow the protein profile of alkane containing cell lysate fractions to be compared to non-alkane containing fractions. In this way several hypothetical proteins that may be involved in *Desulfovibrio* alkane synthesis were identified.

Table of Contents

List of Tables

List of Figures

Chapter 1. Introduction

1.1 Fossil Fuels

Fossil fuels are a finite resource that underpin the economic prosperity of the modern world (Petherick, 2015). Although it is difficult to accurately determine what remains of global fossil fuel reserves, there has been a marked decline in production from existing oil fields of up to 6.7% per year (IEA, 2008). This decline may indicate fossil fuel production has surpassed its 'peak' (De Almeida & Silva, 2009). Closely tied up with the economic issues surrounding fossil fuel production is the political unrest that has arisen in oil producing nations over recent years (Humud, Pirog and Rosen, 2015). Without a uniform distribution of fuel production across the globe, politics will continue to be a defining issue in fuel security.

Combustion of fossil fuels has a detrimental impact on the environment; fossil fuel use has been identified as the primary factor contributing to rise in atmospheric carbon dioxide (CO_2) – a major contributor to global climate change (IPPC report, 2007). Annual global CO_2 emissions from fossil fuel combustion rose by 22% over nine years from 26.4 $GtCO_2$ in 2005 (IPPC report, 2007) to 32.2 $GtCO_2$ in 2014 (IEA report, 2015). Increase in atmospheric CO_2 contributes to global climate change and the associated environmental impacts such as; increased frequency of extreme weather events, rise in sea level, ocean acidification and raised global mean temperature (Rosenzweig *et al.*, 2001; Doney *et al.*, 2009; IPCC 2013). Recent studies show a near-linear relationship between CO_2 emissions and global mean temperature change (Matthews *et al.*, 2009). Increasing mean temperatures and unstable weather conditions pose a threat to food security (Schmidhuber & Tubiello, 2007) and biodiversity, with one study predicting up to 37% of species may be 'committed to extinction' by 2050 using current climate change models (Thomas *et al.*, 2004).

Increase in global population will have a significant impact on fuel demand and reliance on fossil fuels in the future. Recent UN projections estimate the global population will rise from 7.3 billion to between 9.6 and 12.3 billion by 2100, contrary to previous data that predicted global population would peak this century (Garland *et al.*, 2014). Not only is the global population increasing, but the proportion of 'middle class' people in developing countries is rising (Ravallion, 2010) resulting in increased demand for transportation to facilitate both business and leisure pursuits. The number of light duty vehicles in use is

estimated to at least double by 2050, with demand for transport fuels increasing between 30 to 82 percent by 2050 (World Energy Council, 2011).

With the size of the transport sector projected to increase significantly over the next 50 years and with a large proportion of greenhouse gas emissions being attributed to this sector (27% of total greenhouse gas emissions in the US in 2013, US Environmental Protection Agency, 2016]) development of carbon neutral transport fuels has become increasingly important. As governmental and social awareness of factors effecting climate change has increased, government policies have changed to reduce human impact. One of the main areas targeted by global governments is the use of petroleum based transport fuels and how reliance on such fuels can be reduced to mitigate CO_2 output from the growing transport sector.

Numerous incentives for oil companies to increase their delivery of transport fuels derived from renewable sources (biofuels) have been implemented by governments. The European Union has set targets for biofuels to make up 10% of European transport fuels by 2020 (European commission, 2016) and the US Energy Independence and Security Act of 2007 established a Renewable Fuel Standard (RFS2) requiring increased biofuel use in all light duty vehicles (Anderson *et al.*, 2009). However, this demand for immediate upscale in biofuel production has led to existing food crops being used for biofuel (ethanol) production in an unstainable way which is likely to have economic and environmental repercussions in the future (Moore, 2008).

1.2 First Generation Biofuels

First generation biofuels are fuels, such as fatty acid methyl esters (FAME i.e., bio-diesel) and ethanol, derived from food crops. Ethanol has been used as a transport fuel for over a century (Nattale Netto, 2005) and as demand for alternatives to petroleum based fuels has increased, oil companies have turned to ethanol for several reasons. Ethanol is relatively simple to produce via fermentation of sugars produced by crops such as *Saccharum officinarum* (sugar cane) and *Zea mays* (maize/corn), followed by distillation. Furthermore, net CO_2 output from ethanol production and use is low compared to petroleum (CO_2 is sequestered during growth of the feedstock). Ethanol is also industrially appealing as a biofuel as the infrastructure is well established – ethanol has been

produced on an industrial scale in Brazil for over 40 years due to the 'Pro alcohol' initiative (Leite *et al.*, 2009).

However, there are some major drawbacks to ethanol as a biofuel; for example, ethanol can only be used as an additive fuel in the majority of current combustion engines. The 'blend wall' – the amount of ethanol that may be mixed with petroleum-based fuels whilst having no detrimental effects on the conventional petrol engine and vehicle performance, currently stands at around 10% (E10). However, a higher blend wall of 15% (E15) has been introduced by the US environmental protection agency (EPA) with the aim to reduce fuel prices and petroleum consumption (Qiu, Colson & Wetzstein, 2014). Some vehicles have been engineered to run on up to 100% ethanol (Andrietta *et al*., 2007), and 'flex fuel' engines which can utilise both conventional petroleum fuel and petroleum blended with up to 85% ethanol, have been introduced (Zhu, 2014). However, it would take a substantial combustion engine infrastructure remodel for ethanol to fully replace its fossil fuel counterparts and this would have high economic and environmental costs.

The food versus fuel argument is also an important factor when considering the impacts of increased reliance on ethanol as a transport fuel (Graham-Rowe, 2011). The increased use of arable land to cultivate crops for fuel production has had major repercussions on global food security with numerous studies stating biofuel production is a major contributing factor to inflated food prices (Mitchell, 2008). Collins (2008) attributed 60% of the surge in maize price between 2006 and 2008 to an increased use of maize for ethanol production.

The other first generation biofuel currently produced for retail blends is biodiesel. Biodiesel is made up of fatty acid methyl esters (FAME) produced from vegetable oils or animal fats. Blends of biodiesel with conventional diesel have been shown to reduce hydrocarbon particulate matter and carbon monoxide emissions but increase emissions of toxic nitrogen oxides (Qi *et al.*, 2010). Like ethanol, biodiesel is used primarily as an additive fuel (i.e., blended with conventional fuel) and can only compete with conventional diesel in price due to government subsidies (Gerpen, 2005). The high cost of raw materials and of processing these to produce functional fuels are major barriers to up scaling this industry. Vegetable oil prices account for 60-75% of the cost of biodiesel and this will only increase, as more agricultural land is required to produce food for a rapidly expanding population (Fangrui & Hanna, 1999).

1.3 Second Generation Biofuels

Global agriculture primarily cultivates plants rich in easily digestible energy sources such as oils, sugars and starch. However, lignocellulose is a fourth energy rich element that makes up a considerable proportion of the dry mass of all plants and has potential as a biofuel feedstock (Kreith & Krumdieck, 2014). Lignocellulose is the main component of plant cell walls, made up of cellulose (beta 1-4 linked chains of glucose molecules), hemicellulose (various 5-6 C sugars such as arabinose, xylose, galactose and glucose) and lignin (a polymer of three phenol alcohols). These complex structure makes lignocellulose indigestible, so this fraction of food crops is wasted or used as low value commodities such as animal bedding.

Second generation biofuels are defined as fuels derived from non-food crops, or parts of food crops that cannot be used to make food products – i.e. biofuels derived from lignocellulose. Lignocellulosic material may be converted into liquid biofuels either through hydrolysis and fermentation, which yields bioethanol, or via gasification which can yield various products such as bio-diesel, bio-SNG (synthetic natural gas – can be converted to bioethanol) and bio-DME (dimethylether, Naik *et al.,* 2010).

The agriculture and forestry industries generate a range of byproducts including straw, corn-stover and saw dust, all potential feed-stocks for biofuel production. However, to meet demand, plants that yield higher proportions of lignocellulose than sugars and starch are starting to be grown for the purpose of second generation biofuel production. These include short rotation forestry crops such as bamboo and willow, perineal grasses such as switch grass, and non-food crops such as sweet sorghum (Naik *et al*., 2010).

There is no direct competition between manufacture of second-generation biofuels and food production, as is seen with first generation biofuel production, due to the feed-stocks being waste products or non-food crops. However, where crops are grown specifically for second-generation biofuel production, the use of agricultural land that may otherwise be used for food production continues to be an issue (Sims *et al*., 2010).

Lignocellulossic biomass is thought to represent the most abundant global biofuel feedstock yet lignocellulose conversion to usable liquid transport fuels is still largely experimental. Lignocellulose is unamenable to biological degradation and the process of “unlocking” the monosaccharide sugars from lignocellulose (known as pre-treatment) prior to fermentation is very energy, and cost, intensive. Pre-treatments include acid hydrolysis,

often performed at high temperatures, and treatment with relatively high loads of cellulose degrading enzymes to release free glucose from the strong bonds formed with hemi-cellulose and lignin (Kumar *et al*., 2009).

Due to the shortcomings of current biofuels, there is a need to produce a superior alternative. The ideal biofuel would pose no threat to global food security, be suitable for use in current combustion engines without blending and be truly sustainable. Hydrocarbon production in nature has been studied for decades; re-visiting and expanding our knowledge of naturally occurring hydrocarbon production may enable a superior advanced biofuel to be developed.

1.4 Hydrocarbon Synthesis in Living Organisms

The term 'hydrocarbon' is used from this point to describe compounds that are derived from long-chain fatty-acid precursors. Hydrocarbon production in nature spans several taxonomic groups, however, being products of secondary metabolic pathways, yields are not sufficient for industrial exploitation. This being said, improving understanding of biological hydrocarbon production pathways will enable relevant enzymes to be characterised and optimised to improve product yield within the original system or for the enzyme-encoding gene to be engineered into a novel synthetic system.

Several examples of hydrocarbon production in nature have been studied. For example, Birds produce a variety of esters in their uropygial (preen) gland. *Galliform* birds such as chickens and turkeys secrete fatty acid esters of 2,3-alkanediols, while *Anseriformes* (*e.g*. geese) or *Strigiformes* (*e.g*. barn owls) secrete wax monoesters. The final step in biosynthesis of these esters has been identified as fatty alcohol reduction catalysed by a wax synthase (WS) gene also identified in prokaryotic organisms (Biester *et al*., 2012).

The long chain hydrocarbons produced by insects play integral roles in waterproofing and communication (Blomquist *et al.*, 2010). Although different insect species synthesize numerous different hydrocarbons, they may be roughly divided into three groups, *n*-alkanes, methyl-branched alkanes and unsaturated hydrocarbons, all of which have very long carbon chain lengths between C_{21}-C_{33} (Blomquist *et al.*, 2010). In Blattodea species, elongation of acyl-CoA creates long chain fatty acids (LCFAs) which are then converted into alkanes through a decarboxylation reaction catalysed by a cytochrome P-

450 enzyme (Tillman *et al*., 1999; Howard & Blomquist, 2005). Qui *et al* (2012) found P450 enzymes of the CYP4G family to be responsible for oxidative production of alka(e)nes in *Drosophila melanogaster* using RNAi knockdown techniques. In the same study CYP4G2 (from *Musca domestica)* was used to create a recombinant fusion protein with P450 reductase. This fusion protein catalysed aldehyde decarboxylation via a novel mechanism which is NADPH dependent and produces carbon dioxide and water byproducts (see Figure 1, Qui *et al*., 2012).

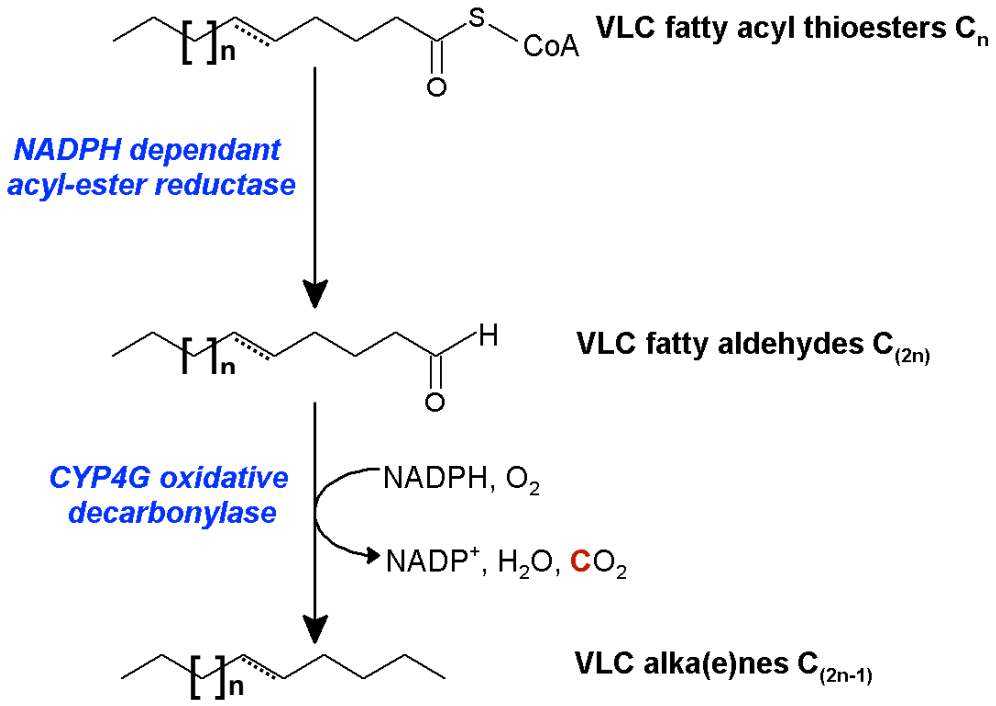

Figure 1. Insect Alkane Synthesis Pathway (adapted from Qiu *et al*.,2012)

Pathway showing formation of very long chain (VLC) alkanes and alkenes in insects via oxidative decarboxylation of VLC fatty aldehydes, catalysed by CYP4G enzymes. Carbon loss is highlighted in red and enzymes are shown in blue.

Many Plant species produce a range of hydrocarbons that make up their cuticular lipid layer, used for waterproofing and protection, in a similar way as esters are used to waterproof bird feathers. Plant cuticular lipids are very long chain fatty acids (VLCFAs) and derivatives thereof such as alcohols, ketones, alkanes and wax esters (Lee & Suh 2015).

The biosynthesis of VLCFAs in *Arabidopsis* has been extensively studied and involves firstly the hydrolysis of C_{16}-C_{18} acyl-acyl carrier proteins to fatty acids catalysed by fatty acyl ACP thioesterase (FATA/FATB). C_{16}-C_{18} fatty acids are then activated by a long chain acyl CoA synthase (LACS) and transported to the endoplasmic reticulum (ER) where they undergo elongation via sequential addition of C_2H_5 units (derived from malonyl-CoA) to form C_{20}-C_{34} VLCFAs (Bonaventure *et al*., 2003; Schnurr *et al*., 2004). Fatty acid elongation is catalysed by a fatty acid elongase (FAE) complex which comprises β-ketoacyl-CoA synthase (KCS), β-ketoacyl-CoA reductase (KCR), 3-hydroxyacyl-CoA dehydratase (HCD) and *trans*-2,3-enoyl-CoA reductase (ECR), These enzymes are responsible for the sequential condensation, reduction, dehydration and second reduction involved in plant VLCFA synthesis (Kunst & Samuels 2009; Li Beisson *et al*., 2013)

VLCFAs are then processed, via one of two pathways, into cuticular lipids (Figure 2). In the acyl reduction pathway, fatty acyl-CoA reductase (*FAR3*/*CER4*) catalyses the formation of primary alcohols which are subsequently condensed into wax esters by the bi-functional wax synthase enzyme *WSD1*. In the second pathway VLCFAs are reduced to aldehyde intermediates before undergoing decarbonylation to form alkanes. A recent study has shown a multi-enzyme complex including the aldehyde decaronylase CER1, the aldehyde forming enzyme *CER3/WAX2/YRE* and the cytochrome b6 isoform *CYTB5* is likely to catalyse this two-step reaction (Bernard *et al*., 2012). A portion of the alkanes produced are then thought to act as precursors in the formation of secondary alcohols and ketones catalysed by the mid-chain alkane hydroxylase 1 enzyme *MAH1* (Greer *et al*., 2007).

Although a wide variety of hydrocarbon products are cultivated in *Arabidopsis,* many of which have potential industrial applications, *A. thaliana* is not an ideal candidate for metabolic engineering or synthetic biology parts to be derived from. This is due to carbon loss through the main hydrocarbon synthesis pathway, as seen in the insect alkane synthesis pathway, which reduces carbon efficiency and therefore economic viability.

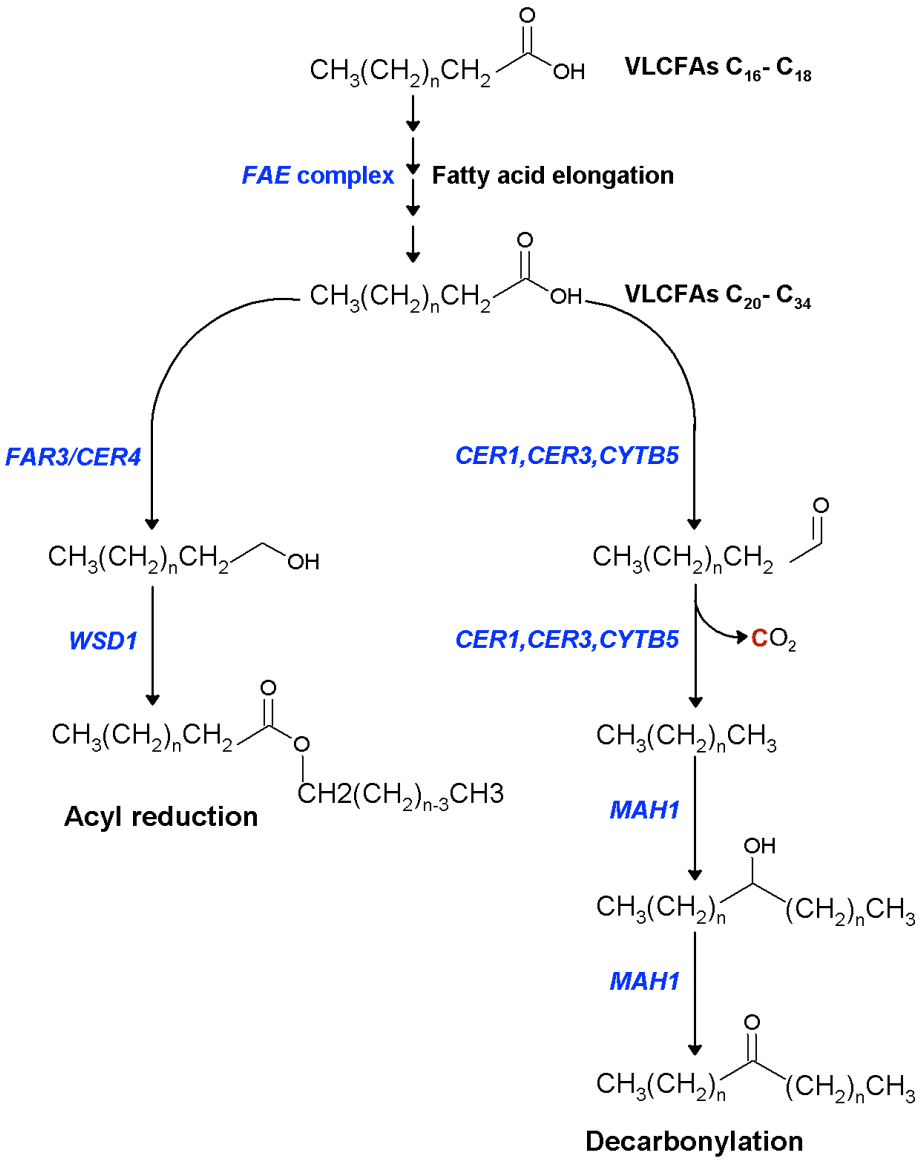

Figure 2. Proposed Metabolic Pathways for Wax Biosynthesis in Arabidopsis

Very long chain fatty acids (VLCFAs) are converted through two biosynthetic pathways to all other cuticular wax components. Fatty acyl-CoA reductase (*FAR3*/*CER4*) catalyses the formation of primary alcohols from VLCFAs, which are then condensed into wax esters by wax synthase enzyme *WSD1*. The decarbonylation pathway yields alkanes from a fatty aldehyde intermediate. This two-step reaction is thought to be catalysed by a multi-enzyme complex including an aldehyde decarbonylase CER1, an aldehyde forming enzyme *CER3/WAX2/YRE* and a cytochrome b6 isoform *CYTB5* (Bernard *et al*., 2012). Mid-chain alkane hydroxylase 1 (MAH1) is proposed to catalyse the conversion of alkanes to secondary alcohols and ketones (Geer *et al*., 2007). Carbon loss is highlighted in red and enzymes are shown in blue.

1.5 Third Generation Biofuels

Numerous microbial species have been identified as hydrocarbon producers. Microalgae, such as *Chlorella spp*., synthesize a variety of lipids and long-chain hydrocarbons (Mata *et al*., 2010). Where a high proportion of lipids are produced, these may be utilised as precursors in biodiesel production, while the longer chain hydrocarbons may be developed into 'drop in' fuels. For example, the green algae *Botryococcus braunii* produces very long chain unsaturated hydrocarbons (these constitute up to 75% of its dry mass, Banerjee *et al*., 2002).

Superficially microalgae possess many qualities that make them well suited to industrial scale production of biofuels; most species require only sunlight and basic nutrients for growth, they are often able to grow on waste water unfit for human consumption and, unlike plants, no valuable agricultural land is required for growth (Mata *et al*., 2010).

However, there are several drawbacks to biofuel production from microalgae, harvesting biomass has been a particular challenge to engineers due to the small size of the algae (approximately 1–20 μm) and their suspension in liquid (Lam & Lee, 2012). Different separation and drying methods to recover biomass (such as centrifugation and natural gas drying) can double overall energy input and generate positive CO_2 emissions, (Sander & Murthy, 2010). The high cost of installing the closed system bioreactors required to achieve optimal product yields is also prohibitive to the economic viability of micro-algal biofuels (Brennan & Owende, 2010). Furthermore, few algal species produce hydrocarbons that match those found in current petroleum based transport fuels so hydrocarbon products would need to be further processed before they can be used as drop in fuels - an expensive and energy intensive process.

Several bacterial species produce hydrocarbons of the same carbon chain lengths found in current transport fuels (C_4-C_{23}), which have potential use as 'drop in' fuels in current combustion engines. For example, *Jeotgalicoccus* spp. synthesize terminal alkenes including 18-methyl-1-nonadecene and 17-methyl-1-nonadecene via decarboxylation of fatty acids catalysed by the P450 enzyme $OleT_{JE}$ (Rude *et al.*, 2011).

Micrococcus Luteus produce long chain alkenes through head to head condensation of fatty acids (or fatty acid derivatives). Four protein families OleABCD are critical to this pathway, with OleA being the most studied. OleA has been shown to catalyse the Claisen condensation of fatty acids to β-ketoacids which then undergo spontaneous

decarboxylation to produce ketones (Frias *et al*., 2011). The role of the other Ole proteins in decarbonylation of the ketones to produce odd chain length alkenes has yet to be fully characterized (Bird and Lynch 1974; Frias *et al*., 2011).

Cyanobacterial species, such as *Synechococcus elogatus* PCC7942 and *Anabaena sp*. PCC7120, have been shown to be reliable alkane producers, synthesizing mainly heptadecane and pentadecane through a well characterized secondary metabolic pathway (Tan *et al*., 2011; Schirmer *et al.*, 2010). The pathway involved was identified through genomic comparison of strains positive and negative for alkane synthesis as well as "knock in" and "knock out" experiments of candidate genes. The specific activity of the genes involved (acyl-ACP reductase, AAP and aldehyde deformylating oxygenase, ADO) was confirmed through their heterologous expression in *E. coli* (Schirmer *et al*., 2010).

Although being photosynthetic makes cyanobacteria industrially appealing as biofuel producers, the alkane yield is too low to make the process commercially viable. Furthermore, production of such a narrow range of alkane products (C_{17} and C_{15}) would not allow for direct replacement of petroleum fuels in current combustion engines, as a mix of different chain length and branched alkanes (and alkenes) would be required to achieve this.

However, recent advances in synthetic biology have facilitated research into overcoming these shortfalls. A novel method of synthesizing tailored alkanes of various chain lengths in *E. coli* has been developed (Howard *et al*., 2013). *E. coli* were transformed with a fatty acid reductase (FAR) complex from *Photorhabdus luminescens* and an aldehyde deformylating oxygenase (ADO) gene from *Nostoc punctiforme* to enable the bacteria to synthesize alkanes from free fatty acids. Alkane carbon chain lengths were predictably altered via manipulations to the fatty acid pool (Howard *et al*., 2013), resulting in a tailored product that could replace its fossil fuel counterpart. Several other research groups have designed similar synthetic pathways (Harger *et al*., 2012; Akhtar *et al*., 2013; Choi *et al*., 2013) however yield has yet to be much improved. Low yields and carbon loss through the pathway prevent this system of advanced biofuel production being up-scaled.

Long-chain alkane and alkene production in different bacterial species is summarised in the following diagram (Figure 3).

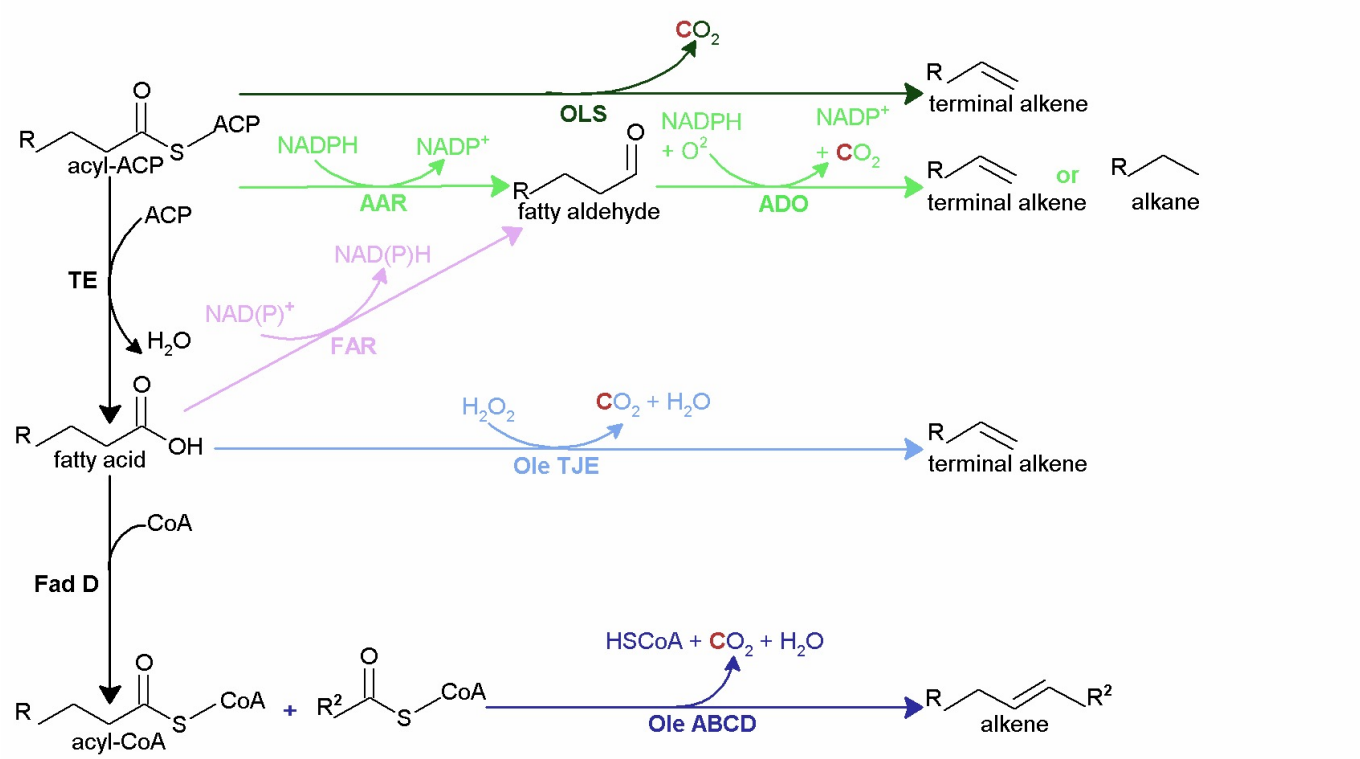

Figure 3. Overview of Fatty Acid Based Alkane/Alkene Biosynthesis in Bacteria

Five different pathways are shown here: an endogenous cyanobacterial pathway (light green) shows reactions catalysed by acyl-ACP reductase (AAR) and aldehyde deformylating oxygenase (ADO, Schirmer *et al.*, 2010); *Micrococcus luteus* pathway (dark blue) shows formation of long chain alkenes via head condensation of fatty acid derivatives, catalysed by Ole ABCD (Frias *et al.*, 2011); terminal alkene production pathway ubiquitous in the genus Jeotgalicoccus (light blue) catalysed by fatty-acid decarboxylase $OleT_{JE}$ P450 enzyme (Rude *et al.*, 2011); conversion of acyl-ACP to terminal alkenes and dienes in marine cyanobacteria *Synechoccus* sp. PCC7002, (dark green) catalysed by OLS, a multi-domain polyketide synthase (Mendez-Perez, Begemann and Pfleger, 2011); and a synthetic pathway (lilac) enabling free fatty acids in *E. coli* to be converted into petroleum replica alkanes (Howard *et al.*, 2013). Carbon loss in each pathway is highlighted in red, enzymes are in bold.

1.6 Synthetic Biology

Plants and microbes produce a wide variety of compounds, many of which hold potential value as replacements for products currently derived from unsustainable sources, such as plastics and fuel. Whilst there are numerous examples of living organisms being directly exploited as 'biological factories' (e.g., agriculture, forestry) many products of commercial interest are too low yielding for this to be economically viable. A further barrier to harnessing products from certain living organisms is complex growth conditions or nutritional requirements making large scale growth impractical and expensive.

Synthetic biology is a pioneering field of research that aims to combine biological 'parts' and 'devices' into rational systems that produce desirable products in a sustainable way (Nielson & Moon, 2013). In most cases the 'parts' are enzyme-encoding genes with well understood biological functions, but this term may also include tools for gene expression optimization such as promotors and riboswitches. The aim of synthetic biology is to create standardized modular systems whereby novel biological pathways may be engineered to allow economically viable product formation using selected 'parts' from existing natural pathways that may span several species. Once designed and characterized, the synthetic pathway may be introduced into a suitable industrial host, such as the yeast *Saccharomyces cerevisiae* or the gram-negative bacterium *Escherichia coli,* which can grow rapidly in a fermenter with basic growth requirements.

Synthetic biology success stories to date include; production of the anti-malarial drug artemisinin (usually derived from *Artemisia annua* - sweet wormwood) in *E. coli* (Martin *et al.,* 2013), and *E. coli* engineered to produce higher alcohols such as isobutanol and 1,2-butandiol, which have uses as biofuels and precursors to production of valuable polymers (Atsumi, 2008; Yim *et al.*, 2011). Muconic acid (a precursor to several plastics) has been synthesized in *Saccharomyces cerevisiae* by introducing a three step synthetic pathway based on enzymes found in less industrially viable microbes (Curran *et al.*, 2013). There have also been steps forward in synthetic biofuel research; *E. coli* transformed with the synthetic alkane production pathway CEDDEC, has been proven to produce tailored petroleum replica alkanes, albeit on a small scale (Howard *et al.*, 2013).

Synthetic biology therefore has an immense potential to allow the chemical, fuel and pharmaceutical industries to synthesize products from their existing portfolios, and to

create new and enhanced products, in an environmentally responsible way so they may sustain the needs of modern society.

1.7 *Desulfovibrio*

Desulfovibrio species are gram negative, non-spore forming, anaerobic bacteria that are widely distributed among both terrestrial and aquatic environments. A defining metabolic characteristic of *Desulfovibrio spp*. is their ability reduce sulphate to sulfide according to the following reaction (Voordouw, 1995).

$$SO_4^{2-} + ATP + 8H^+_{in} + 8e^- \longrightarrow HS^- + AMP + 2P_i$$

The ability of *Desulfovibrio spp*. to reduce sulfur makes them part of a broad group of bacteria known as sulphate reducing bacteria (SRB). The hydrogen sulfide produced by *Desulfovibrio spp*. creates an unpleasant smell often associated with the anoxic canal waters from which these bacteria were initially isolated (Beyerinck, 1895).

Desulfovibrio spp. can utilise a variety of electron donors for sulphate reduction, such as hydrogen, organic acids, alcohols, and components of crude oil (Postgate, 1984; Matias *et al*., 2005). When lactate serves as the electron donor, energy (ATP) for sulphate reduction is acquired via oxidation of lactate to pyruvate and then to acetyl-CoA which is subsequently converted to acetate yielding one ATP from ADP. Conversion of lactate to acetate yields four electrons of the eight electrons required for sulphate reduction; therefore, lactate and sulphate are utilised in a 2:1 molar ratio according to the following reaction (Price *et al*., 2014).

$$2C_3H_6O_3\,(\text{lactate}) + SO_4^{2-} \longrightarrow HS^- + 2C_2H_3O_2^-\,(\text{acetate}) + 2CO_2$$

Although thought of as strict anaerobes, *Desulfovibrio* species have been shown to survive aerobic environments by reducing oxygen to water (Cypionka, 2000). In *D. gigas* this respiratory pathway is well studied and the enzyme responsible for oxygen reduction, ubredoxin:oxygen oxidoreductase (ROO), has been characterized (Frazao *et al*., 2000).

Desulfovibrio spp. play an essential role in the biological sulfur cycle and, along with other dissimilatory sulphate reducing bacteria such as *Desulfotomaculum spp*, facilite the release of sulfide ions from metal sulphates (Pfenning, 1975). Due to their metabolism locally increasing pH, *Desulfovibrio spp*. have been industrially exploited for remediation

of toxic metals such as copper (II), nickel (II) and cadmium, which precipitate as metal sulfides in the presence of *Desulfovibrio* (Heidelberg *et al.,* 2004). However, *Desulfovibrio spp.* are generally associated with negative economic impacts particularly affecting the oil industry, as they produce toxic sulfide ions that can lead to corrosion of ferrous metals (drilling and pipeline equipment) as well as 'souring' oil products (Heidelberg *et al*., 2004; Miranda, 2006).

Desulfovibrio spp. were first identified as producing C_{10}-C_{25} aliphatic hydrocarbons, including alkanes, over seventy years ago (Jankowski & ZoBell, 1944). However, prior to the present study, analysis did not distinguish metabolic hydrocarbon production from contamination with 'white oil' (hydrocarbons found ubiquitously on all manufactured goods) leading to unreliable data regarding which strains produce hydrocarbons.

Desulfovibrio spp. produce higher alkane yields than other microorganisms studied to date (0.8–2.25% of total dry biomass, [Ladygina, 2006]). However, *Desulfovibrio spp.* are not suited to industrial scale alkane production due to slow growth, requiring carefully monitored anaerobic conditions and complex growth media. However, genes which encode enzymes involved in the *Desulfovibrio* alkane synthesis pathway may prove integral to future synthetic biology efforts to produce an ideal biofuel from engineered bacteria. For example, *Desulfovibrio* alkane synthesis genes may be isolated and introduced into a model bacterium such as *E. coli* for further characterization and optimization (already achieved with genes from cyanobacteria [Schirmer *et al*., 2010]). Following this, desirable genes may be integrated into an alkane synthesis pathway in a host suitable for industrial scale growth.

A hypothetical *Desulfovibrio* alkane synthesis pathway has previously been suggested (Bagaeva, 1998). Isotopic labelling experiments were used by Bagaeva (1998) to investigate conversion of lactate to hydrocarbons in *D. desulfuricans*. Bagaeva concluded formate is a direct product of CO_2 reduction catalysed by formate dehydrogenase, and formate is also involved in acetate biosynthesis. He goes onto suggest hydrocarbons are produced by decarboxylation of free fatty acids, as seen in cyanobacteria. This was based on the observation that ^{14}C derived from methyl groups of labelled acetate was preferentially incorporated into alkane products over ^{14}C from carboxylic groups giving evidence for a decarboxylation step. Formate feeding into fatty-acid biosynthesis would provide an explanation for why alkanes of both odd and even carbon chain lengths were observed in *D. desulfuricans*, however the incorporation of ^{14}C from labelled formate into

alkanes is not discussed here so it remains unclear whether odd chain fatty acids were produced and the role they played in alkane synthesis. Bagaeva's proposed pathway is shown overleaf (Figure 4).

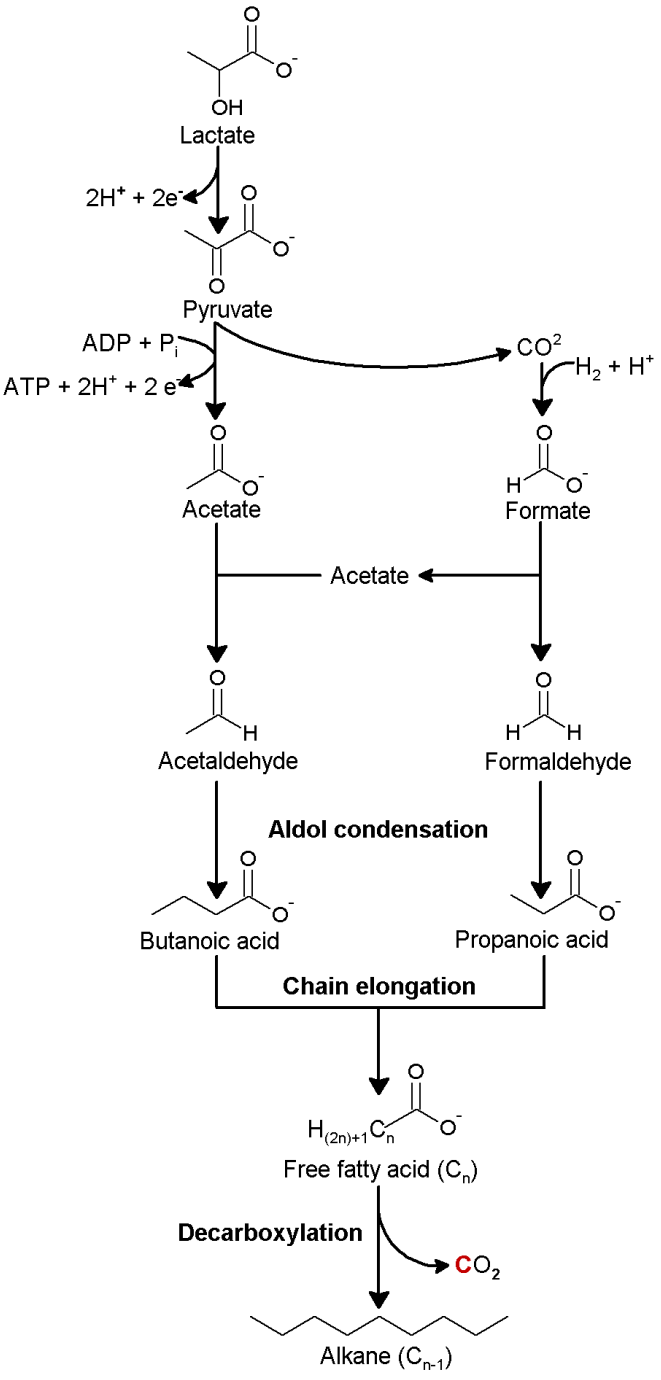

Figure 4. *Desulfovibrio* Alkane Synthesis Pathway Proposed by Bagaeva (1998)

A pathway where odd or even-chain fatty acids undergo decarboxylation to produce alkanes in *Desulfovibrio* was proposed by Bagaeva based on ^{14}C from labelled methyl groups of acetate being incorporated into alkane products more actively than ^{14}C from labelled carboxyl groups, giving evidence to support a decarboxylation reaction. Carbon loss is highlighted in red.

The genes involved in *Desulfovibrio* alkane synthesis have yet to be identified, and there are several barriers to achieving this. First, there is no reliable transformation protocol available for this genus ruling out conventional molecular biology methods such as genetic manipulation. *Desulfovibrio vulgaris* Hildenborough has been successfully transformed (Keller, Bender & Wall, 2009), however the *Desulfovibrio* strain used was likely "lab-adapted" and other strains are more recalcitrant to transformation.

Second, initial in-silico transcriptome comparison of the alkane producing *Desulfovibrio desulfuricans desulfuricans* 8326 with 11 non-alkane producing *Desulfovibrio* strains identified approximately 280 enzymes unique to the alkane producing strain (Rob Lee, Internal Shell report), which does not significantly narrow down potential genes involved in alkane synthesis.

Alkane biosynthesis pathways were successfully investigated through various biochemical methods decades prior to genomic data becoming readily accessible (Dennis & Kolattukudy 1992; Bird & Lynch, 1974). It was hoped a non-genetic, biochemistry approach could provide valuable insight in this project, as the molecular 'toolkit' for this genus is yet to be established.

The current study aimed to screen different *Desulfovibrio* strains for alkane synthesis using isotopically labelled growth media to achieve a definitive alkane profile for each strain, which may be used to inform a novel hypothesis for alkane synthesis in the genus. This hypothesis was then tested by observing the effects of exogenously supplied potential competitive inhibitors or substrates had on alkane synthesis. The study then progressed to a proteomics based approach based around the detection of alkanes in *Desulfovibrio desulfuricans desulfuricans* 8338 cell lysate. Several methods were employed to fractionate cell lysates from 3 alkane producing *Desulfovibrio* strains, prior to alkane analysis using GC/MSD, to narrow down the proteins that may be associated with alkanes. Once this was achieved, two-dimensional difference electrophoresis was used to separate and visualise distinct proteins present in alkane containing cell lysate fractions. These were then compared to non-alkane containing cell lysate fractions from the same *Desulfovibrio* strain and different *Desulfovibrio* strains with the aim of identifying the most likely proteins to be associated with alkanes in the cell lysate.

Chapter 2. Materials and Methods

Unless otherwise stated all chemicals were obtained from Sigma Aldrich. The anaerobic workstation was a Whitley A35 anaerobic workstation (Don Whitley Scientific) with an internal atmosphere of ANO_2 (10% H_2, 10% CO_2 and 80% N_2) and N_2 at regulated pressures of approx. 3 bar, temperature was 30 °C and humidity 65 %. *Desulfovibrio* strains were obtained from the Lebniz Institute DSMZ-German Collection of Microorganisms, the American Type Culture Collection (ATCC) and the National Collection of Industrial, Food and Marine Bacteria (NCIMB).

2.1 *Desulfovibrio* Culture

Desulfovibrio were cultured in 50 ml Falcon tubes (Thermo Fisher Scientific), except where larger volumes were required (i.e., for cell lysate preparation) then 250 ml or 500 ml glass Duran bottles (Duran group) were used. All culture vessels were placed in an anaerobic workstation overnight to remove oxygen prior to culture inoculation. *Desulfovibrio* were cultured in modified Postgate B (PGB) medium (Postgate, 1979) made with type 1 ultra pure water (18.2 megohm, from a GenPure x-CAD Water Purification System, Thermo Fisher Scientific) and the following compounds: KH_2PO_4 (0.5 g l^{-1}; 3.67 mM), NH_4CL (1 g l^{-1}; 18.69 mM), $CaSO_4$ (1 g l^{-1}; 7.35 mM), $MgSO_4.7H_2O$ (2 g l^{-1}; 8.11 mM), $FeSO_4.7H_2O$ (0.5 gl^{-1}; 1.80 mM), ascorbic acid (0.1 gl^{-1}; 0.57 mM), sea salts (10 g l^{-1}), yeast extract (1 g l^{-1}), lactic acid (6 ml l^{-1}; 80.33 mM), ammonium thioglycoalte (0.2 ml l^{-1}; 2.18 mM) and Resazurin (1 ml l^{-1} of a 1 g l^{-1}solution; approx. $4x10^{-3}$ mM). Where 10% D_2O PGB was used PGB was prepared with D_2O (99.8% HPLC grade, 100 ml l^{-1}) and ultra pure water (900 ml l^{-1}). Where ^{13}C lactate PGB was used, PGB was prepared with 4.5 g l^{-1} ^{13}C lactate in place of lactic acid. Deuterium depleted PGB (Dd PGB) was prepared with deuterium depleted water in place of ultra pure water. All variations of PGB medium were adjusted to between pH 7.2 – 7.4 with KOH (1 M) before being autoclaved. Medium was transferred to an anaerobic workstation directly following sterilization to cool and for any residual oxygen to be removed before being inoculated (1 ml inoculum in 45 ml media) with *Desulfovibrio* taken from stock cultures. Cultures were incubated in an anaerobic workstation (30 °C) for between 7-21 d depending on strain and desired product to be harvested.

HPLC sample preparation

Samples of *Desulfovibrio* cultures (1 ml) were transferred to 1.5 ml Eppendorf tubes and centrifuged at 21,630 *g*, 10 °C for 10 min to pellet cell debris and FeS. Clarified supernatant was transferred to 200 μl glass insert vials prior to HPLC analysis to determine culture growth. Lactic acid and acetic concentrations were quantified by comparison to known standards. The HPLC used was a Dionex 3000, with Shodex RI (Thermo Fisher Scientific). The column was an aminex HPX-87H (Bio-Rad) fitted with a cation H cartridge set. The column was operated at 65°C, samples were injected at a rate of 15 µl/s. Mobile phase used was an aqueous solution of 0.005% HCL. Refractive Index detector conditions were as follows; temperature 50°C, data collection rate 10 Hz, positive polarity, rise time 1.5 s, integrator range 500 µRIU/V and recorder range 512 µRIU.

2.2 Alkane Extraction and Analysis

Desulfovibrio culture samples (10-45 ml) were centrifuged at 23,450 *g* at 10 °C for 12 min and the supernatant discarded. Pellets were re-suspended in 25 ml ultra pure water, transferred to PTFE tubes (30 ml, cleaned with DCM prior to use) and centrifuged at 17,230 *g* at 10 °C for 12 min. Supernatant was discarded and wash step repeated. Pelleted samples were transferred to a -80 °C freezer for 30 min before being being uncapped and transferred to a freeze dryer to dry overnight. No internal hydrocarbon standard was added at this point from which to calculate alkane extraction efficiency (as is best practice) as this was deemed unessential as results focused on presence (or absence) of alkanes rather than concentration. 1 ml or 500 μl DCM was added to freeze-dried samples using a clean glass syringe before they were placed in a sonnicating water bath for 45 min (25 °C or room temp). Samples were retrieved and a clean glass syringe used to withdraw 200 μl from each sample, needles were replaced with 4 mm Puradisc syringe filters (PVDF membrane, 0.2 μm pore size Whatman, GE Healthcare Life Sciences) and samples transferred to glass vials. Samples were run on a 7890A GC with a 5975C MSD attached (Agilent) alongside a mixed external standard (C_8-C_{20} n-alkanes, 4 mg l^{-1}) and blanks of DCM. The column used was a DB-5 30 m 0.25-0.25 μm (Agilent) and the carrier gas was He supplied at a flow rate of 1.5 ml/min. GC/MSD method was as follows: inlet 280 °C, 1 μl splitless injection, temp programme was 30 °C to 300 °C at 15 °C per min. Analysis software used was ChemStation (Agilent).

2.3 Preparation for Exogenously Supplied Hydrocarbon Screen

0.5 mmol of all hydrocarbons screened were transferred to 50 ml Falcon tubes and incubated for up to 30 min (until solids melted) at 80 °C. Tubes were then inverted and vortexed (15 s) to coat the internal surface with hydrocarbon and rotated for 20 s on ice to solidify. All Falcon tubes containing hydrocarbons were transferred to an anaerobic workstation and lids loosened to remove O_2 overnight. Cultures of *Desulfovibrio desulfuricans desulfuricans* 8338 (*Dd* 8338) were then set up as previously described. Controls were cultured in blank Falcon tubes. All *Dd* 8338 cultures were incubated for 14 d - 21 d.

Cultures were transferred into clean Falcon tubes (1 ml was taken for HPLC analysis and 10 ml for protein analysis at this point) before performing alkane extraction and analysis.

2.4 Cell Lysate Preparation, Fractionation and Protein Analysis

Cell lysis

Desulfovibrio culture samples (10 ml for protein quantification or 250 ml for ammonium sulphate precipitation) were centrifuged to pellet cells (23,450 *g*, 4 °C for 20 min or 11,880 *g* for 22 min where 250 ml volumes used) and supernatant discarded. Pellets were then re-suspended in ice-cold sterile PBS, centrifuged and supernatant discarded as above. Pellets from 10 ml culture samples were re-suspend in 300 μl PBS, pellets from 250 ml culture samples were re-suspend in 5 ml PBS, cell suspensions were transferred to Eppendorf tubes prior to being frozen in liquid nitrogen. Samples were then transferred to a water bath (37 °C) for 20 min. This freeze-thaw cycle was repeated twice. Samples were then centrifuged at 21,630 *g*, 4 °C for 20 min to pellet cell debris. Clarified supernatant (cell lysate) was then transferred to clean Eppendorf tubes and stored at -20 °C.

Quibit® protein quantification assay (Thermo Fisher Scientific)

Working solution (WS) was prepared according to manufacturers protocol. 190 μl WS and 10 μl protein standard (standards #1-3) or 10 μl cell lysate was transferred to thin wall 0.5 ml PCR tubes (supplied by the manufacturer) and vortexed for 2-3 s. All assays were incubated at room temp for 15 min before being analysed using a Qubit® 2.0 Fluorometer according to the manufacturer's protocol.

SDS-PAGE

Novex® Bolt™pre-cast gels and reagents (Thermo Fisher Scientific) were used throughout. Cell lysate (upto 6.5 μl, if using less volume was made up with ultra pure water), 4X LDS sample buffer (2.5 μl) and 10X reducing agent (1 μl) were combined in Eppendorf tubes and vortexed (3 s) before being incubated at 70 °C for 10 min.

The LDS sample buffer contained lithium dodecyl sulphate (pH 8.4) which is an anioic detergent used to solubulise proteins at low temperatures and optimise activity of the reducing agent. 500 mM dithiothreitol (DTT) was used to disrupt intramolecular and intermolecular disulfide bonds, achieve complete protein unfolding and to maintain the reduced state of the proteins during electrophoresis.

4-12 % bis-tris plus mini gels were loaded with 5-10 μl of SeeBlue® Plus2 protein standard (diluted 1:10 with ultra pure water, Invitrogen) in the first well, and cell lysate samples in remaining wells. Gels were run in 1X MES running buffer at 165 V for 35 min. Peirce® silver stain kit was used according to the manufacturers protocol to stain protein bands. Gel images were taken using myECL imaging system (Thermo Fisher Scientific).

Amicon Ultra-2ml centrifugal filters (Merck, Millipore)

PBS was used as a negative control throughout. Amicon Ultra- 2 ml devices were inserted into filtrate collection tubes. Up to 2 ml of cell lysate was transferred to each device before being centrifuged at 7,500 *g*, 10 °C for 22 min (if using 100 kDa cut off device) or 15 min (if using 50 kDa cut off device). Devices were retrieved from centrifuge and filtrate collection tube transferred to ice. Concentrated samples were recovered by inverting device, attaching collection tube and centrifuging at 1000 *g*, 10 °C for 2 min. Filtrate and concentrated cell lysate fractions were stored on ice or in -20 °C freezer until needed.

Ammonium sulphate precipitation

8-10 ml of *Desulfovibrio* cell lysate was transferred to 50 ml Falcon tubes. Ammonium sulphate (salt, molecular biology grade) was added to reach the desired percentage saturation according to the following equation:

$$X = 0.1G(S_2 - S_1)/(1 - (VG/1000)S_2)$$

Here, X equals grams of $(NH_4)_2SO_4$ to be added to 100 ml of solution with saturation S_1 to reach a solution with saturation S_2, G = grams of $(NH_4)_2SO_4$ in 1 L of saturated solution, and V = apparent specific volume of $(NH_4)_2SO_4$ in a saturated solution.

Samples were stirred on ice for 1 h using magnetic stir plates set to 250 rpm, transferred to multiple 2 ml Eppendorf tubes and centrifuged at 21,630 *g*, 4 °C for 15 min. Clarified supernatants were transferred to clean 50 ml Falcon tubes and ammonium sulphate added to reach next desired saturation (precipitates were stored on ice). This was then stirred and centrifuged as previously described and the process repeated until all ammonium sulphate saturations had been performed. Precipitates were re-suspended in ice-cold PBS to approx. 1/3 original volume. 500 μl of cell lysate and each cell lysate fraction obtained from different ammonium sulphate saturations were transferred to clean PTFE tubes and freeze-dried overnight prior to alkane analysis.

2.5 2D difference gel electrophoresis (2D-DIGE)

2D gel electrophoresis separates proteins based on both their isoelectric point and molecular mass, allowing greater resolution of proteins than SDS-PAGE (where proteins are separated based solely on molecular mass). Furthermore, in 2D difference gel electrophoresis, each protein fraction is labelled with a unique fluorescent dye, enabling gel images to be overlaid, and spots representing proteins more highly expressed in one fraction than another to be clearly visualised and quantified using complementary computer software.

2D-DIGE was outsourced to Applied Biomics Inc (Hayoward, CA). The methods used by Applied Biomics were as follows:

Sample preparation: protein sample buffer was exchanged into 2D cell lysis buffer (30 mM Tris-HCl, pH 8.8, containing 7 M urea, 2 M thiourea and 4% CHAPS). Protein concentration was measured using Bio-Rad protein assay method. Internal standard was made by mixing equal amounts of protein from each sample.

CyDye labelling: for each sample, 30 μg of protein was mixed with 1.0 μl of diluted CyDye, and kept in dark on ice for 30 min. Samples were labelled with Cy2, Cy3 and Cy5 respectively. The labeling reaction was stopped by adding 1.0 μl of 10 mM Lysine to each sample, and incubating in dark on ice for additional 15 min. The labelled samples were

then mixed. The 2X 2D sample buffer (8 M urea, 4% CHAPS, 20 mg ml^{-1} DTT, 2% pharmalytes and trace amount of bromophenol blue), 100 µl de-streak solution and rehydration buffer (7 M urea, 2 M thiourea, 4% CHAPS, 20 mg ml^{-1} DTT, 1% pharmalytes and trace amount of bromophenol blue) were added to the labelling mix to make the total volume 250 µl for use with 13 cm IPG strips. Samples were mixed and spun before being loaded into strip holder.

IEF and SDS-PAGE: IEF (pH 3-10 linear) was run following the protocol provided by GE Healthcare. IPG strips were incubated in equilibration buffer-1 (50 mM Tris-HCl, pH 8.8, containing 6 M urea, 30% glycerol, 2% SDS, trace amount of bromophenol blue and 10 mg ml^{-1} DTT) for 15 min with gentle shaking. Strips were rinsed in equilibration buffer-2 (50 mM Tris-HCl, pH 8.8, containing 6 M urea, 30% glycerol, 2% SDS, trace amount of bromophenol blue and 45 mg ml^{-1} Iodoacetamide) for 10 min with gentle shaking. IPG strips were rinsed in the SDS-gel running buffer before transferring into 12% SDS-gels. The SDS-gels were run at 15 ^{o}C until the dye front ran out of the gels.

Image scan: Gel images were scanned immediately following the SDS-PAGE using Typhoon TRIO (GE Healthcare).

Analysis of 2D-DIGE gel images was performed using ImageJ software (National Institutes of Health, US).

Chapter 3. Results

3.1 Screen of *Desulfovibrio* Strains for Alkane Production

Desulfovibrio spp. have previously been shown to produce alkanes (Bagaeva and Chernova, 1994; Ladygine, 2006). However, the literature does not provide reliable information regarding which precise strains produce which alkanes. The experiments described below aim to clarify which *Desulfovibrio* strains produce alkanes, and the alkane profile of each alkane producing strain, using stable isotope labelled media components. This information provides the basis for a hypothetical *Desulfovibrio* alkane production pathway.

21 sequenced *Desulfovibrio* strains were cultured in PGB and PGB where 10% of the water was replaced with deuterium oxide (D_2O). Labeling growth media with "heavy water" allowed metabolically produced alkanes to be distinguished from possible contaminants. This distinction was possible due to a marked increase in the 58 ion to 57 ion ratio of metabolically produced alkanes, corresponding to an increase in alkane fragments where deuterium was incorporated. Typical alkane mass spectra give a base peak (most abundant peak) with a mass to charge ratio (m/z) of 57, this represents the high proportion of $^{12}C_4H_9$ fragment ions. Where a deuterium atom is incorporated into this fragment (from metabolism of supplied 10% D_2O PGB), the m/z is 58 due to the additional 1 Dalton mass of deuterium compared to hydrogen. The relative abundance of each different fragment ion may be extracted from a total ion count (TIC) chromatogram trace using ChemStation software, this allows the relative abundance of each fragment ion to be compared to those with a different m/z and to the TIC.

In controls cultured in normal PGB, 58 ion peaks were not more than 6% of the height of the corresponding 57 ion peak. Where *Desulfovibrio* were cultured in 10% D_2O PGB, 58 ion alkane fragment peaks ranged from 20-50% of the height of the corresponding 57 ion peak (Figures 5-11).

This screen identified six *Desulfovibrio* strains that produced alkanes; *D. gabonesis* 10636 (*Dg* 10636), *D. desulfuricans desulfuricans* 8326 (*Dd* 8326), *D. desulfuricans desulfuricans* 8338 (*Dd* 8338), *D. marinus* 18311 (*Dm* 18311), *D. Paquesii* 16681 (*Dp* 16681) and *D. gigas* 9332 (*Dg* 9332).

Following this initial screen, all six alkane producing strains and *Desulfovibrio giganteus* STg 4370 (*Dg* 4370, chosen as a closely related negative control) where cultured in PGB,

10% D_2O PGB and PGB where the lactate was substituted with ^{13}C lactate. Using ^{13}C labelled lactate as the primary carbon source enabled definitive determination of metabolically produced alkanes due to ^{13}C alkanes having a major 61 ion peak not seen in alkanes from cultures with no ^{13}C supplied. The 61 ion peak corresponds to an abundance of $^{13}C_4H_9$ fragment ions from parent alkanes, concluding they are formed from metabolism of ^{13}C lactate. 61 ion peaks are not apparent in alkane analysis of control cultures grown with no exogenous ^{13}C supply due to the minimal probability of 4 naturally occurring ^{13}C atoms combining sequentially.

Overlaid 57 ion ($^{12}C_4H_9$), 58 ion ($^{12}C_4H_8D_1$) and 61 ion ($^{13}C_4H_9$) chromatograms are shown from GC/MSD analysis of alkanes extracted from cultures samples of *Dg* 4370, *Dg* 10636, *Dd* 8338, *Dm* 18311, *Dp* 16681 and *Dg* 9332 (Figures 5-10). Clear 61 ion peaks in chromatograms corresponding to cultures grown in ^{13}C lactate PGB represent alkanes that are true products of *Desulfovibrio* metabolism, as opposed to contamination with 'white oil'. Several, relatively small alkane peaks that were shown to be non-metabolically produced due to having identical fragment ion ratios when grown in all media types were identified in GC/MSD analysis of the non-alkane producing *Dg* 4370. These peaks were attributed to white oil contamination and are labelled as 'wo' in subsequent analysis of alkane producing strains. Alkane extraction of *Dd* 8326 cultures from the ^{13}C lactate experiment was unsuccessful, so chromatograms for this species are taken from the initial screening using only two media types (Figure 11).

Dp 16681 produced only octadecane, *Dg* 10636, *Dd* 8338 and *Dg* 9332 produced octadecane and eicosane, with octadecane being the most abundant product except in *Dg* 9332 where eicosane is more abundant. *Dm* 18311 also produced both octadecane and eicosane as well as being the only alkane producing strain shown to definitively synthesize nonadecane. This varies from previous analysis using deuterium labelled media (10% D_2O PGB) where a small nonadecane peak was also detected in *Dg* 10636. Analysis of *Dd* 8326 cultures showed clear octadecane and eicosane production and a small deuterated nonadecane peak is also seen; however, this is similar to the peak seen in the closely related D*g* 10636 which was deemed a false positive when verified with ^{13}C lactate PGB. It is therefore likely that *Dd* 8326 does not produce nonadecane however this is not definitive.

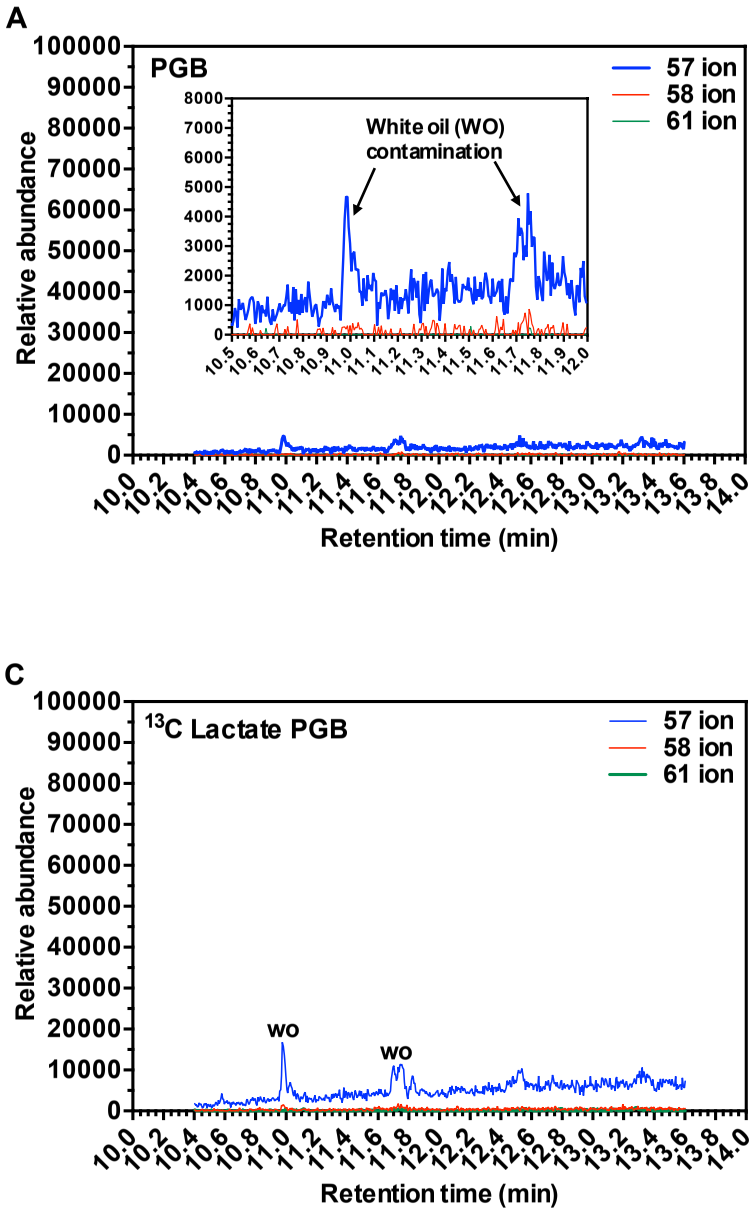

Figure 5. Chromatograms Showing Alkane Production in *Desulfovibrio giganteus STg* 4370

Dg 4370 was cultured in three media types: Post Gate B (PGB, A); 10% D_2O PGB (B); PGB where lactate was replaced with ^{13}C lactate (C). When lactate had been consumed (determined by HPLC analysis), bacteria were harvested by centrifugation. Pellets were washed and freeze-dried overnight and alkanes extracted into dichloromethane prior to GC/MSD analysis. Graphs show overlaid 57 ion (main alkane fragment ion, blue trace), 58 ion (abundance of this alkane fargment ion increases when bacteria are grown in duterium labelled media, red trace) and 61 ion (main alkane fragment ion when bacteria are grown in ^{13}C lactate PGB, green trace) chromatograms. wo indicates white oil contamination.

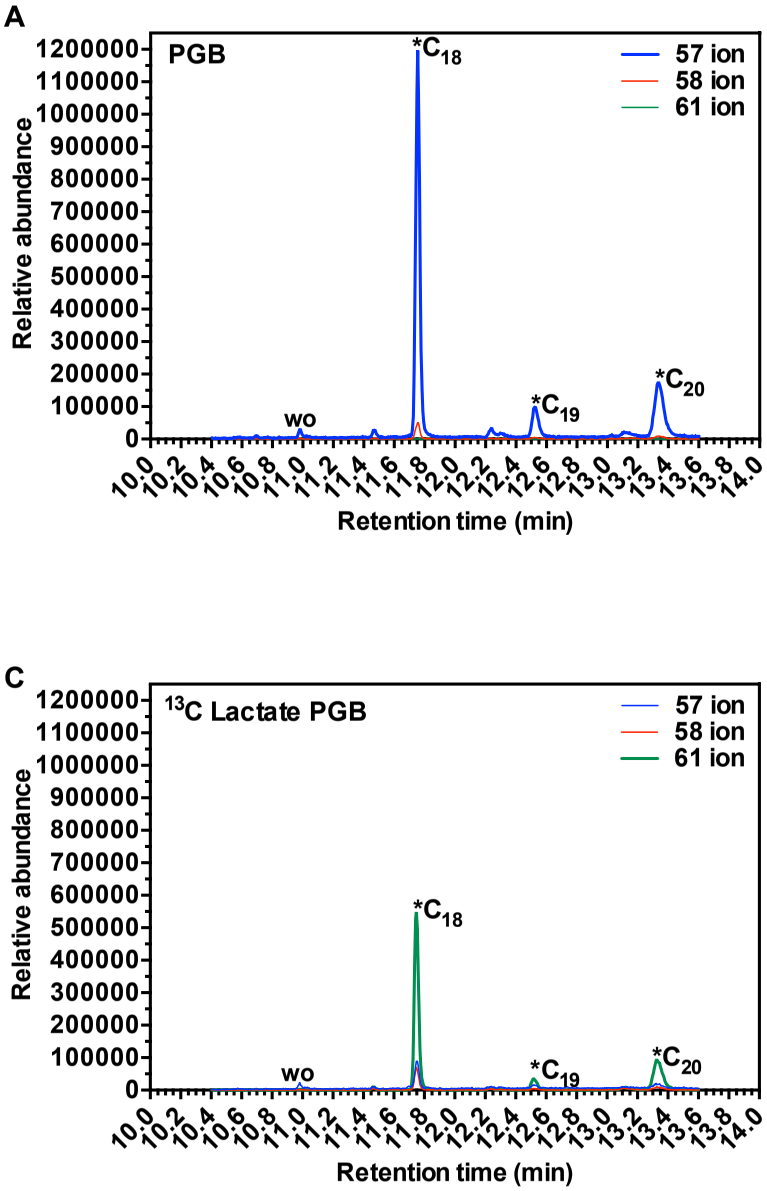

Figure 6. Chromatograms Showing Alkane Production in *Desulfovibrio marinus* 18311

Dm 18311 was cultured in: PGB (A); 10% D_2O PGB (B); PGB where lactate was replaced with ^{13}C lactate (C). When lactate was consumed (determined by HPLC analysis), bacteria were harvested by centrifugation. Pellets were washed and freeze-dried overnight and alkanes extracted into dichloromethane prior to GC/MSD analysis. Graphs show overlaid 57 ion (main alkane fragment ion, blue trace), 58 ion (abundance of this alkane fargment ion increases when bacteria are grown in duterium labelled media, red trace) and 61 ion (main alkane fragment ion when bacteria are grown in ^{13}C lactate PGB, green trace) chromatograms. Peaks labelled with asterisks represent alkanes that are true metabolic products based on the change in ratio of these fragment ions when bacteria were cultured in different media types. wo indicates contamination as seen in negative control.

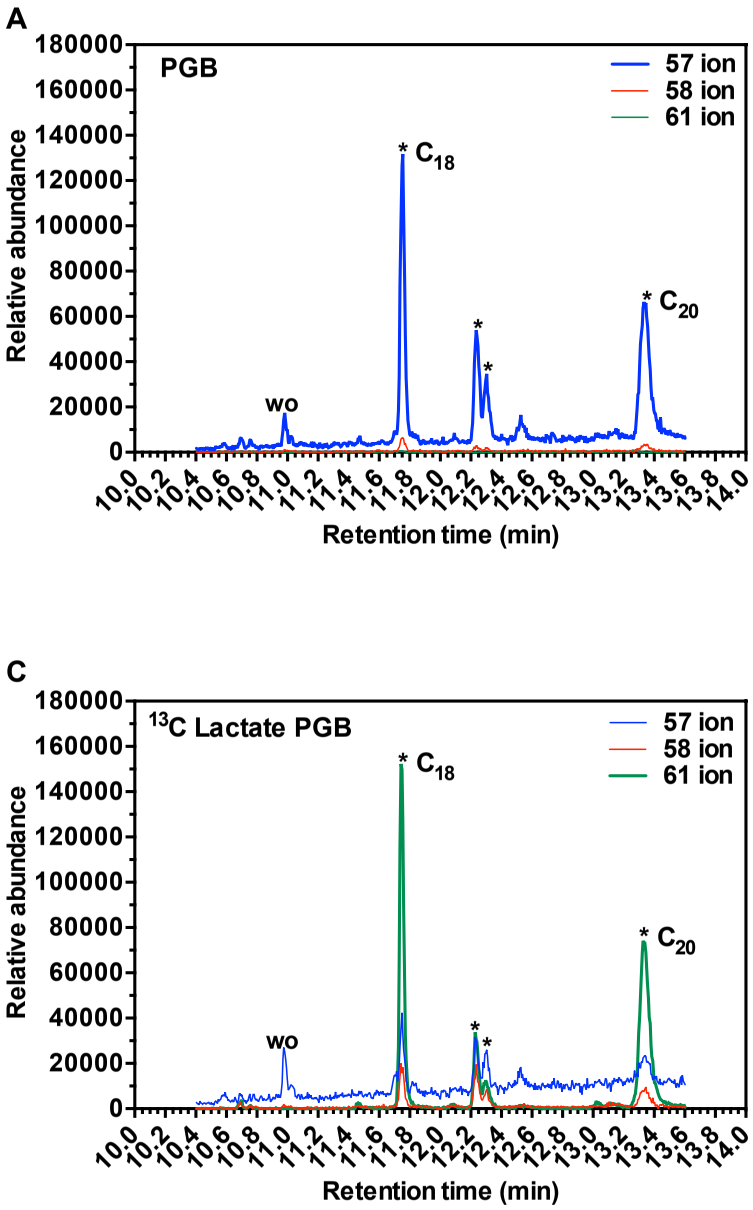

Figure 7. Chromatograms Showing Alkane Production in *Desulfovibrio desulfuricans desulfuricans* 8338

Dd 8338 was cultured in: PGB (A); 10% D_2O PGB (B); PGB where lactate was replaced with ^{13}C lactate (C). When lactate was consumed (determined by HPLC analysis), bacteria were harvested by centrifugation. Pellets were washed and freeze-dried overnight and alkanes extracted into dichloromethane prior to GC/MSD analysis. Graphs show overlaid 57 ion (main alkane fragment ion, blue trace), 58 ion (abundance of this alkane fargment ion increases when bacteria are grown in duterium labelled media, red trace) and 61 ion (main alkane fragment ion when bacteria are grown in ^{13}C lactate PGB, green trace) chromatograms. Peaks labelled with asterisks represent alkanes (when labelled with C_n) or other hydrocarbons that are true metabolic products based on the change in ratio of these fragment ions when bacteria were cultured in different media types. wo indicates contamination as seen in negative control.

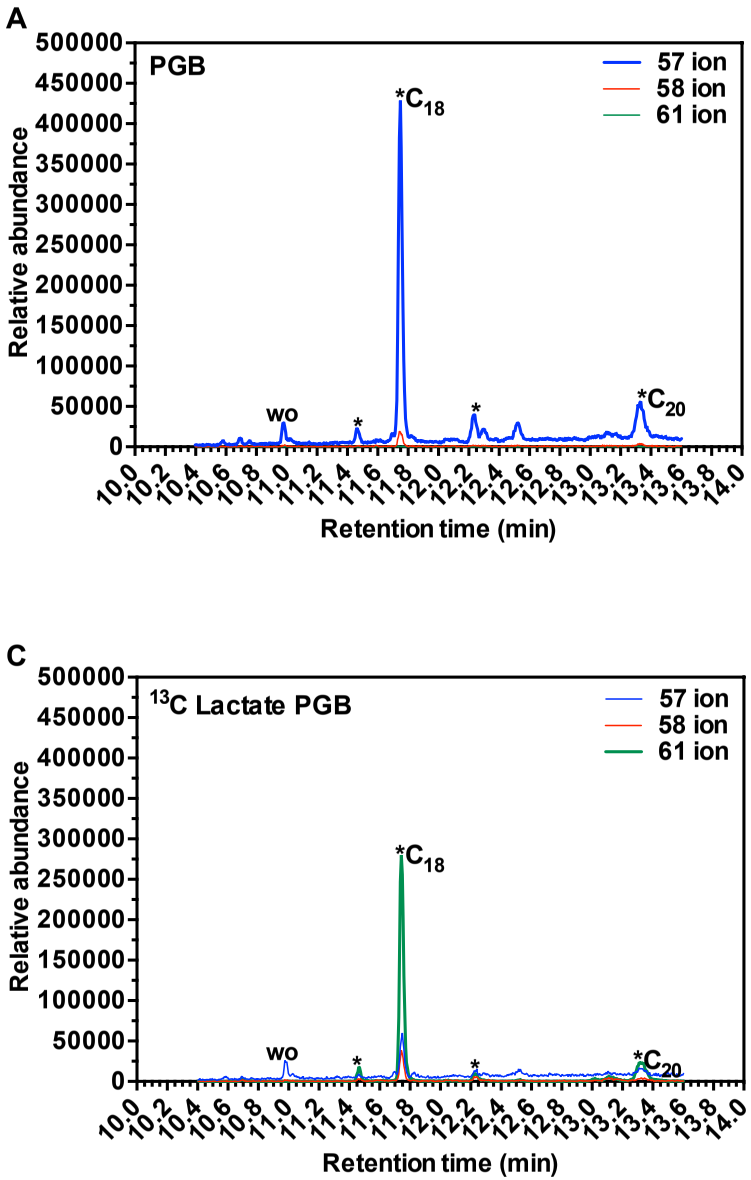

Figure 8. Chromatograms Showing Alkane Production in *Desulfovibrio gabonensis* 10636

Dg 10636 was cultured in: PGB (A); 10% D_2O PGB (B); PGB where lactate was replaced with ^{13}C lactate (C). When lactate was consumed (determined by HPLC analysis), bacteria were harvested by centrifugation. Pellets were washed and freeze-dried overnight and alkanes extracted into dichloromethane prior to GC/MSD analysis. Graphs show overlaid 57 ion (main alkane fragment ion, blue trace), 58 ion (abundance of this alkane fargment ion increases when bacteria are grown in duterium labelled media, red trace) and 61 ion (main alkane fragment ion when bacteria are grown in ^{13}C lactate PGB, green trace) chromatograms. Peaks labelled with asterisks represent alkanes (when labelled with C_n) or other hydrocarbons that are true metabolic products based on the change in ratio of these fragment ions when bacteria were cultured in different media types. wo indicates contamination as seen in negative control.

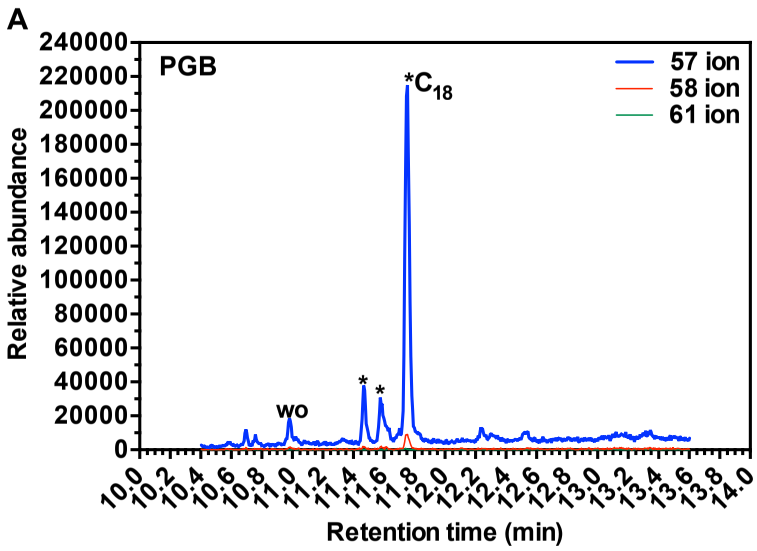

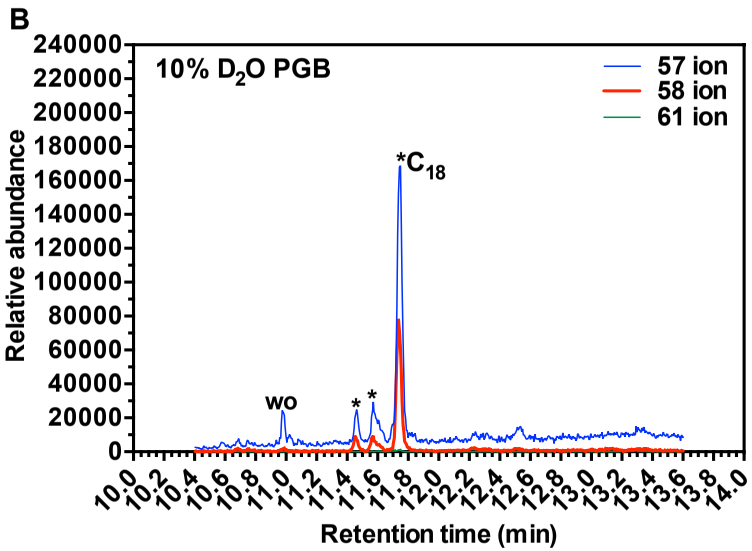

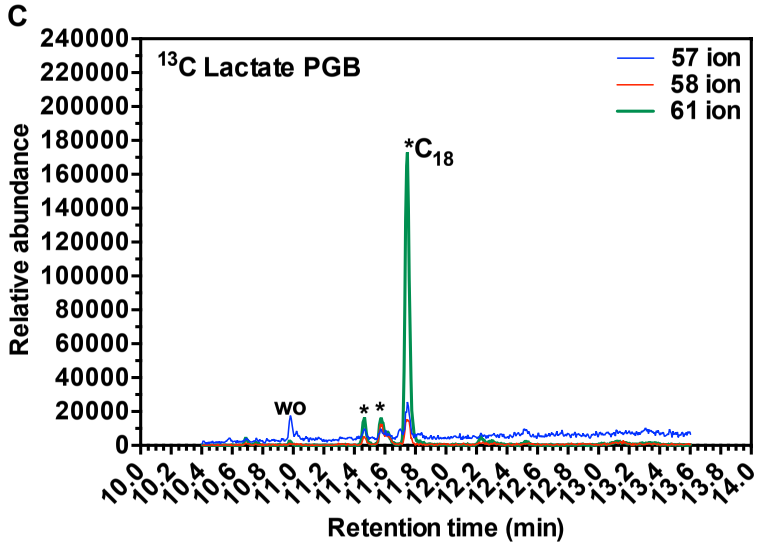

Figure 9. Chromatograms Showing Alkane Production in *Desulfovibrio paquesii* SB1 16681

Dp 16681 was cultured in: PGB (A); 10% D_2O PGB (B); PGB where lactate was replaced with ^{13}C lactate (C). When lactate was consumed (determined by HPLC analysis), bacteria were harvested by centrifugation. Pellets were washed and freeze-dried overnight and alkanes extracted into dichloromethane prior to GC/MSD analysis. Graphs show overlaid 57 ion (main alkane fragment ion, blue trace), 58 ion (abundance of this alkane fargment ion increases when bacteria are grown in duterium labelled media, red trace) and 61 ion (main alkane fragment ion when bacteria are grown in ^{13}C lactate PGB, green trace) chromatograms. Peaks labelled with asterisks represent alkanes (when labelled with C_n) or other hydrocarbons that are true metabolic products based on the change in ratio of these fragment ions when bacteria were cultured in different media types. wo indicates contamination as seen in negative control.

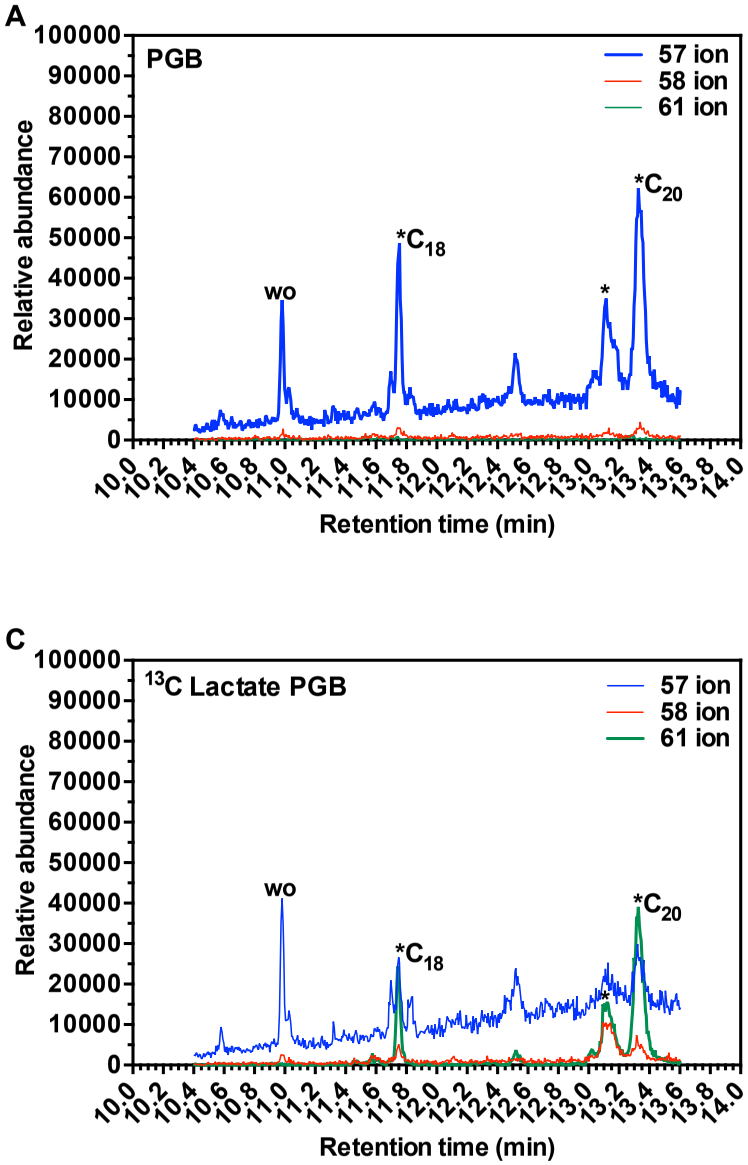

Figure 10. Chromatograms Showing Alkane Production in *Desulfovibrio gigas* 9332

Dg 9332 was cultured in: PGB (A); 10% D_2O PGB (B); PGB where lactate was replaced with ^{13}C lactate (C). When lactate was consumed (determined by HPLC analysis), bacteria were harvested by centrifugation. Pellets were washed and freeze-dried overnight and alkanes extracted into dichloromethane prior to GC/MSD analysis. Graphs show overlaid 57 ion (main alkane fragment ion, blue trace), 58 ion (abundance of this alkane fargment ion increases when bacteria are grown in duterium labelled media, red trace) and 61 ion (main alkane fragment ion when bacteria are grown in ^{13}C lactate PGB, green trace) chromatograms. Peaks labelled with asterisks represent alkanes (when labelled with C_n) or other hydrocarbons that are true metabolic products based on the change in ratio of these fragment ions when bacteria were cultured in different media types. wo indicates contamination as seen in negative control.

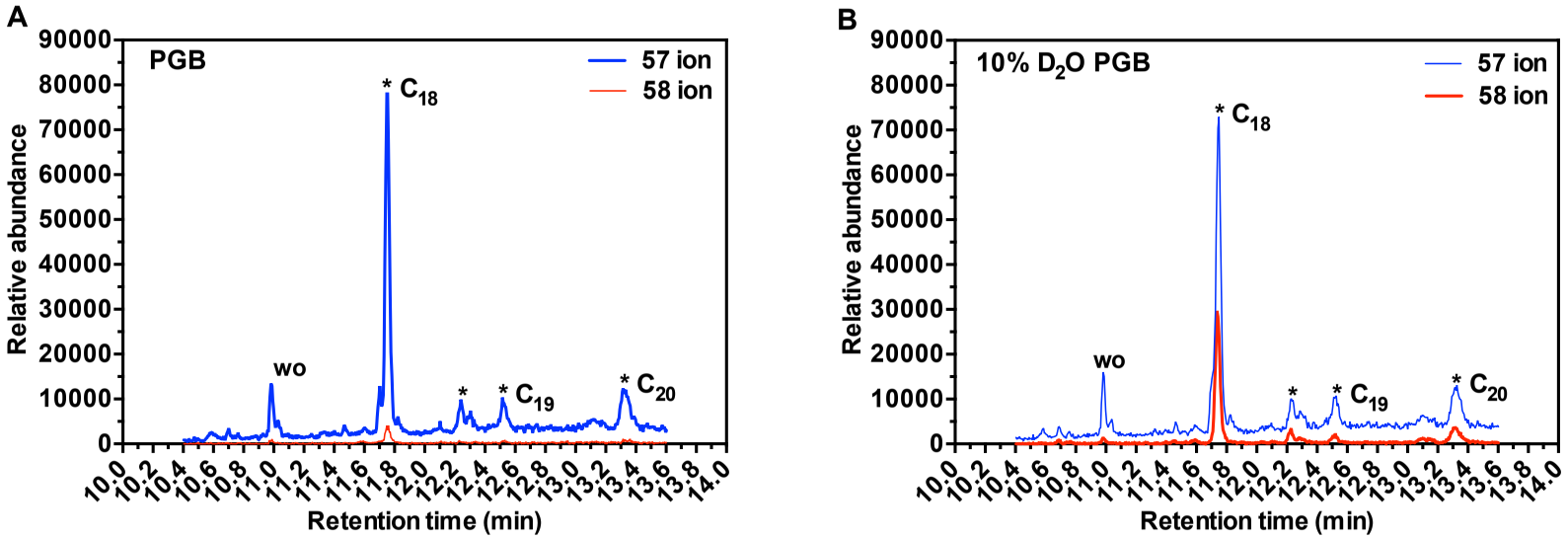

Figure 11. Chromatograms Showing Alkane Production in *Desulfovibrio desulfuricans desulfuricans* 8326

Dd 8326 was cultured in: PGB (A) and 10% D_2O PGB (B). When lactate was consumed (determined by HPLC analysis), bacteria were harvested by centrifugation. Pellets were washed and freeze-dried overnight and alkanes extracted into dichloromethane prior to GC/MSD analysis. Graphs show overlaid 57 ion (main alkane fragment ion, blue trace) and 58 ion (abundance of this alkane fargment ion increases when bacteria are grown in duterium labelled media, red trace) chromatograms. Peaks labelled with asterisks represent alkanes (when labelled with C_n) or other hydrocarbons that are true metabolic products based on the change in ratio of these fragment ions when bacteria were cultured in different media types. wo indicates contamination as seen in negative control.

Figure 12 shows the ratios of 58 ions to 57 ions (A) for each of the 7 *Desulfovibrio* species cultured in 10% D_2O PGB. The greater the 58 ion: 57 ion ratio, the greater the certainty that the peaks at relevant retention times correspond to metabolically produced alkanes. However, due to 58 ion fragments being ubiquitous in relatively small amounts in many hydrocarbon mass spectra, there is a relatively high level of background 'noise' making results from Figure 12 A unclear. In Figure 12 B the 61 ion to 57 ion ratios are shown for 6 of the *Desulfovibrio* species cultured in ^{13}C lactate PGB. As 61 ion fragments are not ubiquitous in the mass spectra of other hydrocarbons and as^{13}C was the primary carbon source in the medium supplied to *Desulfovibrio* in this experiment (as opposed to D_2O making up just 10% of the liquid volume of the medium when 10% D_2O was used), there is much less background 'noise' and the ratio values are much greater allowing more definitive clarification of differences between alkane production in each species.

Results from alkane analysis of all 21 *Desulfovibrio* strains analysed are summarised in Table 1. The relative abundance of alkanes produced by strains positive for alkane production was derived from 61 ion peak heights where cultures were grown in media with ^{13}C lactate as the main carbon source. 61 ion peak height was deemed the most reliable data due to the high likelihood of this specific fragment ion only occurring as the by-product of ionization of a parent ^{13}C alkane. Data for *Dd* 8326 is taken from the initial screen from cultures grown in 10% D_2O PGB media and numbers refer to alkane 57 ion peak height (hydrocarbon extraction of *Dd* 8326 cultures grown in ^{13}C lactate PGB was unsuccessful).

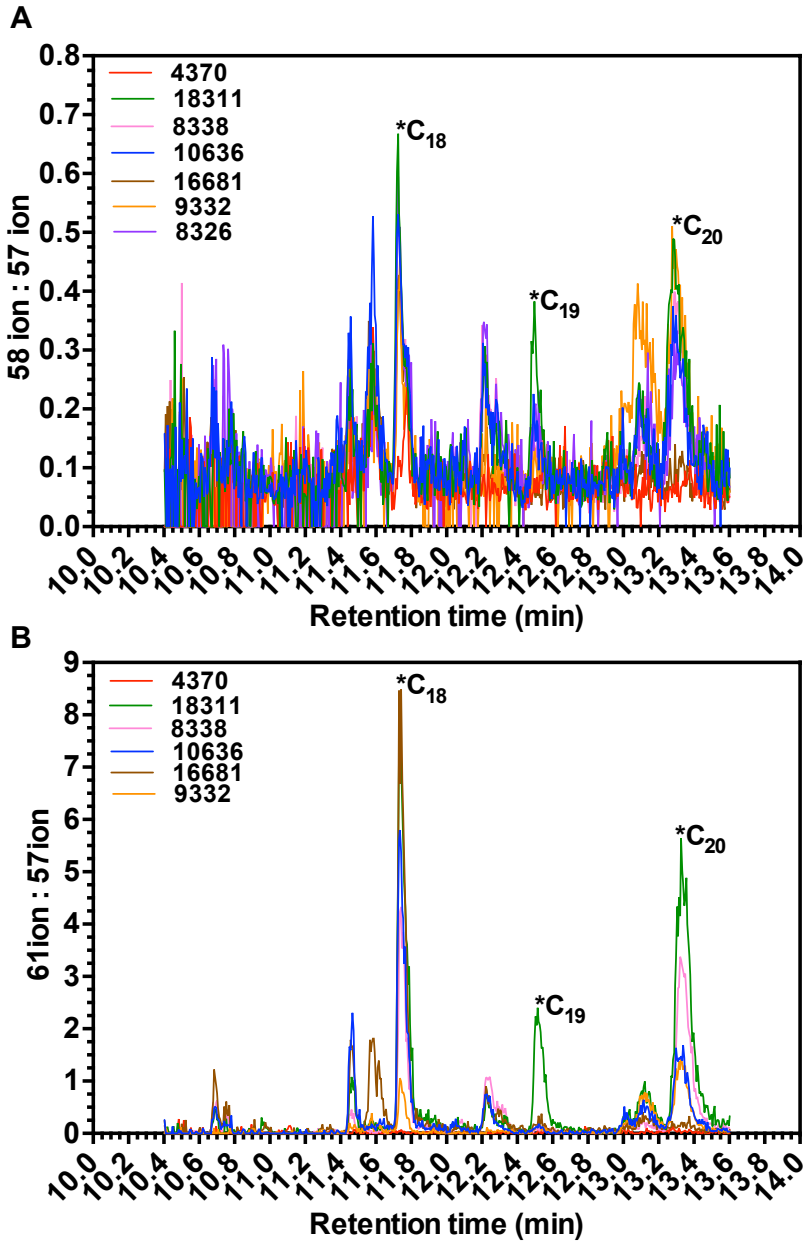

Figure 12. Alkane Fragment Ion Ratios from GC/MSD Analysis of 7 *Desulfovibrio* Species Cultured in Media Supplemented with Stable Isotope Labelled Components

D. giganteus 470 (negative control), *D. marinus* 18311, *D. desulfuricans* 8338, *D. gabonensis* 10636, *D. paquesi* 16681, *D. gigas* 9332 and *D. desulfuricans* 8326 were cultured in modified Post Gate B medium supplemented with 10% D_2O in place of water (A) or ^{13}C lactate in place of ^{12}C lactate (B). Alkanes from each culture were extracted into dichloromethane prior to GC/MSD analysis. Metabolically produced alkanes were determined by quantifying the ratio of 58 ion:57 ion (A) and 61 ion: 57 ion (B) fragments at retention times matched to known external alkane standards. Using ^{13}C lactate as the primary carbon source provided a clearer portrayal of alkane production in each species, compared to using media supplemented with 10% D_2O, due to the greater ratio of stable isotope incorporated fragment ions.

Phylogeny (not to scale)	*Desulfovibrio* species and strain	Culture collection catalogue number (DSM, NCBI, ATTC)	Relative abundance of alkanes (arbitrary units)		
			Octadecane	Nonadecane	Eicosane
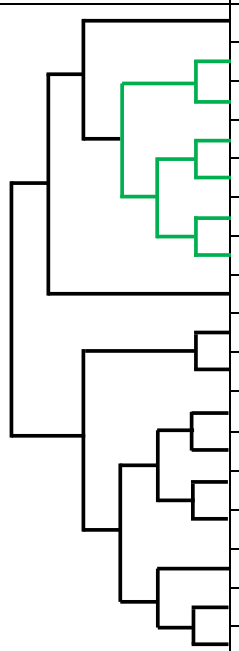	*D. giganteus* STg	4370	0	0	0
	D. paquesii SB1	16681	172992	0	0
	D. gigas	1382, 9332, 19364	25352	0	39120
	D. desulfuricans desulfuricans California27.137.5	8326	*72952	0	*11494
	D. gabonensis	10636	280064	0	18200
	D. desulfuricans desulfuricans CubaHC29.130.4	8338	152256	0	73232
	D. marinus	18311	548736	30512	89704
	D. sp/gigas	496, 12906, 29494	0	0	0
	D. africanus africanus Walvis Bay	8397	0	0	0
	D. africanus africanus Benghazi1	2603	0	0	0
	D. alaskensis G20	17464	0	0	0
	D. alaskensis	16109, 13491	0	0	0
	D. vulgaris Miyazaki F	19637	0	0	0
	D. vulgaris Vulgaris Hildenborough	644, 8308, 29577	0	0	0
	D. piger	749, 29098	0	0	0
	D. desulfuricans desulfuricans MB	12833, 27774	0	0	0
	D. desulfuricans desulfiuricans Essex 6	642, 8307, 29577	0	0	0
	D. desulfuricans aestuarii Sylt3	9335, 29578	0	0	0
	D. alcohoilivorans	5433, 49738	0	0	0
	D. longus	6739, 51456	0	0	0
	D. tunisiensis RB22	19275, 14400	0	0	0

Table 1: Summary of Results from Screening *Desulfovibrio* Strains for Alkane Synthesis

Alkane presence and relative abundance was determined through use of stable isotope labelled media and GC/MSD analysis. Relative abundance values for alkanes were calculated from 61 ion peak heights at the retention times specific to each alkane from *Desulfovibrio* species cultured in PGB medium where ^{13}C lactate was the primary carbon source. Alkane abundance units are arbitrary because no internal standard was used to calculate absolute values. Phylogeny was determined from whole genome comparison (pers comms. P. Dousseaud, 2016). Green branches highlight alkane producing strains. *Data for *Dd* 8326 is taken from the initial screen from cultures grown in 10% D_2O PGB media and numbers refer to alkane 57 ion peak height (hydrocarbon extraction of *Dd* 8326 cultures grown in ^{13}C lactate PGB was unsuccessful).

Following GC/MSD analysis of the six alkane producing *Desulfovibrio* strains a hypothetical alkane synthesis pathway was constructed (Figure 13) based on a series of reduction reactions converting octadecanoic and ecosanoic acids to *n*-alkanes of the same carbon chain length. This hypothesis is based around the fact that long-chain fatty acids produced in bacteria are generally always of an even carbon chain length so to produce even chain length alkanes, such as the octadecane and eicosane produced in *Desulfovibrio*, it is unlikely that a decarbonylation reaction is involved (decarbonylation is integral to alkane production in other micro-organisms). However, this hypothesis does make the assumption that no odd chain length long-chain fatty acids are synthesized in *Desulfovibrio*. Testing this assumption through analysis of the fatty acid profile in *Desulfovibrio* would give further evidence to support this hypothesis.

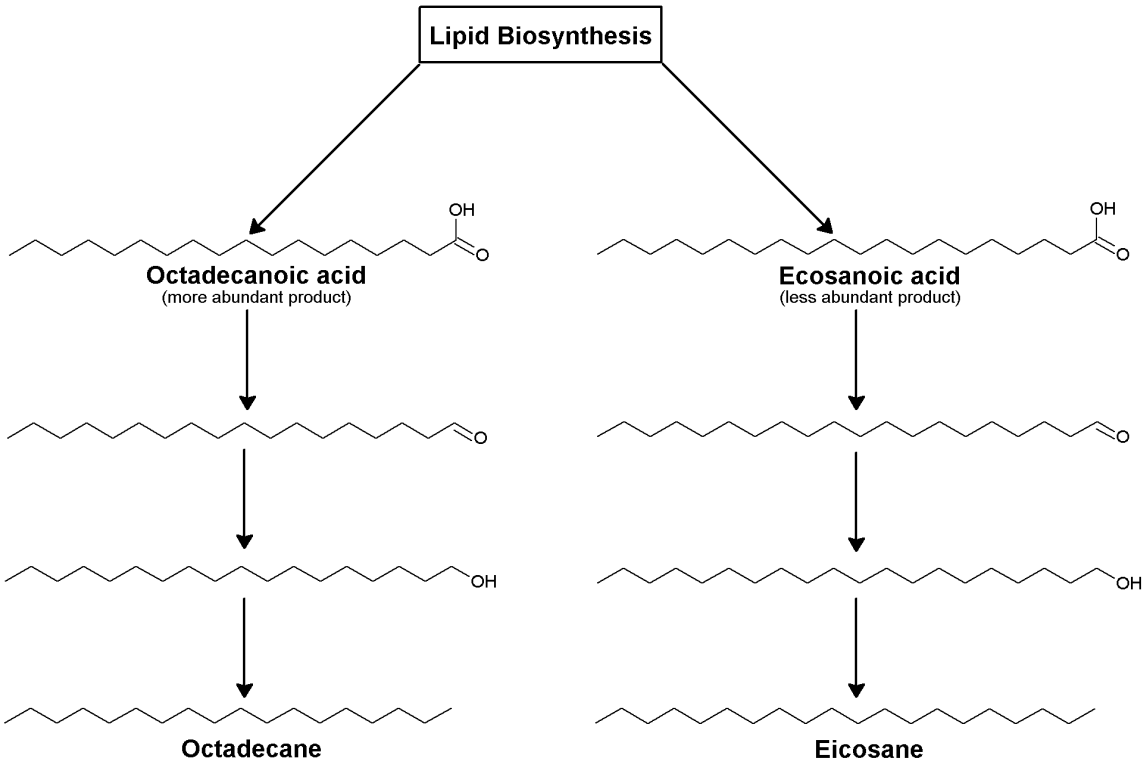

Figure 13. Hypothetical *Desulfovibrio* Alkane Synthesis Pathway

This scheme outlines the proposed *Desulfovibrio* alkane synthesis pathway: a series of reduction reactions whereby octadecanoic and ecosanoic acids are converted to *n*-alkanes with zero carbon loss. As direct alcohol reduction is mechanistically difficult, it is likely that the alcohol group of the precursor fatty acid is activated (possibly via sulfonylation) prior to reduction, This hypothesis is based on GC/MSD analysis of six alkane producing *Desulfovibrio* strains where octadecane and eicosane were the main alkane products. As much less eicosane was produced compared to octadecane in most strains analysed, it is hypothesised that octadecanoic acid is the most abundant long-chain fatty acid present within *Desulfovibrio* cells.

Alternatively, it is possible that octadecane and eicosane are formed from uneven chain length fatty acid precursors via a more conventional decarboxylation reaction, as seen in most alkane producing organisms. However, this scenario seems less likely than the hypothetical pathway illustrated here, due to Shell Biodomain being unable to detect uneven C-chain FAs in *Desulfovibrio* using 2D-GC analysis (Rob. Lee & David Parker, *Pers comm*) and uneven C-chain FAs being scarce throughout nature.

3.2 Growth Kinetics of *Desulfovibrio*

Desulfovibrio growth is typically measured using optical density (Gilmore *et al*., 2011; Meyer *et al*., 2013). Due to the production of black iron sulfide early in the growth cycle, optical density measurements are likely to give an inaccurate representation of growth. Time-course analysis of proteins, alkanes, lactic acid and acetic acid produced (or utilised in the case of lactic acid) by *Dd* 8338 was performed to compare different methods of quantifying growth. A reliable set of *Desulfovibrio* growth data will allow cultures to be incubated for comparable time-frames to achieve an optimal output of desired product (alkanes or proteins) for further analysis in future experiments. This data may also provide a reliable, quantitative measurement to normalise alkane production.

Utilisation of lactic acid and production of acetic acid follow a similar pattern in *Dd* 8338 grown in both PGB and 10% D_2O PGB media types. From HPLC data, clear phases of growth can be estimated (Figure 14). Minimal change in acid concentration between 0 h and 48 h resembles lag phase, a sharp rise/decrease in concentration between 48 h and 108 h indicates exponential phase and a plateau between 108 h and 264 h suggests stationary phase. Measurements of lactic acid and acetic acid are not definitive measurements of growth but they do provide a simple and replicable method of determining when the main carbon source has been utilised, which is related to growth of the bacteria.

In a separate experiment, lactic acid consumption and acetic acid production in the five other alkane producing *Desulfovibrio* strains was monitored over an 8-day period (Figure 15). The length of lag phase varied between strains, lasting between 48 h and 120 h post inoculation, with exponential phase lasting between 48 h and 72 h.

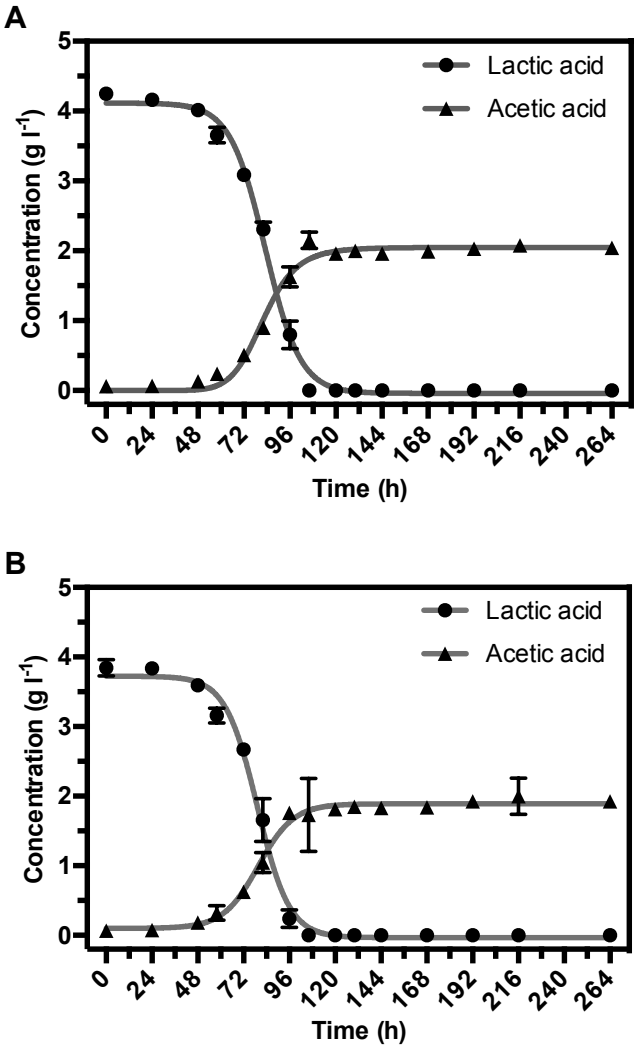

Figure 14. Change in Lactic Acid and Acetic Acid Concentrations Over 11 Days in *Desulfovibrio* d*esulfuricans desulfuricans* 8338 cultures

Dd 8338 was cultured in PGB (A) and PGB where 10% of the water was replaced with D_2O (B). 1 ml samples were taken from 3 biological replicates of *Dd* 8338 cultured in each media type at regular intervals over a 264 h period. 200 μl of clarified supernatant from each sample was transfered into a glass vial and samples analysed using high performace liquid chromatography (HPLC). Concentrations of lactic acid and acetic acid in each sample were quantified against known standards. Error bars represent +/- 1 standard error, n=3. Where error bars cannot be seen they are covered by the symbol. Trend-lines represent nonlinear regression of each data set (curve fit).

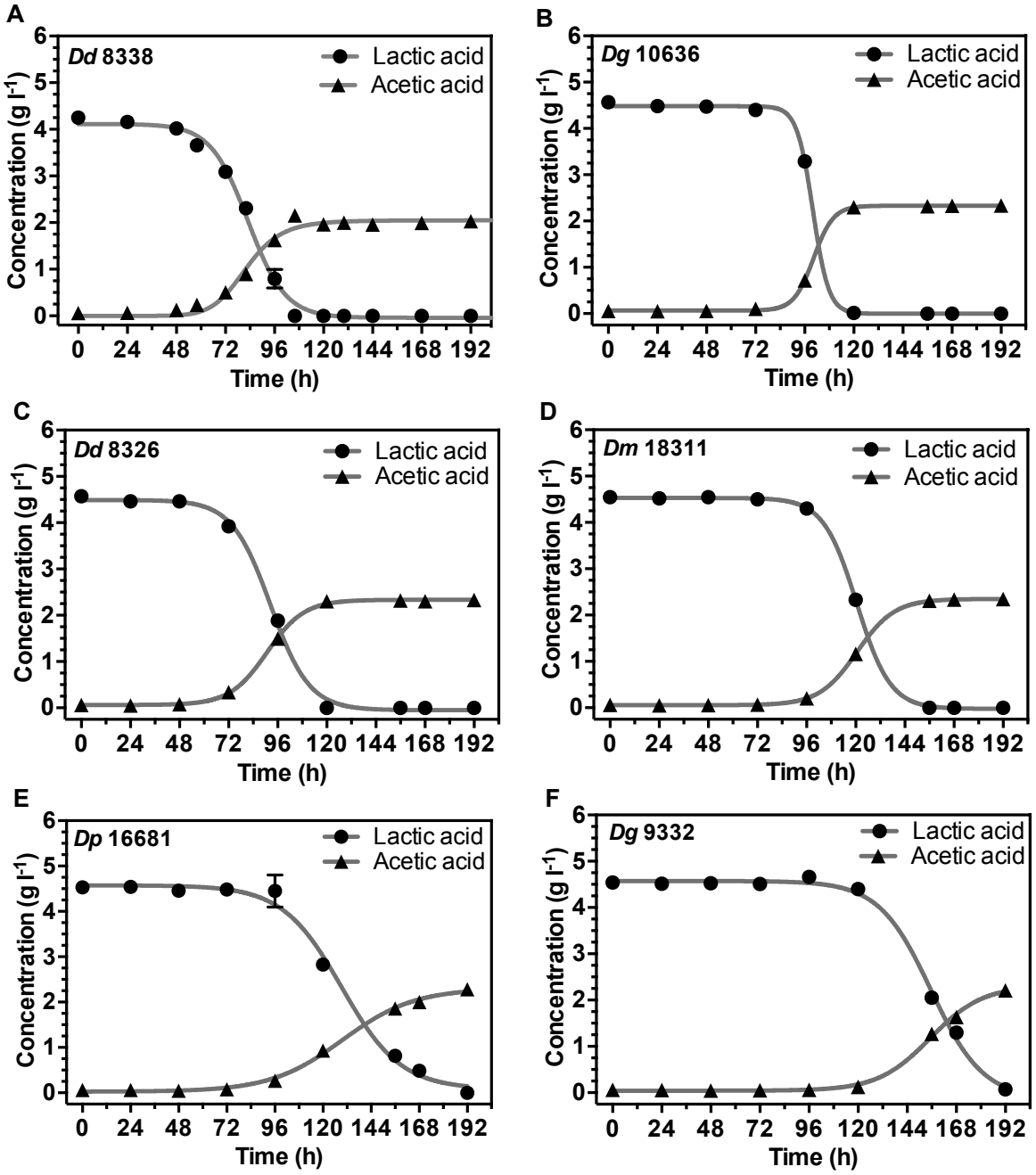

Figure 15. Change in Lactic Acid and Acetic Acid Concentration in Alkane Producing *Desulfovibrio* Strains over an 8 Day Period

Dd 8338 (A – this graph is taken from figure 14 and time-scale adjusted to be comparable to other graphs shown here) *Dg* 10636 (B), *Dd* 8326 (C), *Dm* 18311 (D), *Dp* 16681 (E) and *Dg* 9332 (F) were cultured in PGB medium for 8 days. 1 ml samples were taken from 2 biological replicates of each strain at 24 h intervals. 200 μl of clarified supernatant from each sample was transferred into a glass vial and samples analysed using high performance liquid chromatography (HPLC). Concentration of lactic acid and acetic acid in each sample were quantified against known standards. Error bars represent +/- 1 standard error, n=2 (except A where n=3). Where error bars cannot be seen they are covered by the symbol. Trend-lines represent nonlinear regression of each data set (curve fit).

Protein concentrations of clarified *Dd 8338* lysates were analysed using a Qubit® 2.O Fluorometer (Qubit, Figure 16). The trend in *Dd* 8338 lysate protein concentration over a 264 h period is similar for *Dd* 8338 grown in both media types, however lysates from bacteria cultured in 10% D_2O PGB have greater mean protein concentrations throughout the time-course. Phases of growth are less clearly defined from protein concentration data than from analysis of lactic acid and acetic acid. Protein concentration rises steadily between 0 h and 96 h, remains fairly constant until 120 h at which point it begins to decline.

To gain a visual representation of protein concentrations to compare against Qubit readings, as well as gain further information on the protein profile of *Dd* 8338, cell lysate samples from each time-point were analysed using SDS-PAGE (Figure 17).

Protein band intensities were in the most part consistent with Qubit protein measurements. The highest band intensities are seen in lanes corresponding to *Dd* 8338 cell lysate taken from cultures 96 h and 106 h post inoculation for cultures grown in both media types. This is concurrent with Qubit measurements and with acetic acid production which peaks at approximately 108 h. However, band intensities of these SDS-PAGE gels are not accurate representations of protein concentration due to silver staining giving saturated band intestines above a certain protein concentration.

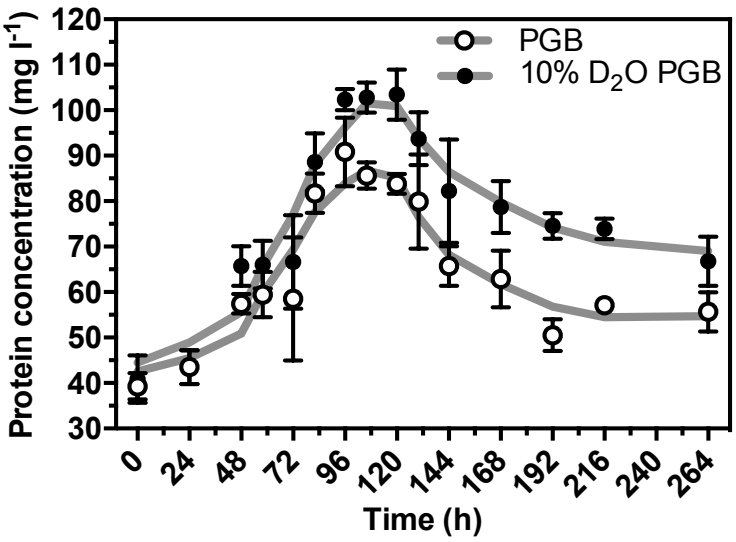

Figure 16. Protein Concentrations from *Desulfovibrio desulfuricans desulfuricans* 8338 Cell Lysate Analysed Using a Quibit 2.0 Fluorometer

Dd 8338 was cultured in PGB and PGB where 10% of the water was replaced with D_2O. 10 ml samples were taken from cultures at regular intervals over a 264 h period, and bacteria harvested by centrifugation. Pellets were resuspended in PBS and cells lysed by freeze-thaw. Protein concentration of clarified cell lysate was quantified using a Qubit 2.0 fluorometer. Error bars represent +/- 1 standard error, n=3. Curved trend-lnes represent 4th order smoothing of the data points.

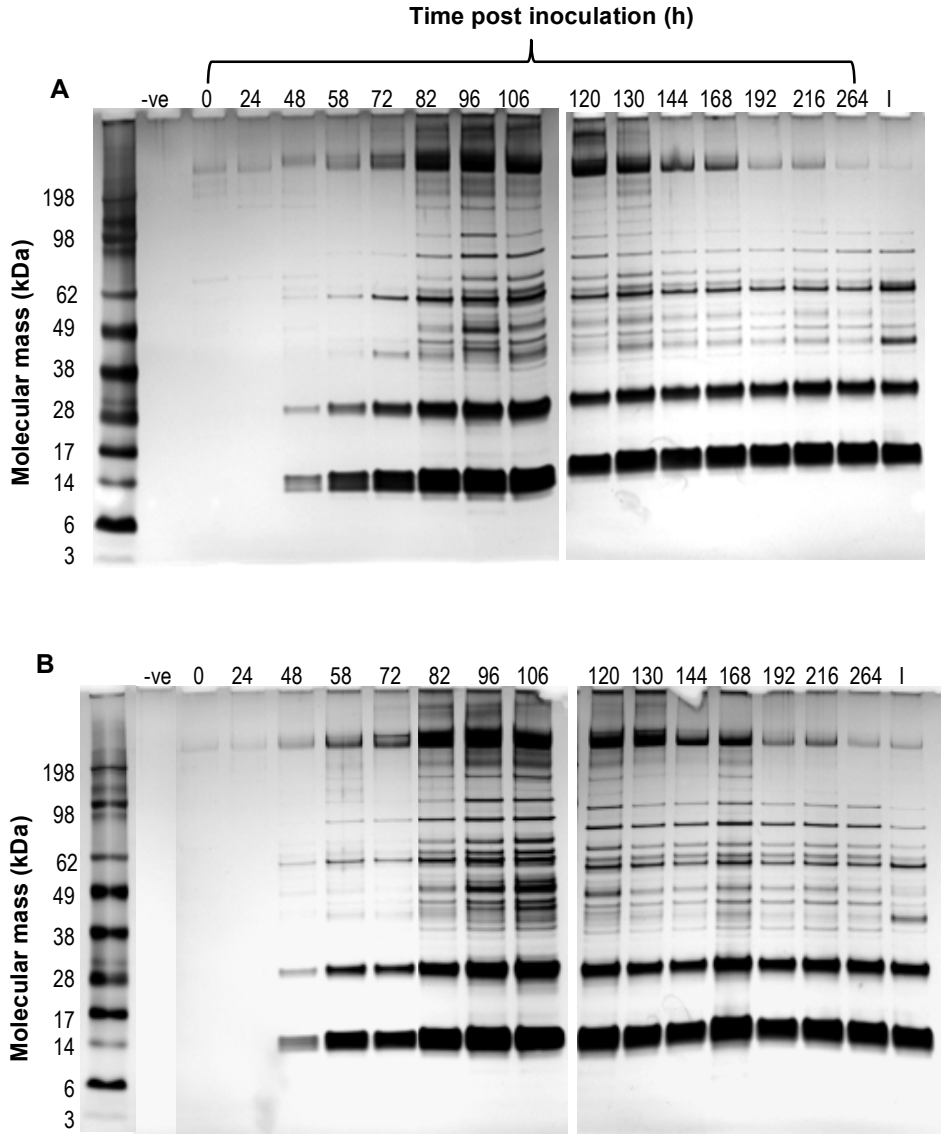

Figure 17. SDS-PAGE Gel Images of Time-Course Cell Lysate Samples from *Desulfovibrio desulfuricans desulfuricans* 8338

Images of SDS-PAGE gels run with lysate of samples from *Dd* 8338 cultured in PGB (A) and 10% D_2O PGB (B). Clarified cell lysates were combined with LDS sample buffer and reducing agent (Bolt, Novex, Life Technologies) and incubated (10 min, 70 °C) before being loaded into 4-12% Bis-Tris pre-cast SDS-PAGE mini gels and run at 165 V for 35 min. Ladder used was SeeBluePlus2 pre-stained protein ladder (Novex, Life Technologies). Gels were stained with Pierce silver stain kit according to the manufacturer's protocol. Well labels indicate time (h) cultures were incubated for before samples were taken. The negative control used (-ve) was blank media and 'I' refers to cell lysate prepared from the inoculum culture.

The change in relative abundance of octadecane and eicosane over an 11 day time-course was analysed (Figure 18). Production of both alkanes increases rapidly between 60 h and 96 h, in-line with exponential growth phase estimated from HPLC analysis of lactic acid and acetic acid. Alkane production continued to steadily increase until the final time point at 264 h, unlike other metabolites measured which plateaued or decreased after 120 h. Relative abundance of octadecane and eicosane is lower in *Dd* 8338 cultured in 10% D_2O PGB compared to *Dd* 8338 cultured in PGB. In both media types *Dd* 8338 produces eicosane at a slower rate than octadecane.

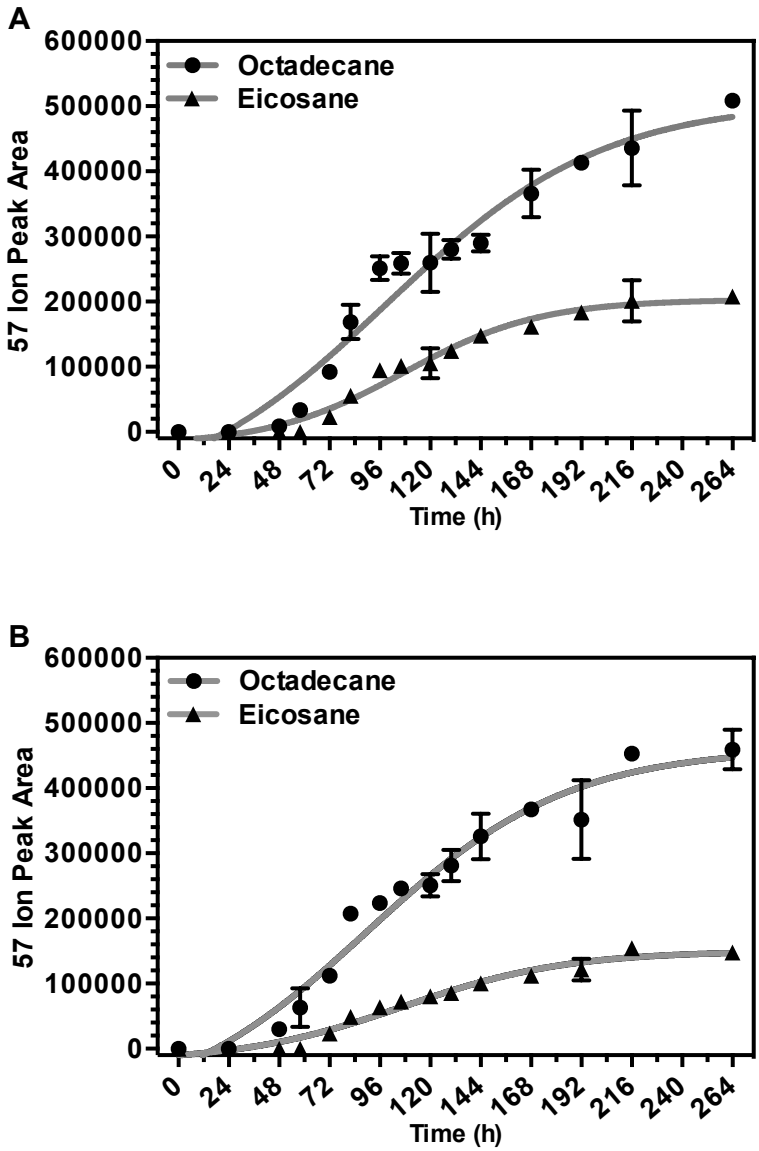

Figure 18. Relative Abundance of Ocatdecane and Eicosane over an 11 Day Time-Course in *Desulofvibrio desulfuricans desulfuricans* 8338 Cultures

Dd 8338 was cultured in PGB (A) and PGB where 10% of the water was replaced with D_2O (B). 35 ml culture samples were taken at 12 h or 24 h intervals over a 264 h period and bacteria harvested by centrifugation. Pellets were freeze-dried and alkanes extracted into DCM. Alkane pofiles were analysed using GC/MSD, enabling the 57 ion peak area of ocatdecane and eicosane to be calculated. Error bars represent +/- 1 SE, n=3. Where error bars cannot be seen they are covered by the symbol. The curved lines represent nonlinear fit regressions of each data set (curve fit).

3.3 Effect of Exogenously Supplied Hydrocarbons on Alkane Production

This experiment aimed to identify hydrocarbons that affected alkane synthesis in *Dd* 8338 cultures to which they were exogenously supplied. Hydrocarbons that have a significant affect on alkane synthesis may be potential substrates or inhibitors of the alkane forming enzyme(s). This line of experimentation was conceived from the observation that crystal structures of hydrocarbon forming enzymes, for example aldehyde deformalating oxygenase (ADO, Schirmer *et al*., 2010) contain bound fatty acid substrates in the hydrophobic pocket. Also it appears that the release of the alkane products is relatively slow (Schirmer *et al*., 2010) therefore, supplying an abundance of long chain hydrocarbons to alkane forming enzymes may interfere sufficiently with substrate affinity to guide enzyme identification. A candidate compound could be used to further investigate the *Desulfovibrio* alkane synthesis pathway, for example, by using a radioisotope labelled version of the compound to follow progression of alkane synthesis and uncover intermediate metabolites in the alkane synthesis pathway.

In a pilot experiment, *Dd* 8338 cultures were exposed to eight exogenously supplied hydrocarbons: 1-tetradecanol, 2-tetradecanol, 3-tetradecanone, 1-hexadecanol, 2-hexadecanol, 2-hexadecanone, 3-hexadecanone and 1-octadecanol. 1-octadecanol was hypothesized to be the most likely substrate for alkane synthesis in *Dd* 8338, due to being the fatty alcohol precursor of octadecane (the major alkane produced in *Dd* 8338) in the hypothesized reductive pathway.

The effect compounds had on alkane production in *Dd* 8338 was determined through GC/MSD analysis of samples and comparison with control cultures exposed to no exogenous hydrocarbons. All *Dd* 8338 were cultured in 10% D_2O PGB so metabolically produced alkanes could be clearly identified and their abundance measured. Change in abundance of C_{18} and C_{20} alkanes produced was analysed (Figure 19) as well as the ratio of 58:57 ion peak heights for these alkanes, a shift in which may indicate incorporation of the non-deuterated compound (or a fragment thereof) into the deuterated alkane product (Figure 19).

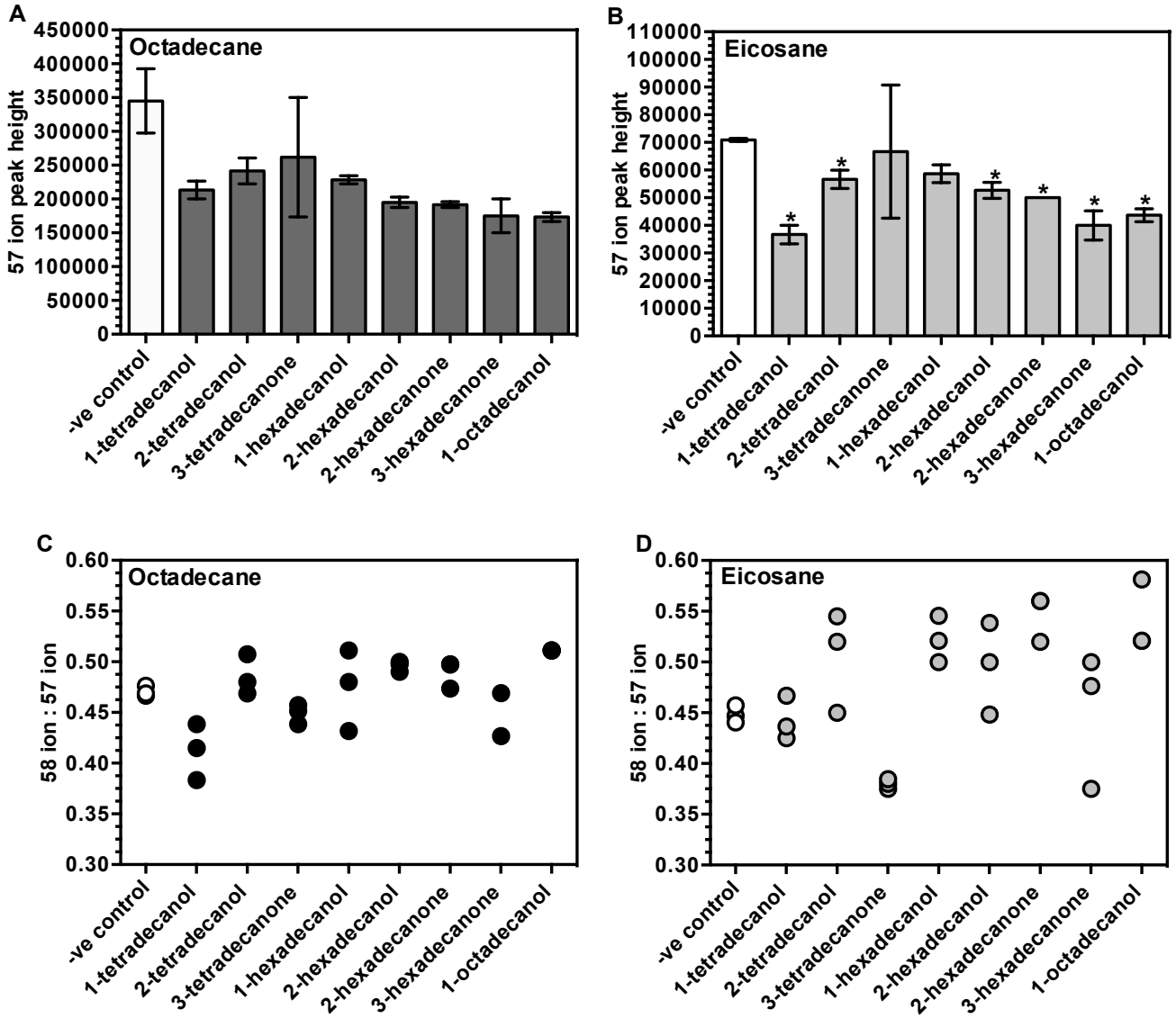

Fig 19. Effect of Exogenously Supplied Hydrocarbons on Alkane Synthesis in *Desulfovibrio desulfuricans desulfuricans* 8338

Octadecane (A) and eicosane (B) 57 ion peaks heights and ratio of 58 ion:57 ion octadecane (C) and eicosane (D) peak heights from GCMS analysis of samples taken from *Dd* 8338 cultured in the presence of 0.5 mmol of the stated hydrocarbon. The negative control was *Dd* 8338 cultured with no external hydrocarbon exposure. 0.5 mmol of each hydrocarbon was used to coat the inside of Falcon tubes in which *Dd* 8338 was cultured. Following 14 days incubation, alkanes were extracted from cultures using dichloromethane and alkane content analysed using GC/MSD. Error bars (A and B) represent +/- 1 standard error, n=3. Asterisks highlight data significantly different from control data ($P<0.05$). In C and D all data points are shown as values correspond to ratios making mean and error calculations inappropriate.

Paired T-Tests were performed on data for alkane 57 ion peak heights to analyse the statistical significance of results compared to controls (all P values are two-tailed and statistically significant is defined here as having a P value < 0.05). Data sets where values correspond to ratios were not analysed statistically in this experiment due to difficulty of correct error propagation.

Analysis of data from the pilot experiment (Figure 19) gave no significant differences between octadecane production in *Dd* 8338 cultures grown in the presence of exogenous hydrocarbons compared to control cultures. However, cultures supplied the following compounds produced significantly less eicosane than control cultures based on the 57 ion peak height (p values are shown in brackets): 1-tetradecanol (0.0126); 2-tetradecanol (0.0424); 2-hexadecanol (0.0176); 2-hexadecanone (0.0007); 3-hexadecanone (0.0266); 1-octadecanol (0.0086).

Analysis of difference in 58:57 ion peak height ratios between cultures exposed to exogenous hydrocarbons and control cultures was difficult to analyse statistically due to the data being ratios. An increase in 58:57 ion ratio was not expected as no additional deuterium was provided from the exogenous hydrocarbons, however a marked increase in eicosane 58:57 ion peak ratio was seen in cultures supplied 1-hexadecanol, 2-hexadecaneone and 1-octadecanol. A decrease in 58:57 ion ratio may point to incorporation of part of the non-deuterated compound into the alkane product which would result in a greater abundance of C_4H_9 (57 ion) fragments and reduce the abundance of $C_4H_8D_1$ (58 ion) fragments produced from metabolism of the 10% deuterated media. Such a decrease in the 58:57 ion ratio was only seen for eicosane produced by cultures of *Dd* 8338 supplied exogenous 3-tetradecanone.

The hydrocarbon screen was repeated with selected compounds and alkane abundance normalised to protein concentration to increase comparability of results (Figure 20). No marked difference was observed between controls and sample cultures when octadecane abundance was normalised to protein concentration, consistent with 57 ion peak height results from the pilot screen. Eicosane abundance normalised to protein concentration was consistently less than controls in *Dd* 8338 exposed to exogenous 1-tetradecanol. From this data the most likely inhibitor to alkane production in *Dd* 8338 was 1-tetradecanol, however reduction in eicosane abundance was the only consistent outcome.

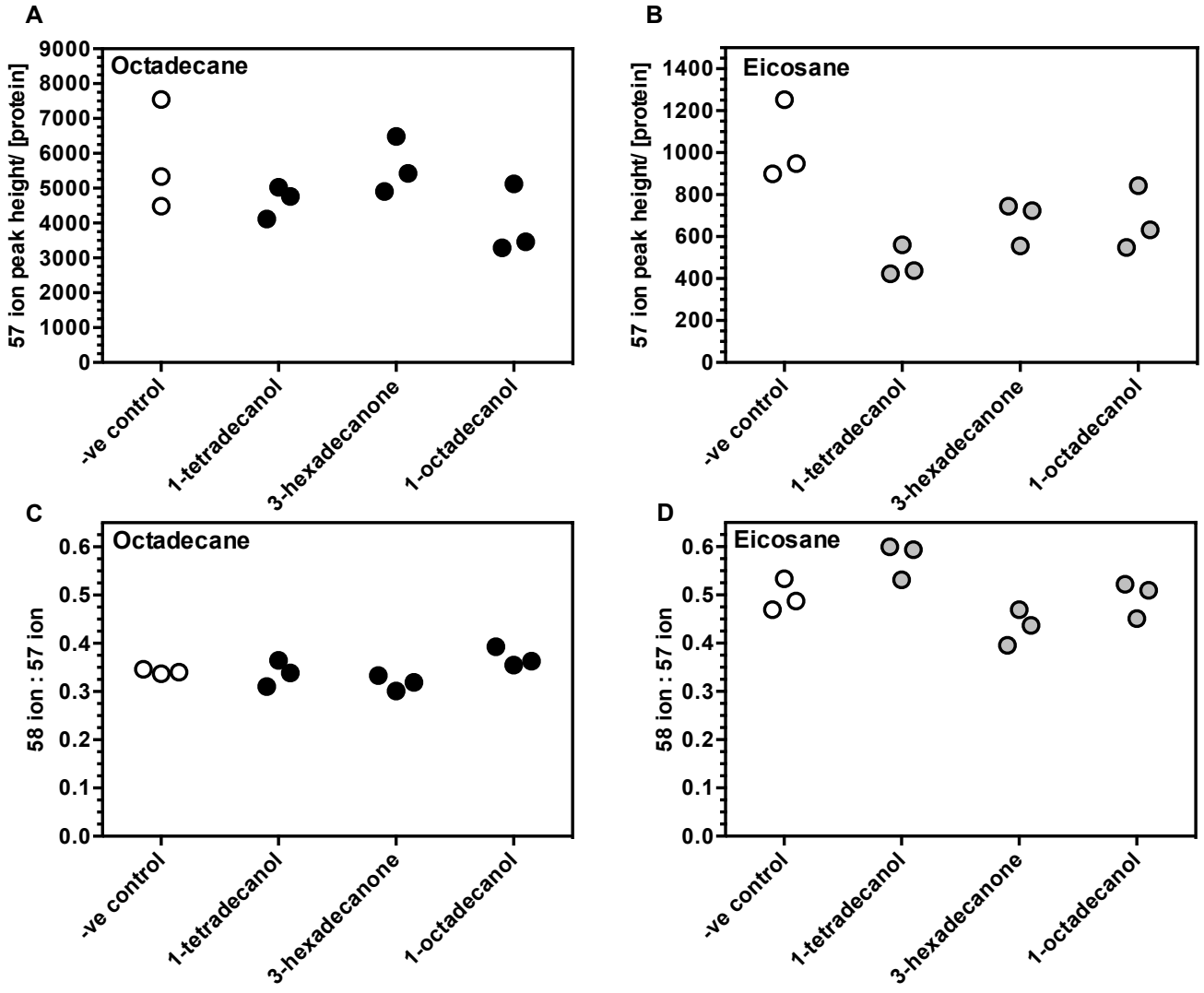

Fig 20. Effect of Exogenously Supplied Hydrocarbons on Alkane Synthesis in *Desulfovibrio desulfuricans desulfuricans* 8338 - Repeats from Initial Experiment

Octadecane (A) and eicosane (B) 57 ion peaks heights normalised to cell lysate protein concentrations, and ratio of 58:57 ion peak heights for octadecane (C) and eicosane (D) from GC/MSD analysis of samples taken from *Dd* 8338 cultured in the presence of 0.5 mmol of the stated hydrocarbon. The negative controls were *Dd* 8338 cultured with no external hydrocarbon exposure. 0.5 mmol of each hydrocarbon was used to coat the inside of Falcon tubes in which *Dd* 8338 was cultured. Following 14 days incubation, alkanes were extracted from cultures using dichloromethane and alkane content analysed using GC/MSD. All data points are shown, as values correspond to ratios making mean and error calculations inappropriate.

Effect of Exogenously Supplied Deuterated Hydrocarbons on Alkane Synthesis

Dd 8338 cultures were exposed to nine fully deuterated hydrocarbons with the aim of identifying potential substrates or inhibitors to the alkane synthesis pathway. Although there is some overlap, it was not possible to obtain the deuterated form of all of the hydrocarbons used in the previous screen. However, with only 1-tetradecanol showing a significant effect on alkane synthesis, it was deemed appropriate to perform this experiment with a slightly different range of hydrocarbons: tridecane d28, 1-tridecanol d27, tetradecane d30, 1-tetradecanol d29, hexadecane d34, 1-hexadecanol d33, heptadecane d36, octadecane d38 and 1-octadecanol d37.

After 21 days incubation, HPLC analysis of clarified culture supernatant showed cultures had utilised all lactic acid provided in the growth media and had likely reached stationary phase of growth. This suggests exposure to these 9 different deuterated hydrocarbons had no marked effect on primary metabolism of the bacteria, or that the bacteria were not sufficiently exposed to the hydrocarbons for a change in metabolism to be apparent.

Analysis of GC/MSD data from the pilot screen of deuterated hydrocarbons (Figure 21 A and B), using paired T-tests, showed most compounds tested produced significantly different amounts of octadecane (based on 57 ion peak height) compared to controls. *Dd* 8338 cultures supplied the following deuterated compounds produced significantly less octadecane compared to controls cultured in deuterium depleted PGB (Dd PGB, P values in brackets): tridecane d28 (0.0204); 1-tridecanol d27 (0.0016); tetradecane d30 (0.0357); hexadecane d34 (0.0104); heptadecane d36 (0.0246) and 1-octadecanol d37 (0.0019). Significantly greater octadecane abundance was observed in cultures supplied 1-hexadecanol d33 (0.0467) compared to controls. However, cultures supplied most deuterated hydrocarbons produced significantly greater amounts of octadecane when compared to controls cultured in 10% D_2O PGB (all sample cultures were grown in Dd PGB) except for cultures supplied tridecane, where no significant difference was seen, and cultures supplied 1-tetradecanol d27 and hexadecane d34 which both produced significantly less octadecane.

Desulfovibrio cultures exposed to tridecane d28 (0.0146), tetradecane d30 (0.0057) and hexadecane d34 (0.0034) produced significantly less eicosane than controls cultured in Dd PGB. When compared to controls cultured in 10% D_2O PGB, eicosane abundance

was only significantly less in cultures exposed to hexadecane d34 (0.0444) and significantly greater in cultures exposed to heptadecane d36 (0.0129).

The deuterated hydrocarbon screen was repeated with selected compounds and alkane abundance normalised to protein concentration to increase the comparability of results (Figure 21 C and D). When octadecane abundance was normalised to protein concentration, none of the sample cultures produced consistently less octadecane compared to either controls cultured in Dd PGB or 10% D_2O PGB. A marked increase in octadecane and eicosane abundance was seen in cultures supplied 1-tetradecanol d29 compared to both Dd PGB and 10% D_2O control cultures.

Using 99.9% deuterated compounds enabled any incorporation of these compounds into alkane products to be easily observed in the corresponding GC/MSD data. Incorporation of a fully deuterated compound into the alkane synthesis pathway would yield a reduced abundance of 57 ions (C_4H_9 fragments) in the corresponding alkane product and a greater abundance of 66 ions (C_4D_9 fragments). The 66-ion chromatograms from GC/MSD analysis of this screen were mainly noise; no visible differences were observed in 66-ion peak heights in chromatograms corresponding to cultures supplied deuterated compounds, compared to chromatograms from control cultures. These data are omitted due to insignificance.

From the screen of deuterated compounds only tetradecane d30 had a consistently significant inhibitory effect on eicosane production in *Dd* 8338 compared to controls cultured in Dd PGB. Combing data from both screens, two compounds, 1-tetradecanol and tetradecane d30, were identified that may be of interest due to their potential inhibitory effect on alkane synthesis in *Dd* 8338. However, with the fully deuterated version of 1-tetradecanol increasing alkane production in the deuterated screen, this brings into question the reliability of this result. Furthermore, neither compound had a consistent significant effect on octadecane production, and as this is the major hydrocarbon product in *Dd* 8338, this also reduces the usefulness of these findings. For these reasons this line of experimentation was discontinued.

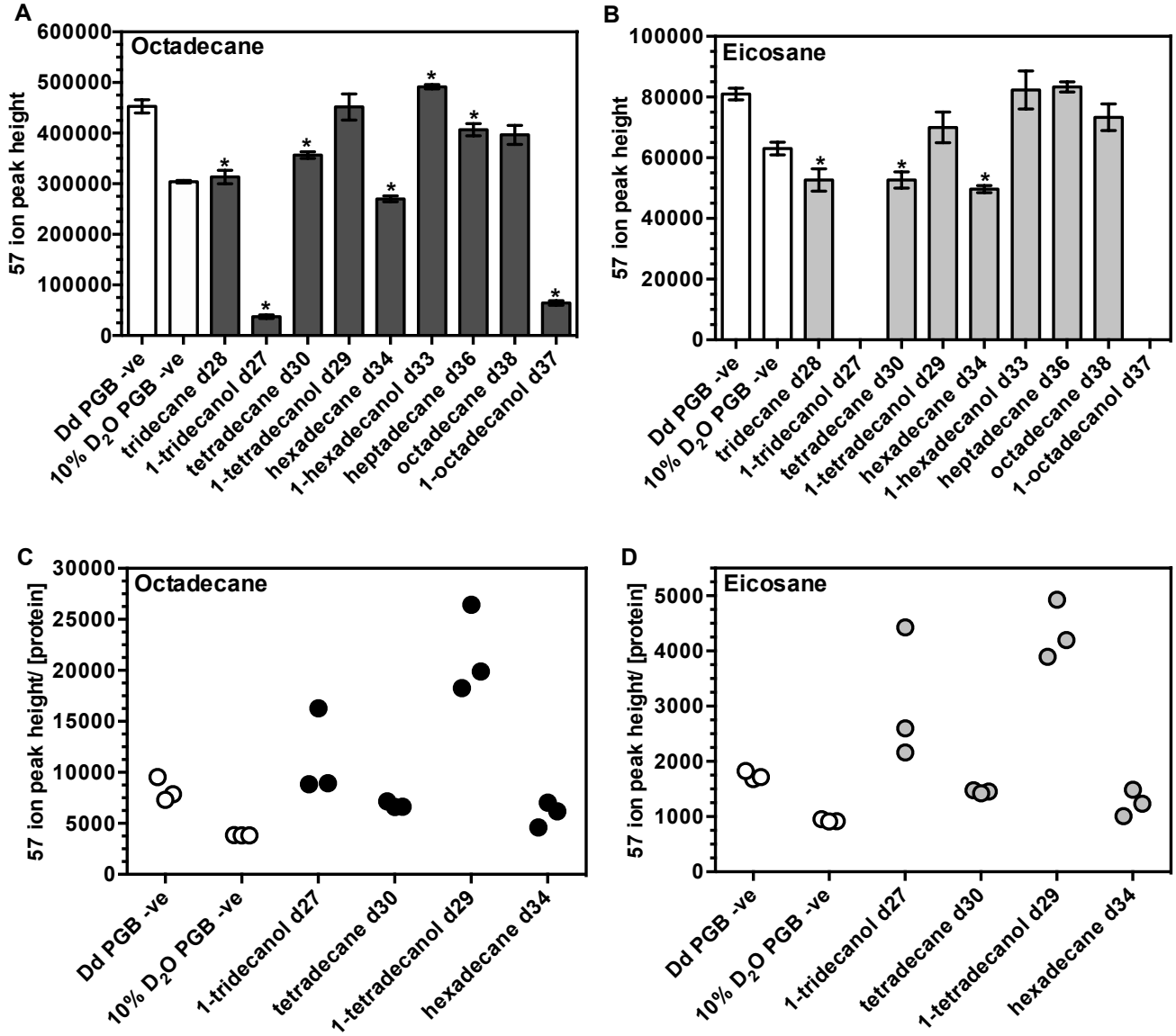

Figure 21. Effect of Exogenously Supplied Deuterated Hydrocarbons on Alkane Synthesis in *Desulfovibrio desulfuricans desulfuricans* 8338

Results from pilot screen: octadecane (A) and eicosane (B) 57 ion peaks heights from GC/MSD analysis of samples taken from *Dd* 8338 cultured in deuterium depleted PGB (Dd PGB) in the presence of 0.5 mmol of the stated hydrocarbon. **Results from repeat screen**: octadecane (C) and eicosane (D) 57 ion peaks heights normalised to cell lysate protein concentrations. Negative controls, *Dd* 8338 cultured with no external hydrocarbon exposure in Dd PGB and 10% D_2O PGB, are shown in white. 0.5 mmol of each hydrocarbon was used to coat the inside of Falcon tubes *Dd* 8338 were cultured in. Following 21 days incubation, alkanes were extracted from each culture using dichloromethane and alkane content analysed using GC/MSD. Octadecane produced by *Dd* 8338 cultured in the presence of 1-octadecene could not be determined due to a large octadecene peak at a similar retention time. Error bars (A and B) represent +/- 1 standard error, n=3. Asterisks highlight data significantly different from Dd PGB control data ($P < 0.05$). In C and D all data points are shown as values correspond to ratios making mean and error calculations inappropriate.

3.4. Identification of Alkanes in *Desulfovibrio* Cell Lysate and Correlation of Crude Protein Fractions to Alkane Signal

A clear deuterated octadecane peak was observed in chromatograms from GC/MSD analysis of clarified *Dd* 8338 cell lysate (bacteria were cultured in 10% D_2O PGB, Figure 21). As *Dd* 8338 cell lysate contains mainly soluble proteins in phosphate buffered saline (original media and cell debris is discarded), this indicates that some octadecane may remain bound to these soluble proteins, possibly in a hydrophobic pocket that is shielded from the aqueous solution. In order to target the proteins that may be associated with alkanes in *Dd* 8338 cell lysate, several methods of cell lysate fractionation were carried out.

Amicon Ultra 2 ml centrifugal filters (Millipore) were used to purify and concentrate cell lysate samples into fractions containing proteins of different molecular weight ranges. These filters were chosen as they were convenient to use and several different molecular weight cut offs were available. Cell lysate fractions were analysed for the presence of deuterated alkane peaks using GC/MSD, with the aim of narrowing down the size range of proteins associated with alkanes. Deuterated octadecane and eicosane peaks were observed in analysis of concentrated cell lysate fractions obtained using 100 kDa and 50 kDa molecular weight cut off Amicon filters (Figure 22). In both cases, no alkane peaks were observed in GC/MSD analysis of the flow-through fractions.

SDS-PAGE was used to visualise the protein profile of each cell lysate fraction obtained using the 100 kDa and 50 kDa Amicon filters. SDS-PAGE analysis (Figure 23) showed that in both concentrated protein fractions a similar protein profile and a broad range of protein sizes are present, however in the flow through fractions only proteins smaller than the molecular weight cut off of the filter used are seen. This confirms these filters are suitable for concentrating protein samples but not for providing clear cut fractions of proteins within a defined size range, as all protein sizes seen in the initial cell lysate are present in the concentrated fraction.

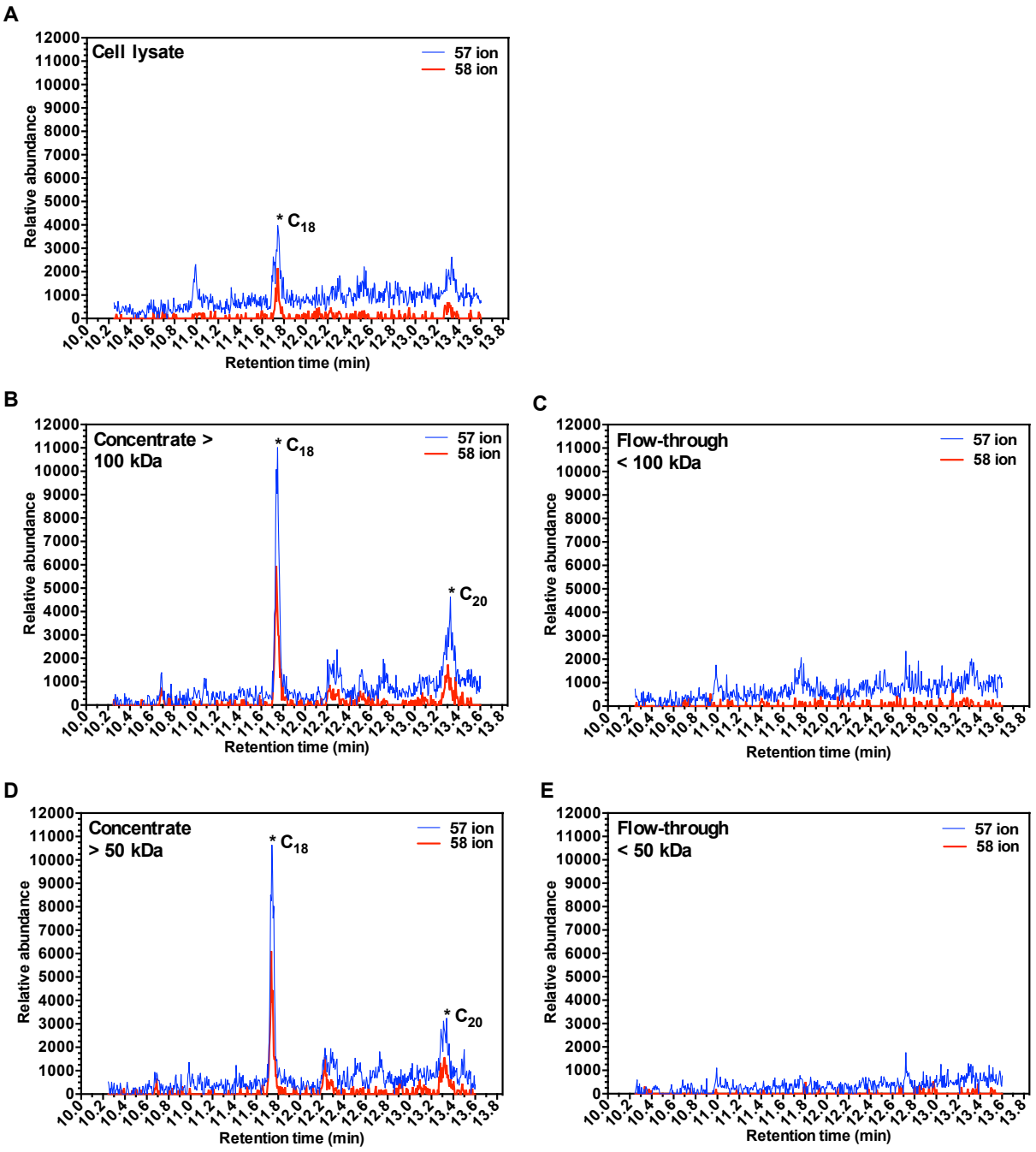

Figure 22. Alkane Analysis of *Desulfovibrio desulfuricans desulfuricans* 8338 Cell Lysate and Cell Lysate Fractions Obtained Using Amicon Ultra Centrifugal Filters

Overlaid 57 ion (blue trace) and 58 ion (red trace) GC/MSD chromatograms from analysis of *Dd* 8338 cell lysate (A) and cell lysate fractions obtained using Amicon Ultra centrifugal filters. Concentrated cell lysate fraction >100 kDa (B) and flow through fraction <100 kDa (C) obtained from use of an Amicon filter with 100 kDa molecular weight cut off. Concentrated cell lysate fraction >50 kDa (D) and flow through fraction <50 kDa (E) obtained from use of Amicon filter with 50 kDa molecular weight cut off. Peaks corresponding to deuterated octadecane and eicosane (products of *Dd* 8338 metabolism) are highlighted with asterisks.

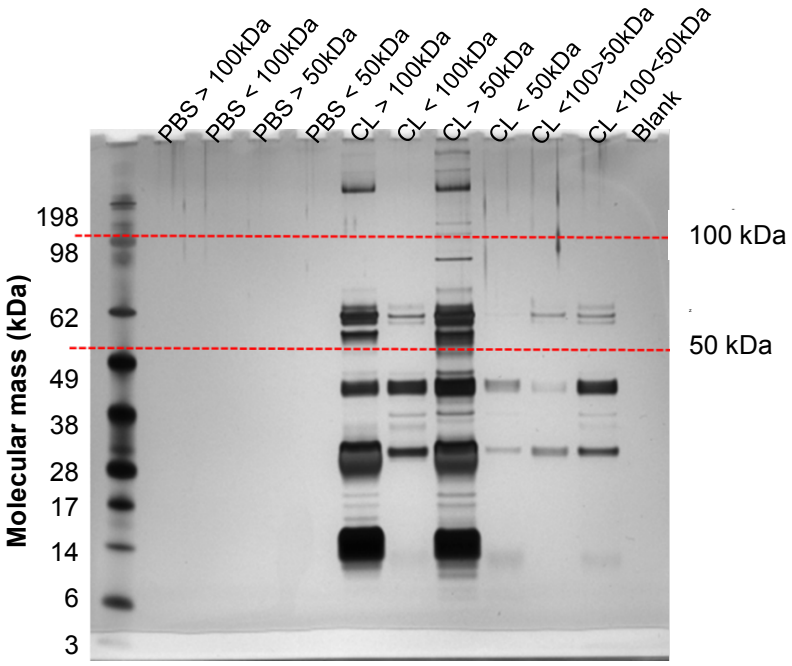

Figure 23. SDS-PAGE Analysis of *Desulfovibrio desulfuricans desulfuricans* 8338 Cell Lysate Fractions Obtained Using Amicon Ultra Centrifugal Filters

SDS-PAGE gel image showing different *Dd* 8338 cell lysate fractions obtained using Amicon Ultra centrifugal filters with 100 kDa and 50 kDa molecular weight cut off membranes. Cell lysate (CL) was prepared by freeze-thaw of *Dd* 8338 culture concentrated in phosphate buffered saline (PBS). Cell debri was then pelleted by centrifugation and clarified cell lysate (supernatant) used in the Amicon filters according to the manufacture's protocol. PBS was used as a negative control throughout. To prepare samples for SDS-PAGE, *Dd* 8338 cell lysate was combined with LDS sample buffer and reducing agent (Bolt, Novex, Life Technologies) and incubated (10 min, 70 °C) before being loaded into a 4-12% Bis-Tris pre-cast SDS-PAGE mini gel and run at 165 V for 35 min. Protein ladder used was SeeBluePlus2 pre-stained ladder (Novex, Life Technologies). Pierce silver stain kit was used according to the manufacturer's protocol. In gel lane labels CL= cell lysate and PBS= phosphate buffered saline.

Ammonium sulphate (AS) precipitation was chosen as a simple method of fractionating cell lysate with minimal risk of denaturing native protein structures, thereby increasing the likelihood of alkanes remaining bound to proteins. The aim of this experiment was to obtain several cell lysate fractions from *Dd* 8338, one containing alkanes (verified with GC/MSD analysis) and one or more not containing alkanes. In this way certain proteins may be excluded or included from further investigation into their role in *Desulfovibrio* alkane synthesis.

In a previous AS precipitation experiment using *Dd* 8338 cell lysate, no precipitate was observed at 25% AS saturation, and clear precipitate observed at both 50% and 75% AS saturations. Alkanes were detected in the 50% AS saturated fraction but not in other fractions (25% AS and 75% AS). From these preliminary results 40%, 50% and 100% AS saturations were chosen for this experiment.

No visible precipitate was formed at 40% AS saturation of *Dd* 8338 cell lysate. At 50% AS saturation, a clear precipitate was observed and at 100% AS saturation a smaller amount of precipitation could be seen. No precipitate was seen in phosphate buffered saline (PBS) controls at any AS saturation. Proteins from *Dd* 8338 cell lysate, and each cell lysate fraction obtained from AS precipitation were analysed using SDS-PAGE; this showed proteins were present in all fractions even when precipitation was not clear (Figure 24).

Alkane content of each *Dd* 8338 cell lysate fraction and the initial cell lysate was analysed using GC/MSD (Figure 25). A clear deuterated octadecane peak can be seen in *Dd* 8338 cell lysate, larger deuterated octadecane and eicosane peaks can be seen in 50% AS saturated cell lysate fraction and no deuterated alkane peaks could be detected in any other fraction. This result suggests alkanes may remain bound to proteins that are present in the 50% AS saturated cell lysate fraction only.

Due to the success of the ammonium sulphate precipitation method in separating cell lysate and isolating a fraction containing alkanes, ammonium sulphate precipitation was performed on two further alkane producing *Desulfovibrio* strains, *Dm* 18311 and *Dg* 10636, and a non-alkane producing strain *Dsp* 496 to act as a negative control. If a similar result were obtained in three different alkane producing *Desulfovibrio* strains, this would provide evidence to support the theory that alkanes may remain associated to certain proteins within the cell lysate and these proteins may play a role in alkane synthesis.

In an initial AS precipitation experiment using *Dm* 18311 and *Dg* 10636 cell lysates, a deuterated alkane peak was observed through GC/MSD analysis of the 40% AS saturated fractions, so 30% AS saturation was used as the initial amount in this experiment. The protein profiles of *Dm* 18311, *Dg* 10636 and *Dsp* 496 cell lysates and cell lysate fractions were analysed using SDS-PAGE (Figure 24).

GC/MSD analysis of *Dm* 18311 cell lysate showed a clear deuterated octadecane peak, with a slightly smaller deuterated octadecane peak being observed in the 30% AS saturated cell lysate fraction. A much larger deuterated octadecane peak and a deuterated eicosane peak were observed in the 50% AS saturated cell lysate fraction and no alkane peaks were detected in the 100% AS saturated cell lysate fraction or the final supernatant (Figure 26).

A clear deuterated octadecane peak was seen in *Dg* 10636 cell lysate, a larger deuterated octadecane peak was observed in the 50% AS saturated cell lysate fraction and no deuterated alkane peaks were detected in any other cell lysate fractions (Figure 27). No deuterated alkane peaks were seen in the negative control *Dsp* 496 cell lysate or AS saturated cell lysate fractions (Figure 28).

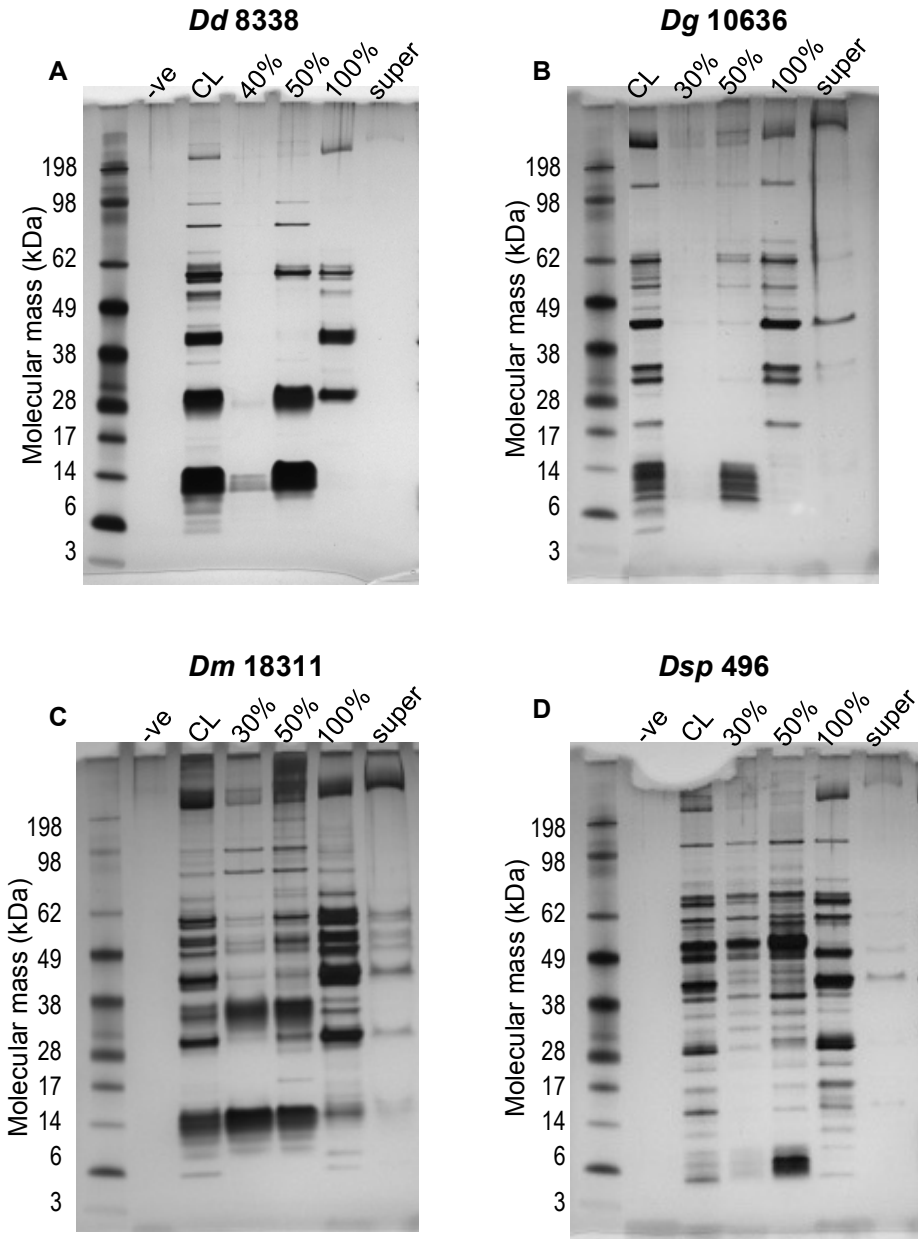

Figure 24. SDS-PAGE Analysis of *Desulfovibrio* Cell Lysate Fractions Obtained from Ammonium Sulphate Precipitation

Images of SDS-PAGE gels run with fractions of cell lysate obtained from ammonium sulphate (AS) precipitation of cell lysate from *Dd* 8338 (A), *Dg* 10636 (B), *Dm* 18311 (C) and *Dsp* 496 (D). Bacteria from 250 ml cultures were harvested by centrifugation and concentrated in 10 ml PBS. Cells were lysed with freeze-thaw and cell debri pelleted. Clarified cell lysate was used for ammonium sulphate precipitations. For *Dd* 8338, 40%, 50% and 100% AS saturations were used. For *Dsp* 496, *Dg* 10636 and *Dm* 18311, 30%, 50% and 100% AS saturations were chosen. All cell lysate fractions were analysed on SDS_PAGE gels alongside the original cell lysate (CL) and the final supernatant obtained after 100% saturation AS precipitation (super). PBS was the negative control throughout. To prepare samples for SDS-PAGE, cell lysate fractions were combined with LDS sample buffer and reducing agent (Bolt, Novex, Life Technologies), incubated (10 min,70°C) and loaded into 4-12% Bis-Tris pre-cast SDS-PGE mini gels run at 165 V for 35 min. The ladder used was SeeBluePlus2 pre-stained protein ladder (Novex, Life Technologies). Protein bands were stained with Pierce silver stain kit according to the manufacturer's protocol.

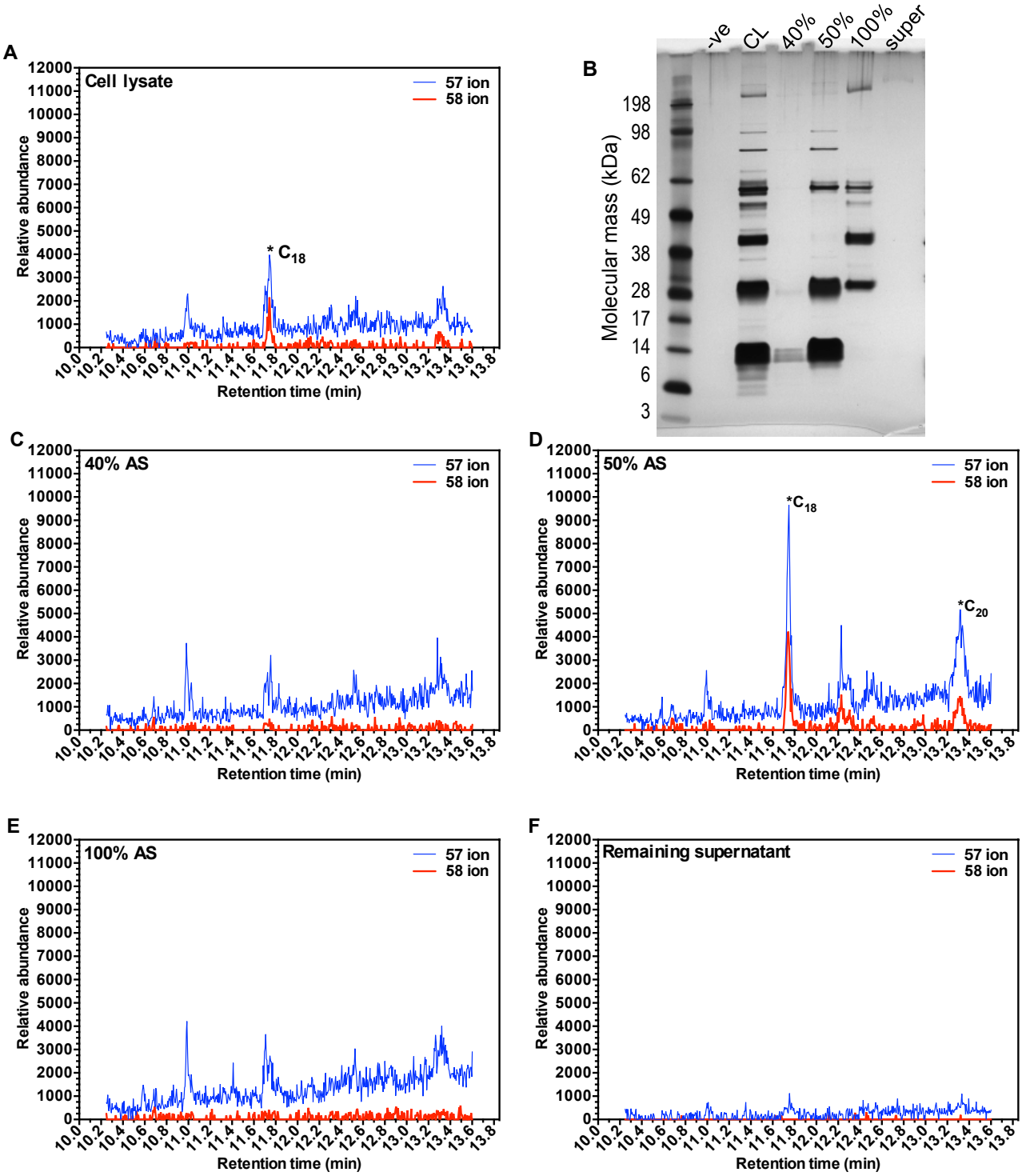

Figure 25. Alkane Analysis of *Desulfovibrio desulfuricans desulfuricans* 8338 Cell Lysate and Cell Lysate Fractions Obtained from Ammonium Sulphate Precipitation

Overlaid 57 ion (blue trace) and 58 ion (red trace) GC/MSD chromatograms from analysis of *Dd* 8338 cell lysate (A). Precipitates obatined from 40% (C), 50% (D) and 100% (E) ammonium sulphate (AS) saturated cell lysate resuspended in PBS, and final supernatant remaining after 100% AS saturation (F) were freeze-dried and alkanes extracted with dichloromethane prior to GC/MSD analysis. Chromatogram peaks corresponding to deuterated octadecane and eicosane are highlighted with asterisks. SDS-PAGE gel image (B) shows the protein profile of *Dd* 8338 cell lysate and each cell lysate fraction.

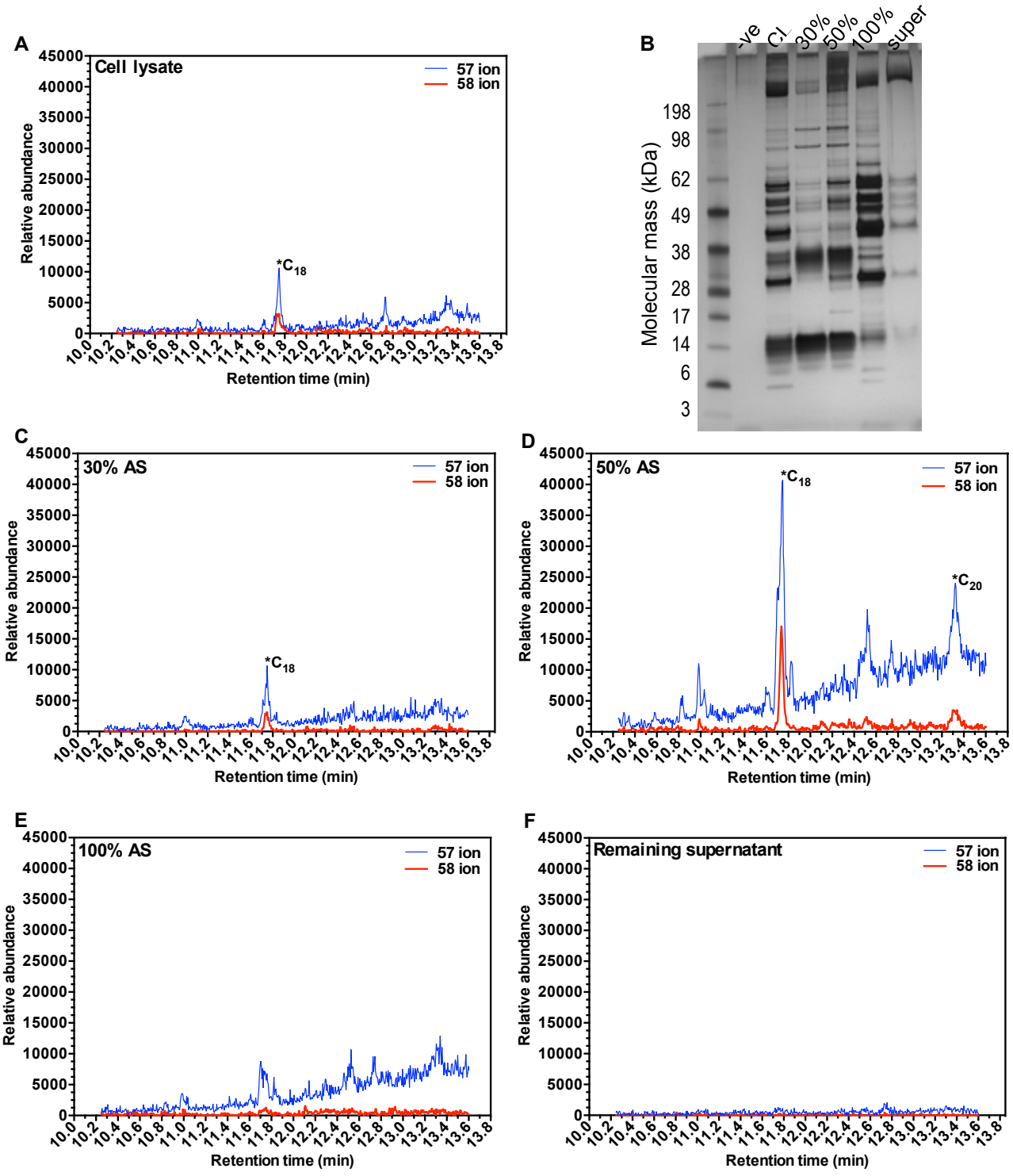

Figure 26. Alkane Analysis of *Desulfovibrio marinus* 18311 Cell Lysate and Cell Lysate Fractions Obtained from Ammonium Sulphate Precipitation

Overlaid 57 ion (blue trace) and 58 ion (red trace) GC/MSD chromatograms from analysis of *Dm* 18311 cell lysate (A). Precipitates obatined from 30% (C), 50% (D) and 100% (E) ammonium sulphate (AS) saturated cell lysate resuspended in PBS, and final supernatant remaining after 100% AS saturation (F) were freeze-dried and alkanes extracted with dichloromethane prior to GC/MSD analysis. Chromatogram peaks corresponding to deuterated octadecane and eicosane are highlighted with asterisks. SDS-PAGE gel image (B) shows the protein profile of *Dm* 18311 cell lysate and each cell lysate fraction.

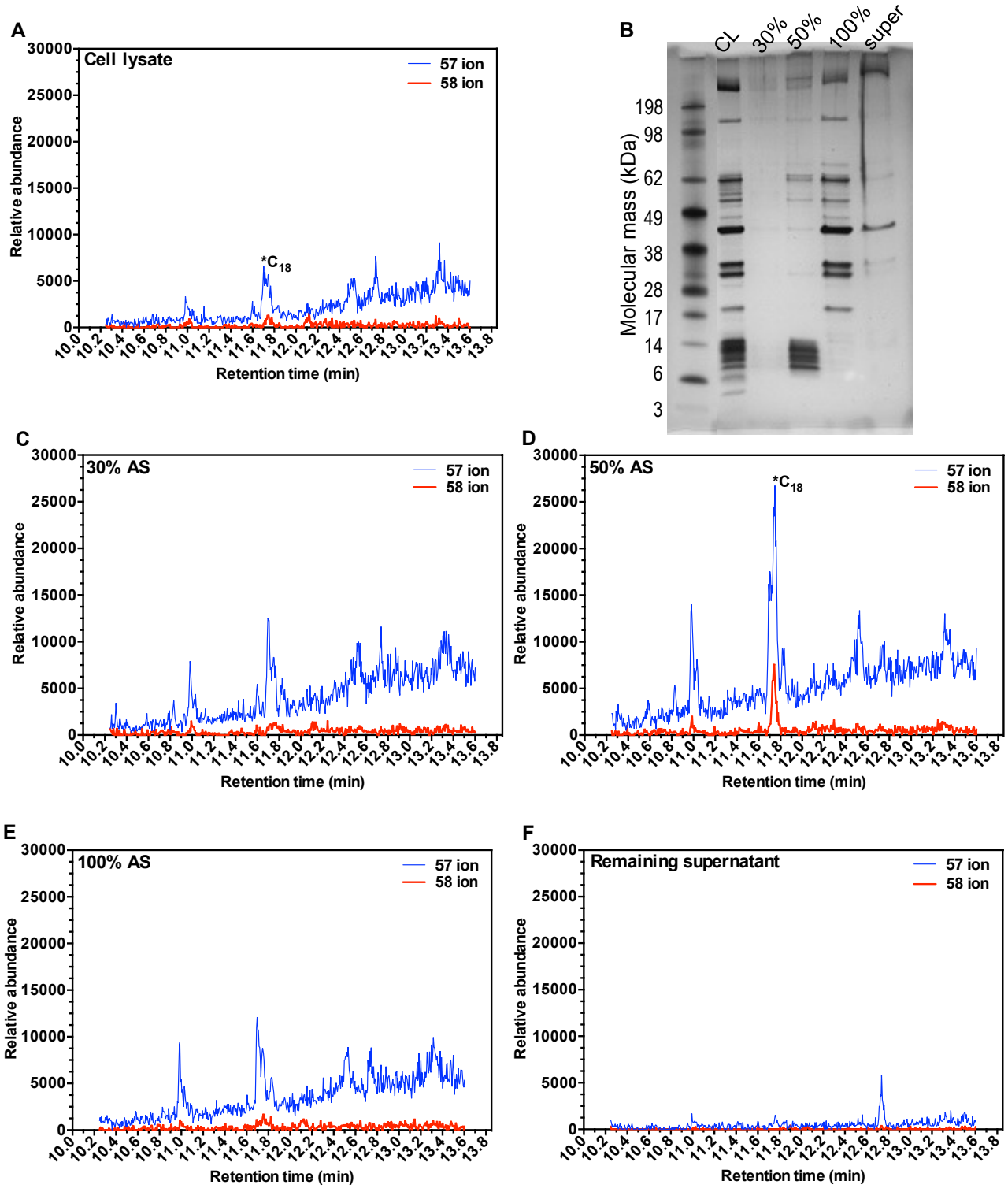

Figure 27. Alkane Analysis of *Desulfovibrio gabonensis* 10636 Cell Lysate and Cell Lysate Fractions Obtained from Ammonium Sulphate Precipitation

Overlaid 57 ion (blue trace) and 58 ion (red trace) GC/MSD chromatograms from analysis of *Dg* 10636 cell lysate (A). Precipitates obatined from 30% (C), 50% (D) and 100% (E) ammonium sulphate (AS) saturated cell lysate resuspended in PBS, and final supernatant remaining after 100% AS saturation (F) were freeze-dried and alkanes extracted with dichloromethane prior to GC/MSD analysis. Chromatogram peaks corresponding to deuterated octadecane and eicosane are highlighted with asterisks. SDS-PAGE gel image (B) shows the protein profile of *Dg* 10636 cell lysate and each cell lysate fraction.

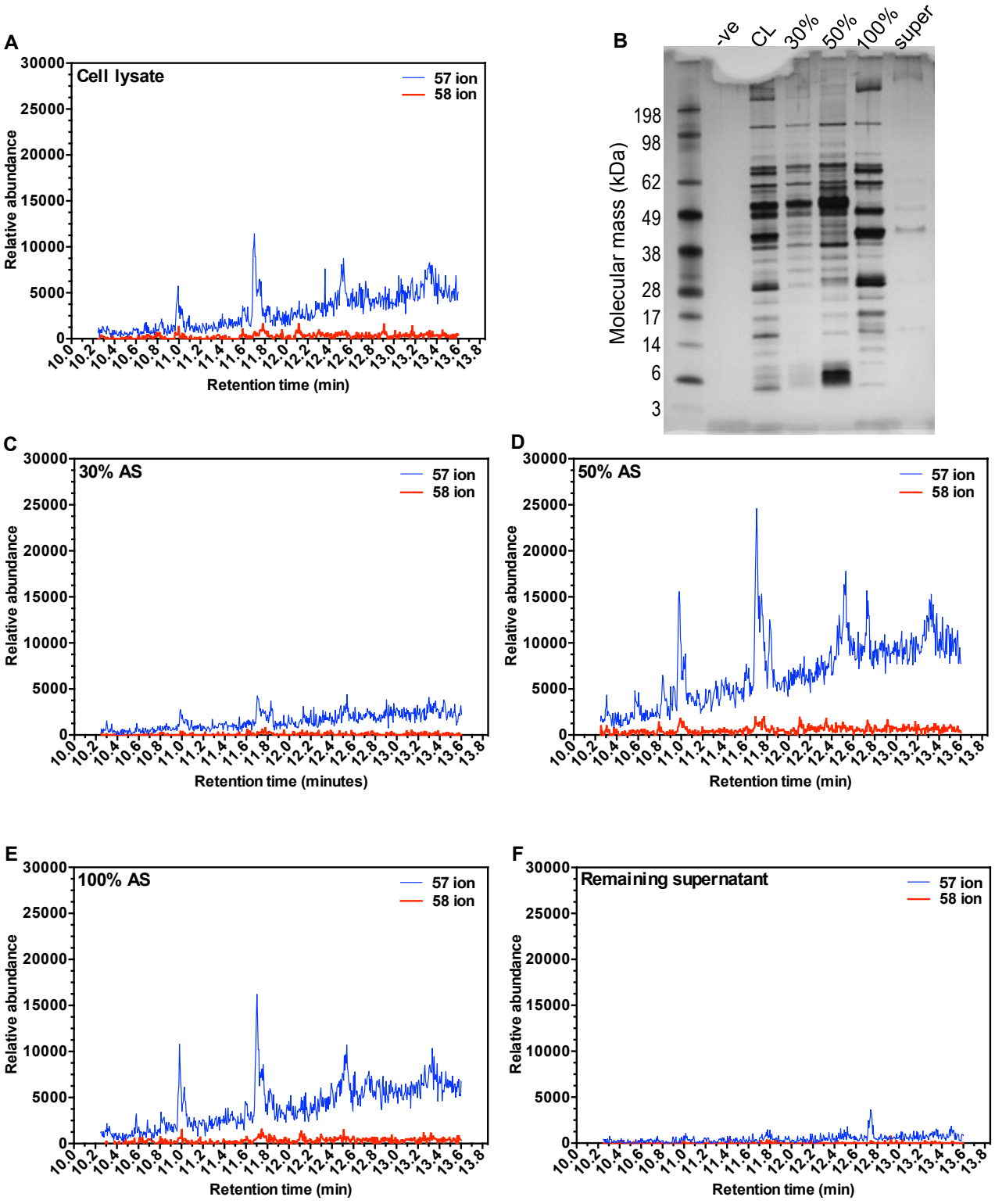

Figure 28. Alkane Analysis of *Desulfovibrio sp 496* Cell Lysate and Cell Lysate Fractions Obtained from Ammonium Sulphate Precipitation

Overlaid 57 ion (blue trace) and 58 ion (red trace) GC/MSD chromatograms from analysis of *Dsp* 496 cell lysate (A). Precipitates obatined from 30% (C), 50% (D) and 100% (E) ammonium sulphate (AS) saturated cell lysate resuspended in PBS, and final supernatant remaining after 100% AS saturation (F) were freeze-dried and alkanes extracted with dichloromethane prior to GC/MSD analysis. Chromatogram peaks corresponding to deuterated octadecane and eicosane are highlighted with asterisks. SDS-PAGE gel image (B) shows the protein profile of *Dsp* 496 cell lysate and each cell lysate fraction.

3.5 Protein Analysis and Comparison of *Desulfovibrio* Cell Lysate Fractions Using 2D Difference Gel Electrophoresis (2D DIGE)

In order to progress from the previous experiment, it was necessary to identify the proteins present in cell lysate fractions that were positive for alkanes. However, as can be seen in Figure 23, SDS-PAGE analysis of the proteins in each cell lysate fraction did not enable proteins present in one fraction but not the other to be identified with confidence. This is due to the proteins from the initial cell lysate having been separated based on their ionic character and not molecular mass, so proteins of the same mass may be present in all fractions. In addition to this, individual bands visualised on an SDS-PAGE gel may represent a number of proteins, each with the same molecular mass, so obtaining information about individual proteins present in these bands and comparing them to proteins present in the corresponding band of a different cell lysate fraction is unachievable.

For these reasons it was decided that two-dimensional gel electrophoresis (2D-GE) would be used to analyse and compare proteins in each cell lysate fraction. 2D-GE separates proteins based on both their molecular mass and iso-electric point, so ionic character is taken into account. Due to not having access to the required equipment and time constraints, 2D-GE of cell lysate fractions from *Dd* 8338*, Dm* 18311, *Dg* 10636 and *Dsp* 496 was outsourced to Applied Biomics Inc., CA. Outsourcing this work also enabled a more advanced technique, 2D difference GE (2D-DIGE), to be used with each cell lysate fraction being labelled with a different cyanine (Cy) dye (Cy2, Cy3 and Cy5) allowing three different samples (all three cell lysate fractions) to be analysed on a single gel.

2D-DIGE gel images for cell lysate fractions from each *Desulfovibrio* strain are shown in Figures 29-32. Protein separation into distinct spots varied between strains, with *Dg* 10636 gel images having a greater number of large smeared areas when compared the negative control *Dsp* 496 where many distinct spots were seen. Also distribution of protein spots across the gel is greater in *Dsp* 496 than in alkane producing strains, however this is more likely to be due to samples from different strains being run on different gels than “real” differences in protein profile.

For each alkane producing *Desulfovibrio* strain, gel images correlating to cell lysate fractions containing no alkanes (30/40% AS and 100% AS) were subtracted from the

image correlating to alkane containing cell lysate fraction (50% AS) using ImageJ software. This allowed protein spots that were present in the alkane containing cell lysate fraction and not present in both other fractions to be accurately determined (Figures 28-30). Similar analysis was performed with gel images from the negative control strain *Dsp* 496 (Figure 32).

In *Dd* 8338 cell lysate fractions two protein spots of interest were identified which remained at high intensity (red colour) when the non-alkane containing fraction images were subtracted from the alkane containing fraction image (Figure 29). In *Dm* 18311 three protein spots of interest were identified in a similar manner. In *Dg* 10636 there were no clear yellow/red spots present in both images obtained when the non-alkane containing fraction images were subtracted from the alkane containing fraction image, as seen in analysis of the previous strains. However, two spots, that are likely unique to the alkane containing fraction but present at a lower intensity, were identified alongside one very small spot (not definitive if this is a real protein spot or contamination) that appeared unique and present at higher intensity (red). The approximate molecular mass range and iso-electric point of each protein spot of interest identified are summarised in Table 2.

None of the protein spots of interest could be matched exactly between strains based on their co-ordinates on the gel images – this was verified using ImageJ synchronization tool. This makes it seem unlikely the same proteins have been identified as being unique to the alkane producing cell-lysate fraction in each *Desulfovibrio* strain analysed. However, samples run on different gels are not directly comparable and proteins conserved across all positive strains can only be definitively determined by excising protein spots of interest and performing mass spectrometry analysis to obtain constituent peptide sequences. Time constraints prevented mass-spectrometry analysis in the current study.

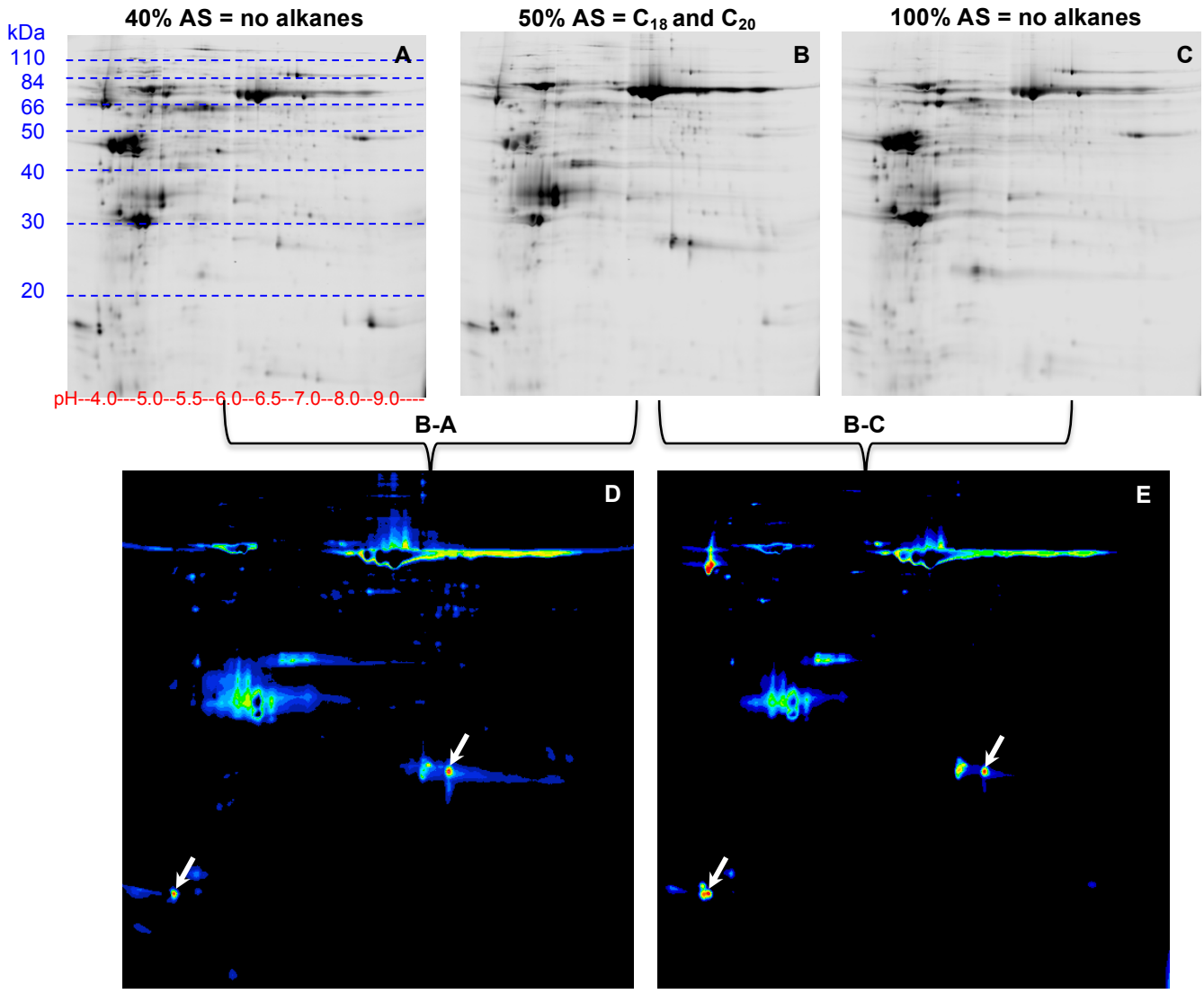

Figure 29. Analysis of *Desulfovibrio desulfuricans desulfuricans* 8338 2D-DIGE Images

2D-DIGE gel images from analysis of *Dd* 8338 cell lysate fractions obtained from different ammonium sulphate (AS) saturations. 2D-DIGE was performed by Applied Biomics Inc, CA. One 2D-DIGE gel run with cell lysate fractions obtained from 40% (A), 50% (B) and 100% (C) AS saturations was excited at different wavelengths to visualise the different dyes used to label each fraction (Cy2, Cy3 and Cy5). The 50% AS saturated cell lysate fraction contained octadecane and eicosane, so this fraction was compared to the other two which contained no alaknes. The image calculator tool in ImageJ was used to subtract (A) from (B) and the resultant image (D) was coloured using the 16 colour lookup table where the most intense spots are warmer in colour (yellow-red). This process was repeated subtracting (C) from (B) to obtain image (E). The white arrows highlight protein spots that are abundant in (B) and absent from both (A) and (C). These spot correlate to *Dd* 8338 cell lysate proteins that are most likely to be associated with alkanes. (A) also shows a scale of approximate iso-electric point (pH) and molecular mass (kDa), which is the same for all gels.

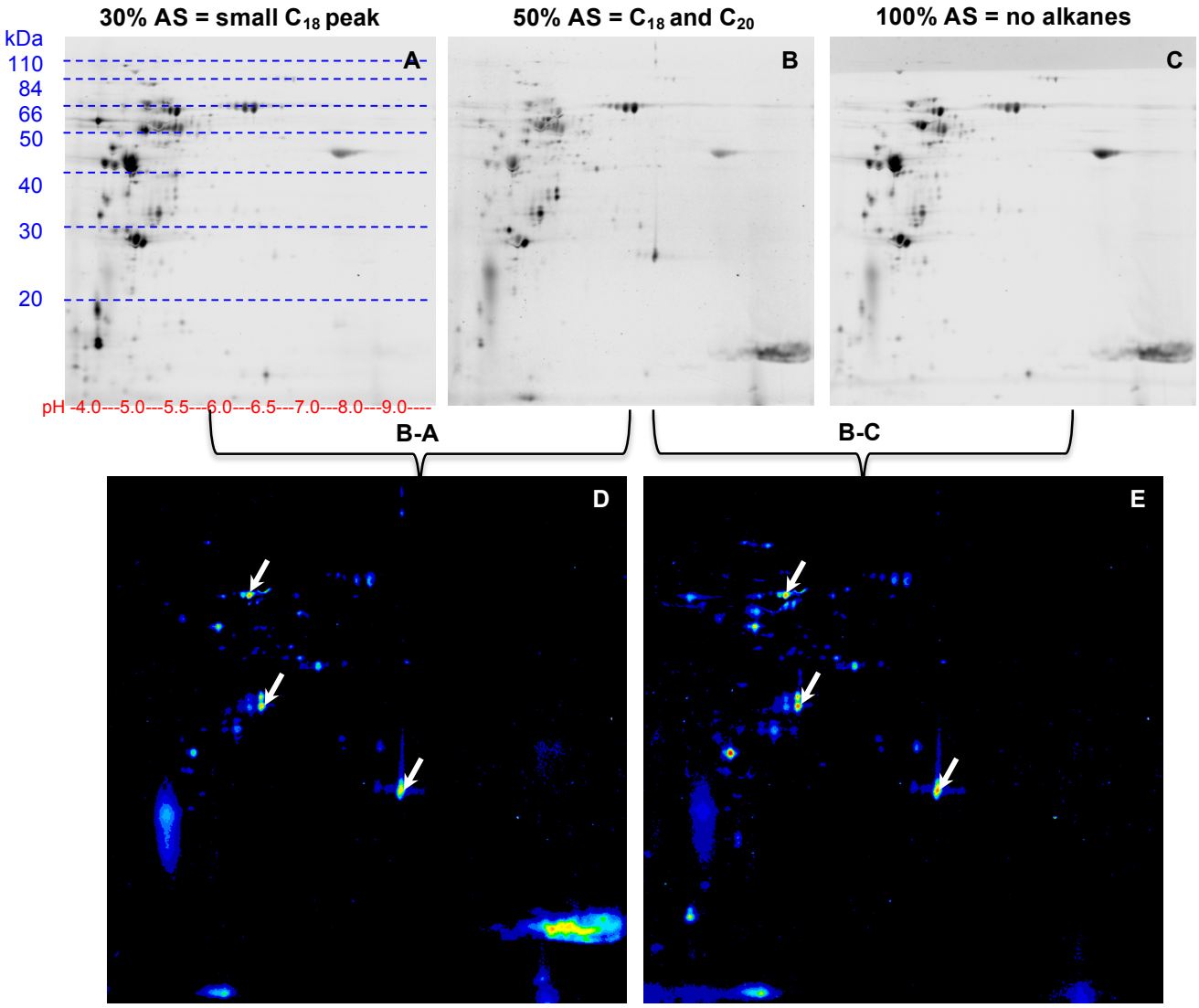

Figure 30. Analysis of *Desulfovibrio marinus* 18311 2D-DIGE Images

2D-DIGE gel images from analysis of *Dm* 18311 cell lysate fractions obtained from different ammonium sulphate (AS) saturations. 2D-DIGE was performed by Applied Biomics Inc, CA. One 2D-DIGE gel run with cell lysate fractions obtained from 30% (A), 50% (B) and 100% (C) AS saturations was excited at different wavelengths to visualise the different dyes used to label each fraction (Cy2, Cy3 and Cy5). The 50% AS saturated cell lysate fraction contained octadecane and eicosane, so this fraction was compared to the other two, the 30% AS fraction contained a small amount of octadecane and no alkanes were identified in the 100% AS fraction. The image calculator tool in ImageJ was used to subtract (A) from (B) and the resultant image (D) was coloured using the 16 colour lookup table where the most intense spots are warmer in colour (yellow-red). This process was repeated subtracting (C) from (B) to obtain image (E). The white arrows highlight protein spots that are abundant in B and absent from both (A) and (C). These spot correlate to *Dm* 18311 cell lysate proteins that are most likely to be associated with alkanes. (A) also shows a scale of approximate iso-electric point (pH) and molecular mass (kDa), which is the same for all gels.

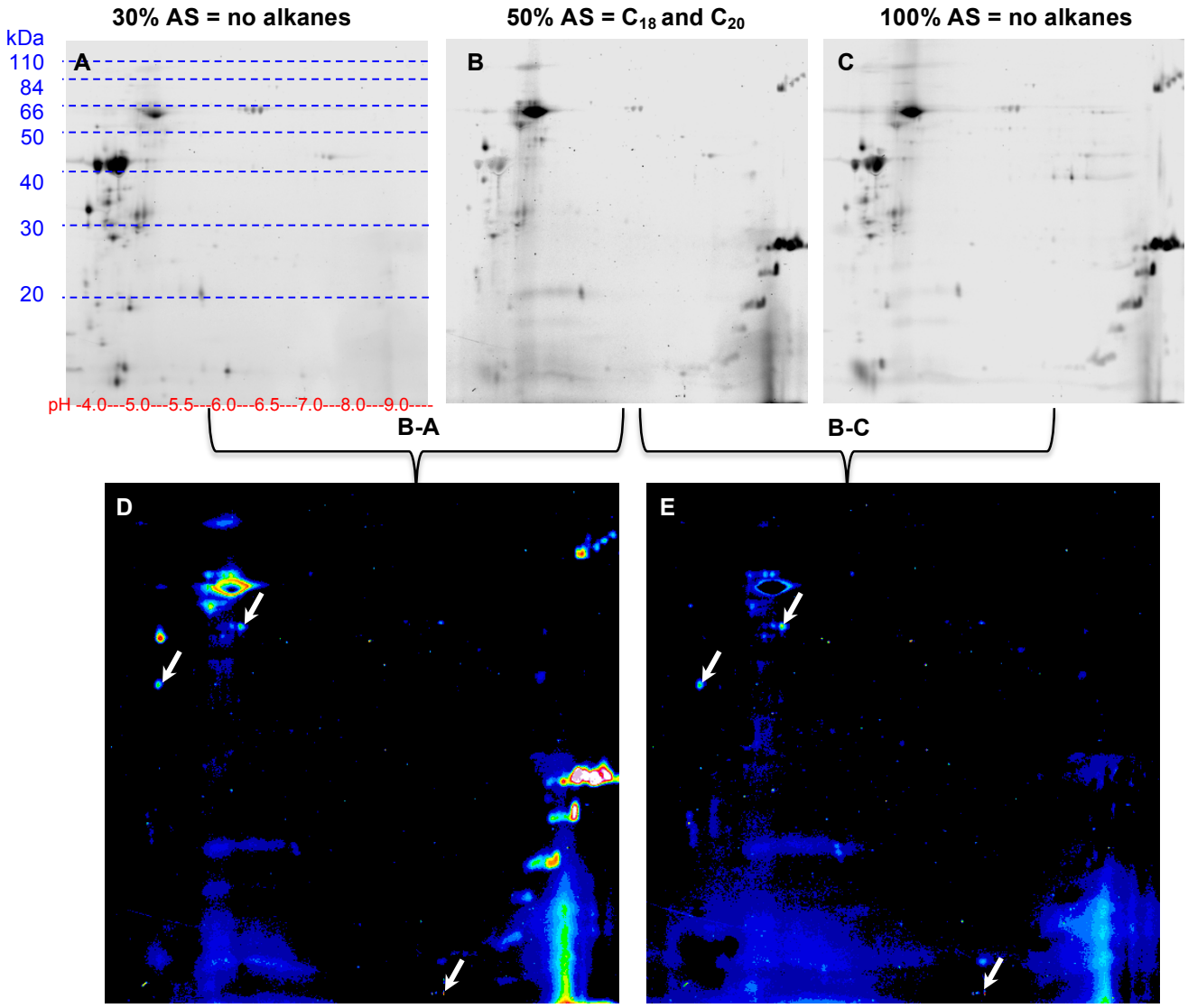

Figure 31. Analysis of *Desulfovibrio gabonensis* 10636 2D-DIGE Images

2D-DIGE gel images from analysis of *Dg* 10636 cell lysate fractions obtained from different ammonium sulphate (AS) saturations. 2D-DIGE was performed by Applied Biomics Inc, CA. One 2D-DIGE gel run with cell lysate fractions obtained from 30% (A), 50% (B) and 100% (C) AS saturations was excited at different wavelengths to visualise the different dyes used to label each fraction (Cy2, Cy3 and Cy5). The 50% AS saturated cell lysate fraction contained octadecane and eicosane, so this fraction was compared to the other two which contained no alkanes. The image calculator tool in ImageJ was used to subtract (A) from (B) and the resultant image (D) was coloured using the 16 colour lookup table where the most intense spots are warmer in colour (yellow-red). This process was repeated subtracting (C) from (B) to obtain image (E). The white arrows highlight protein spots that are relatively abundant in B and absent from both (A) and (C). These spots correlate to *Dg* 10636 cell lysate proteins that are most likely to be associated with alkanes. (A) also shows a scale of approximate iso-electric point (pH) and molecular mass (kDa), which is the same for all gels.

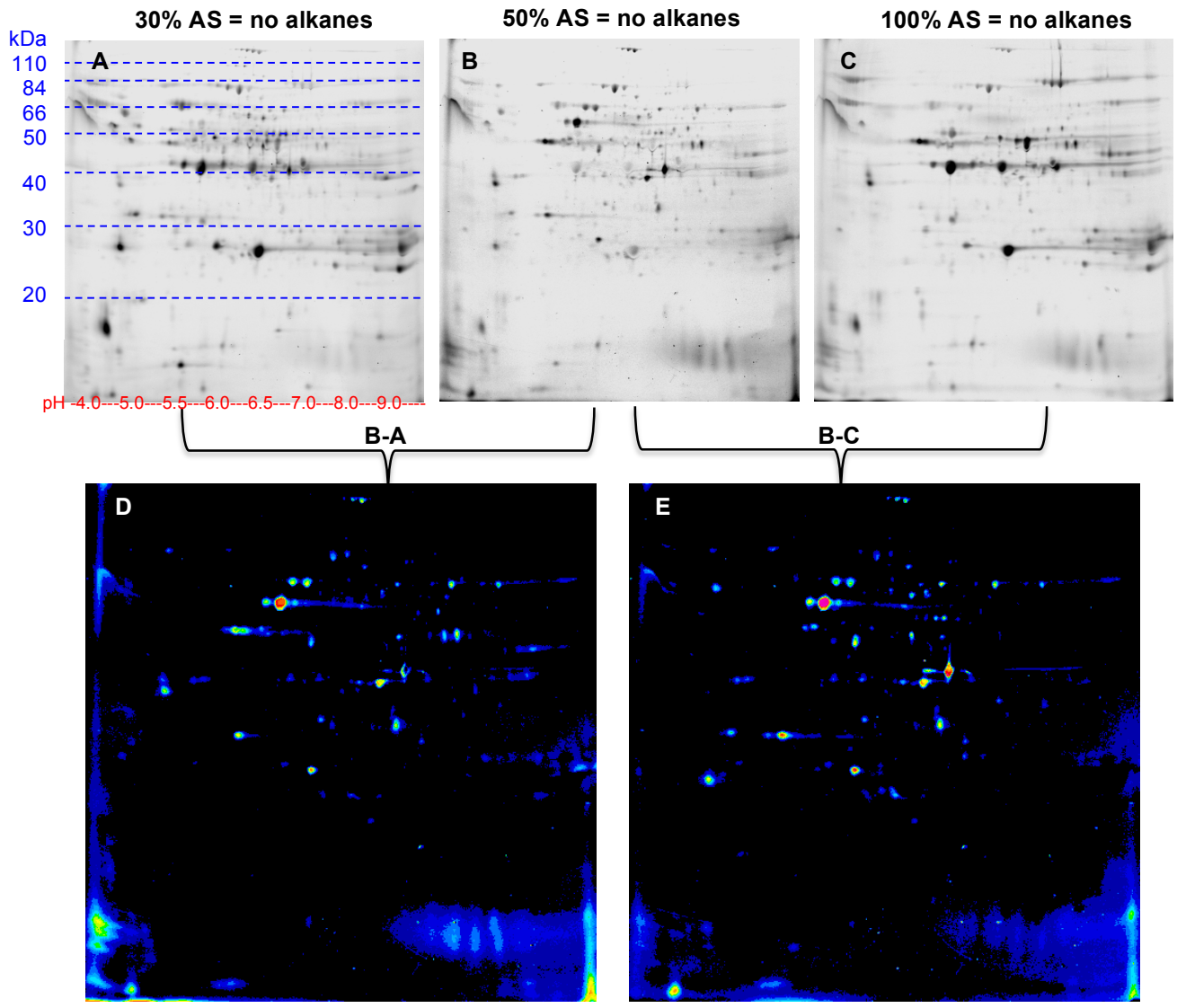

Figure 32. Analysis of *Desulfovibrio sp* 496 2D-DIGE Images

2D-DIGE gel images from analysis of *Dsp* 496 cell lysate fractions obtained from different ammonium sulphate (AS) saturations. 2D-DIGE was performed by Applied Biomics Inc, CA. One 2D-DIGE gel run with cell lysate fractions obtained from 30% (A), 50% (B) and 100% (C) AS saturations was excited at different wavelengths to visualise the different dyes used to label each fraction (Cy2, Cy3 and Cy5). None of the cell lysate fractions contained alkanes, as *Dsp* 496 was the negative control, but, as the 50% AS fraction contained alkanes in the other strains, this fraction was compared to the other two in the same way. The image calculator tool in ImageJ was used to subtract (A) from (B) and the resultant image (D) was coloured using the 16 colour lookup table where the most intense spots are warmer in colour (yellow-red). This process was repeated subtracting (C) from (B) to obtain image (E). (A) also shows a scale of approximate iso-electric point (pH) and molecular mass (kDa), which is the same for all gels.

***Desulfovibrio* strain**	**Protein spot molecular mass (kDa)**	**Protein spot iso-electric point (pH)**
D. desulfuricans desulfuricans 8338	10-18	4
	25-30	7
D. marinus 18311	25-28	6.5
	33-38	5.5
	50-66	5
D. gabonensis 10636	35-40*	4*
	40-50*	5*
	0-5**	7**

Table 2. Summary of Protein Spots Identified as being Unique to Alkane Containing *Desulfovibrio* Cell Lysate Fractions

Analysis of 2D-DIGE gel images using ImageJ software identified several protein spots unique to alkane containing *Desulfovibrio* cell lysate fractions. ImageJ software was used to subtract gel images corresponding to non-alkane containing cell lysate fractions from gel images corresponding to alkane containing cell lysate fractions. The resulting images were coloured using a 16-colour lookup table where colour warmth was positively correlated to spot intensity. *No clear yellow-red spots were identified as being unique to the alkane containing fraction of *Dg* 10636 cell lysate, so two green spots were chosen. **This spot was red in colour but very small so may represent contamination.

Chapter 4. Discussion

4.1 Characterisation of Alkane Synthesis in the *Desulfovibrio* Using Stable Isotopes.

Desulfovibrio were first identified as being capable of alkane synthesis over 70 years ago (Jankowski and Zoebell, 1944), however research into the specifics of alkane production in this genus has, to date, been limited. Often studies will focus on one species or strain of particular industrial interest without comparing this to, or screening other strains to give a fuller picture of alkane synthesis across the genus. This lack in breadth of study has lead to insufficient data being available from which to form a sound hypothesis of the alkane synthesis pathway in *Desulfovibrio,* with the only published hypothetical pathway being based primarily on alkane synthesis in other microorganisms (Bageava, 1998).

In the present study, 21 *Desulfovibrio* strains were screened for alkane production. In this screen, *Desulfovibrio* were cultured in media supplemented with stable isotope components (D_2O or ^{13}C lactate) to allow metabolically produced alkanes to be distinguished from potential contamination with 'white oil' (commonly found on manufactured products). This method of definitively determining alkane synthesis in *Desulfovibrio* had not been employed previously and aimed to provide a benchmark for future alkane synthesis investigation in this genus.

Of the 21 *Desulfovibrio* strains screened, six were positive for alkane production: *Desulfovribrio gabonesis* 10636 (*Dg* 10636), *Desulfovibrio desulfuricans desulfuricans* 8326 (*Dd* 8326), *Desulfovibrio desulfuricans desulfuricans* 8338 (*Dd* 8338), *Desulfovibrio marinus* 18311 (*Dm* 18311), *Desulfovibrio Paquesii* 16681 (*Dp* 16681) and *Desulfovibrio gigas* 9332 (*Dg* 9332). This study identified at least four more alkane producing *Desulfovibrio* strains than previously recorded in literature (available literature only identifies *'Desulfovibrio desulfuricans'* as producing alkanes [Bagaeva and Chernova, 1994; Ladygina, 2006]) giving a broader overview of alkane synthesis in the genus. Phylogenetic analysis identified a close genetic relationship between all six alkane producing strains, however, they may be divided into two more tightly related clades comprising *Dg* 10636, *Dd* 8326, *Dm* 18311 and *Dd* 8338 in one clade and *Dg* 9332 and *Dp* 16681 in the other. A close phylogenetic relationship between all positive strains suggests a common evolutionary origin of the alkane synthesis pathway. All phylogenetic work was performed by Peggy Dousseaud at the University of Exeter (2015).

It is difficult to attribute the difference in phylogeny between the two clades of alkane producing *Desulfovibrio* strains to difference in alkane profile or abundance of alkanes produced however, some general observations can be made. *Dm* 18311, *Dd* 8338 and *Dg* 10636 produced a greater abundance of alkanes than *Dg* 9332 and *Dp* 16681. *Dg* 9332 is the only alkane producing strain where octadecane is not the main alkane product, suggesting a potential difference in alkane synthesis in this strain.

The most abundant alkanes produced by all six alkane producing strains have even carbon chain lengths (C_{18} and C_{20}). This is unusual amongst alkane producing bacteria. For example, heptadecane is the most abundant alkane produced by cyanobacteria (Schirmer *et al*., 2010) and follows the 'n-1' rule for alkane production where, because the final step in synthesis is a decarbonylation reaction, the alkane product has one less carbon compared to the parent long-chain fatty acid. Furthermore, as long-chain fatty acids in nature typically have an even chain length, the resultant products from decarbonylation reactions are odd-chain alkanes. A further example of microbes producing odd chain-length hydrocarbons from fatty acid precursors is the production of long chain alkenes in the genus *Jeotgalicoccus* catalysed by the fatty acid decarboxylase $OleT_{JE}$ P450 (Rude *et al*., 2011).

4.2 A Hypothetical, New Pathway for Alkane Production by *Desulfovibrio*

The production of mainly even chain length alkanes by *Desulfovibrio* suggests an alkane synthesis pathway that bypasses decarbonylation and, instead, follows a reductive route from long-chain fatty acid precursors to alkane products of identical carbon chain length. However, there is a caveat to this hypothesis that *Desulfovibrio*, like the majority of micro-organisms widely studied to-date, only produce even-chain length fatty acids. Bagaeva (1999) suggested *Desulfovibrio* do produce odd-chain length fatty acids; in his hypothetical hydrocarbon synthesis pathway both formate and acetate are precursors to fatty-acid biosynthesis resulting in odd and even chain length fatty acid products. However, Bagaeva's isotope experiments only identified the production of formate, acetate and the incorporation of labelled acetate methyl-groups into alkanes; the incorporation of formate into fatty-acids was not proven and no fatty acid profile was given. A definitive fatty acid profile for *Desulfovibrio* is not available in the literature and

has not been investigated in the current study, so obtaining this data would be important in future work to help strengthen the reliability of this hypothetical, reductive pathway.

Such a pathway would be industrially appealing due to the complete carbon conservation, which would translate to optimal alkane yield and energy efficiency. The working hypothesis of this study was that *Desulfovibrio* produce octadecane and eicosane via a reductive reaction beginning with octadecanoic acid or eicosanoic acid as the respective precursors which then undergo a series of reduction reactions, the first converting them from fatty acids to aldehydes then to fatty alcohols and finally to *n*-alkanes (Figure 12). This hypothetical pathway would require a significant amount of free hydrogen (reducing power) something that is likely to be abundant in *Desulfovibrio* cultures due to the anaerobic hydrogen rich atmosphere.

Dm 18311 was the only alkane producing strain found to produce nonadecane; the only odd-chain alkane observed. Nonadecane may be synthesised via an alternative pathway to the one discussed in the main hypothesis above or may be a product of degradation of eicosane. However, nonadecane abundance only made up 4.6% of the total alkane abundance in this strain and is therefore not a major alkane product.

4.3 Growth Features and Alkane Biosynthesis

After screening *Desulfovibrio* strains for alkane synthesis, it was deemed necessary to identify exactly when in the growth cycle alkanes were being produced to enable alkanes to be harvested within an optimum time frame. Time-course analysis of key metabolites, such as the main carbon source lactic acid, as well as protein concentration, were analysed to determine a reliable method of estimating *Desulfovibrio* growth. In the literature, growth of *Desulfovibrio* has been estimated using optical density (Gilmore *et al*., 2011; Meyer *et al*., 2013) however, due to the iron sulphide precipitate produced, optical density is a unreliable indication of growth. Being confident the bacteria studied have reached the desired phase of growth is imperative to good microbiological research. This time-course experiment gives evidence to support an estimate of growth phase time-frames and enables the identification of a factor that may be used to normalise alkane abundance so it may be more comparable between strains.

For this experiment *Dd* 8338 was selected due to its predictable growth pattern and reliable alkane production, making it a candidate strain for future pathway elucidation experiments. Data from a preliminary time-course experiment indicated exponential phase most likely occurred between 2 and 6 days post inoculation, therefore more regular 10 h or 12 h samples were taken between these time-points as opposed to the 24 h samples taken between 0 to 2 days and 6 to 11 days.

Growth Analysis by Catabolism of Supplied Carbon Source.

High performance liquid chromatography (HPLC) analysis of lactic acid (LA, the main carbon source supplied in the media) and acetic acid in *Dd* 8338 cultures (AA, a major product of lactic acid catabolism) was found to be a simple and reliable method of estimating growth of *Desulfovibrio* with data points resembling a fairly typical bacterial growth curve (see Figure 13). When all other alkane producing *Desulfovibrio* strains were analysed for LA consumption and AA production over an eight-day period, lag phase varied considerably lasting between 48 h and 120 h (See Figure 14), indicating that rate of lactic acid catabolism, as may be expected, is not uniform across the genus. Identifying these varying rates of lactic acid catabolism provides information regarding the optimal incubation times for different strains to reach the same growth phase which may be crucial in future experiments. *Dd* 8338, *Dd* 8326 and *Dm* 10636 all reach stationary phase by 120 h post inoculation, much faster than the other three alkane producing strains. This faster metabolism may increase their suitability for future industrial exploitation.

HPLC analysis of LA and AA provided a simple and rapid method for determining whether or not *Desulfovibrio* cultures grew, but did not provide any other information, for example on culture density or viable cells, that may be used to normalise alkane abundance data. Unless culture samples were collected within the 2-3 day 'exponential' phase, which would not be the case if collecting samples for alkane analysis, HPLC analysis of growth can only give a qualitative answer of 'yes it has grown' (no LA remains and 2-2.5 g l^{-1} AA is produced) or 'no it hasn't grown' (LA remains and little to no AA is produced).

Growth Analysis by Protein Concentration

Analysis of soluble proteins from whole cell lysate of *Dd* 8338 was also performed with samples from all time-points (Figures 15 and 16). *Dd* 8338 cultured in 10% D_2O PGB media produced greater concentrations of soluble proteins compared to *Dd* 8338 grown in PGB media and this difference was deemed statistically significant with a paired t-test of

the two data sets giving a two-tailed P value of <0.0001. A possible explanation for this increase in protein production in *Dd* 8338 cultures supplemented with 10% D_2O is that the deuterium places a metabolic burden on the bacteria such that it triggers overexpression of certain enzymes to compensate for this, increasing protein concentration in the cell lysate.

The overall trend in protein production in *Dd* 8338 was similar to lactic acid consumption and acetic acid production. There was less of a pronounced lag phase seen in soluble protein concentration but a definite phase of exponential increase between 48 h and 96 h in-line with lactic acid catabolism. However, a clear decrease in protein concentration was seen after 120 h. This may indicate after 120 h, when no lactic acid remains as a carbon source, proteins were catabolised to release energy for further cellular development and secondary metabolism. This is a well established response to starvation in *E. coli* (Goldberg and St. John, 1976). A decrease in protein concentration also suggests that, after 120 h, certain enzymes have performed their primary function and so expression of these proteins was switched off as the bacteria enter a more dormant phase.

Comparison of protein-band intensities visualised on SDS-PAGE gels with Qubit protein concentrations gave a consistent picture of the increase in soluble proteins over time. Protein bands reached peak intensity between 96 h and 120 h. However, as silver staining has a narrow linear dynamic range, band intensities are not directly comparable to protein concentrations, and bands corresponding to proteins beyond a certain concentration may be readily saturated with stain. For these reasons, the band intensities from SDS-PAGE gel images, whilst providing an estimate of change in protein concentration over time, are not as reliable a measure of protein concentration as Qubit readings. Nevertheless, these gel images allow the protein profile of *Dd* 8338 to be visualised, and refining this method of cell lysis and protein visualisation was imperative to future work.

It was decided that protein concentration would be used as a measurement to normalise alkane abundance between different *Desulfovibrio* strains. This is because it gives additional information on growth and development of the culture compared to acetic acid analysis, as acetic acid reached very similar concentrations in all strains studied.

Analysis of Alkane Production Relative to Growth

Analysing production of alkanes in *Desulfovibrio* over an 11 day time-course enabled alkane production time-frames to be identified and production rates of different alkanes to

be compared. This was important for future experiments so samples for alkane analysis were taken within an optimal timeframe.

Alkane production in *Dd* 8338 began at a similar time (48 h to 58 h) to both lactic acid consumption and protein production indicating alkane production follows growth; however, alkane production continued much beyond the point of lactic acid depletion (106 h). This implies alkane production is reliant on a substrate and enzyme that remain abundant once the main carbon source has been utilised. From the SDS-PAGE gel images we may also begin to speculate at protein bands correlating to alkane synthesis enzymes by disregarding those that become indistinguishable at later time-points.

From the trend in alkane abundance over time, it may be estimated the optimum time for harvesting alkanes from *Desulfovibrio* cultures, to achieve maximum yield, would be between 11 and 14 days post inoculation. However, this is only an estimate from available data as a true peak abundance was not identified.

In *Dd* 8338 cultured in both PGB and 10% D_2O PGB, production rate of eicosane was slower than the production rate of octadecane, inferring the pre-cursor to octadecane production is more abundant than that of eicosane production. If precurosrs to alkane synthesis are fatty acids of the same carbon chain length as hypothesised, octadecanoic acid may be the primary long-chain fatty acid produced in all alkane producing *Desulfovibrio* strains where octadecane is the main product (all except *Dg* 9332), and ecosanoic acid may be produced at a slower rate via an additional elongation cycle of octadecanoic acid prior to thioesterase cleavage. However, as fatty acids were not analysed in this study this is only a suggested inference from the data available. In future work, analysis of long-chain fatty acids produced by *Desulfovibrio* strains would provide valuable information to test this hypothesis. However, accurate determination of fatty acid abundance can be difficult due to the reactive nature of the carboxylic acid functional groups meaning free fatty acids are generally in low abundance.

4.4 *In Vivo* Screen for Potential Inhibitors and/or Substrates of Alkane Synthesis

Screening for compounds that may effect alkane synthesis in *Dd* 8338 uncovered no clear substrates or competitive inhibitors to the enzymes involved in this pathway. Pilot experiments, screening both hydrocarbons and deuterated hydrocarbons, provided interesting results with several compounds (primary alcohols in the hydrocarbon screen and alcohols and alkanes in the deuterated hydrocarbon screen) having a significant inhibitory effect on alkane production. It was notable that, in some instances, fatty alcohols exhibited an inhibitory effect on alkane synthesis (as measured by 57 ion peak height), as they would be plausible competitive inhibitors to enzymes that convert octadecanol and eicosanol to alkanes.

Protein concentration is not typically used as a measurement to normalise production of a compound against in bacterial cultures due to the potential error associated. However, with conventional growth measurements such as optical density and colony counts being unsuitable for *Desulfovibrio* work, due to the production of black insoluble H_2S, it was thought beneficial to show alkane abundance normalised to protein concentration rather than to no growth factor. Error could not be accurately determined from 57 ion peak height data expressed as a ratio of protein concentration so no robust conclusions could be drawn from these data sets, however they were beneficial as an additional perspective on the raw 57 ion peak height data.

In the pilot screen of deuterium labelled compounds, a significant difference in both octadecane and eicosane production was seen between *Dd* 8338 control cultures grown in deuterium depleted PGB and 10% D_2O PGB. A similar reduction in alkane yield was seen in time-course cultures of *Dd* 8338 grown in 10% D_2O PGB compared to PGB. This suggests, as previously discussed, that the presence of deuterium in the growth media may have an inhibitory effect on alkane synthesis, making it difficult to determine whether the deuterated compounds screened in this experiment had a true inhibitory effect or whether the presence of deuterium was a significant factor in alkane production regulation.

In repeat experiments compounds shown previously to have significant effects on alkane synthesis had smaller, non-significant effects, and in some cases opposite effects reducing the reliability of initial results. Of all seventeen compounds screened, none were shown to have a consistently significant effect on alkane production in *Dd* 8338. There are

several plausible explanations for this: none of the compounds tested were substrates or inhibitors to the alkane synthesis pathway; the compounds were not in the correct state for uptake by the cell (not soluble, may form micelles); the bacteria were not able to metabolise these compounds; the concentration of compounds was not sufficient to significantly effect alkane synthesis. In future, similar experiments performed in a cell free system adding potential substrates directly to cell lysate, may circumvent some of these issues.

Due to the lack of statically significant and consistent data obtained through these experiments, no robust conclusions could be drawn. In retrospect it might have been beneficial to cease this line of experimentation earlier however the industrial supervisor was clear about the need for these experiments to be performed in totality.

4.5 Identification of Proteins Associated with Alkanes *In Vitro*.

Identification of Alkanes in Cell Lysate Fractions

As no substrates or competitive inhibitors to the alkane synthesis pathway were identified a new approach to pathway elucidation was employed. A proteomics based route was taken in the final series of experiments which stemmed from identifying a clear deuterated octadecane peak in GCMS chromatograms of clarified *Dd* 8338 cell lysate from (*Dd* 8338 was cultured in 10% D_2O PGB). It was hypothesised that, due to the cell lysate containing only soluble proteins in phosphate buffered saline, with all original media and cell debris having been discarded, that alkanes may remain bound to a protein or within a protein complex that may play a role in alkane synthesis. With this hypothesis in mind two methods were employed to fractionate cell lysate; protein fractions were then screened for alkane presence in order to narrow down proteins that may be involved in *Desulfovibrio* alkane synthesis.

Use of Amicon Ultra-2ml centrifugal filter devices provided a rapid and effective method of concentrating proteins in *Dd* 8338 cell lysate. GCMS analysis of concentrated cell lysate fractions obtained from the use of filters with two different molecular weight cut off membranes (100 kDa and 50 kDa) yielded clear deuterated octadecane and eicosane peaks. However, when these cell lysate fractions were analysed using SDS-PAGE it became clear the filters did not exclude all proteins lower than the stated molecular weight

cut off from the concentrated fractions, which had similar protein profiles to whole cell lysate in both cases. This made the use of these filters unsuitable for achieving cell lysate fractions with varied protein profiles from which potential alkane associated proteins may be identified.

The un-concentrated flow-through fractions of cell lysate, obtained from use of both the 50 kDa and 100 kDa molecular weight cut off filters, contained proteins with smaller molecular mass than the stated cut off of the filter and no alkanes were identified in the GC/MSD analysis of these flow through fractions. This could imply that proteins present in the flow through cell lysate fractions were not associated with alkanes and may be excluded from further analysis. However, the presence of similar protein bands at higher intensities in the concentrated fractions may suggest that the reduced concentration of these proteins in the flow through compared to the concentrated protein fraction could be responsible for the lack of alkane detection.

In future experiments size exclusion chromatography may prove a superior method of separating *Desulfovibrio* cell lysate into protein fractions based on size, but was not pursued here due to time constraints. Affinity chromatography using a potential substrate, such as a fatty alcohol, bound to resin to selectively bind and purify proteins that might play a role in *Desulfovibrio* alkane synthesis was also considered for this line of experimentation. However, affinity chromatography had been attempted previously in the laboratory and was unsuccessful mainly due to column promiscuity for hydrophobic molecules (C. Edner, pers. comm.).

Ammonium sulphate (AS) precipitation of proteins from *Dd* 8338 cell lysate was a more successful method of obtaining protein fractions with visibly different protein profiles. Although ammonium sulphate precipitates proteins depending on their ionic character and not size, there was clear differences in the protein profiles of cell lysate fractions obtained from ammonium sulphate precipitation, compared to each other and the corresponding whole cell lysate, when proteins were analysed using SDS-PAGE.

Percentage saturations of ammonium sulphate used were optimised to obtain two protein fractions with no detectable alkane presence and one with a clear alkane presence (50% AS) from cell lysate of *Dd* 8338, and *Dg* 10636. GC/MSD analysis following ammonium sulphate fractionation of *Dm* 18311 gave a small octadecane peak in one fraction (30% AS), a much greater octadecane peak and an eicosane peak in the second

fraction (50% AS) and no alkanes in the final fraction. In this case, isolating alkanes to one fraction was less successful but analysis of the 50% AS saturated cell lysate fraction still provides useful information, particularly when compared to the 50% AS saturated fractions from *Dd* 8338 and *Dg* 10636. A non-alkane producing strain, *Dsp* 496, was also subject to the same ammonium sulphate precipitation procedure to act as negative control and allow subtractive protein analysis.

Identification of proteins present in 50% ammonium sulphate saturated cell lysate fractions and not present in other fractions was deemed unachievable from SDS-PAGE analysis. Visible overlap was observed between the molecular mass of protein bands in different cell lysate fractions due to proteins being separated based on ionic character, not mass. In addition to this, if gel bands were excised and subject to mass spectrometry analysis, resultant peptide sequences would likely be unresolved, particularly where the bands are most intense and likely correspond to a large number of different proteins. Performing mass spectrometry analysis of excised SDS-PAGE gel bands would make accurate protein identification extremely difficult. For these reasons, a more comprehensive method of separating the proteins present in different *Desulfovibrio* cell lysate fractions was employed, in order to obtain a better resolution of distinct proteins prior to their identification.

Proteomic Comparison of Cell Lysate Fractions

Two dimensional gel electrophoresis (2D-GE) enables separation of proteins based on both their molecular mass and isoelectric point, giving much higher resolution of individual proteins compared to SDS-PAGE. Due to time constraints and lack of required equipment, it was not feasible to perform such analysis of *Desulfovibrio* cell lysate fractions 'in house', so this work was outsourced to a specialist protein analysis company Applied Biomics Inc., CA.

Outsourcing this work also allowed a more sophisticated type of 2D-GE to be performed, 2D difference gel electrophoreses (2D-DIGE), where three separate samples are analysed on a single gel achieved by the proteins in each sample being labelled with a distinct Cyanine (Cy) dye. 2D-DIGE has several main advantages over conventional 2D-GE: sensitivity is greater (proteins with concentrations as low as 0.2ng are detectable); resolution of protein spots is much higher using specific wavelengths of light to visualise spots labelled with a distinct dye; and most significantly it enables three separate samples

to be analysed on a single gel, making them directly comparable. In conventional 2D-GE samples are analysed on separate gels and then attempts made to match the gel alignment exactly so spots can be compared – this is a difficult task that requires a high level of expertise and can easily lead to false positives. Being able to run three samples on one gel was ideally suited to this experiment where three different cell lysate fractions were obtained for each *Desulfovibrio* strain.

In addition to being an appropriate method of separating and analysing the cell lysate samples prepared in this experiment, 2D-DIGE analysis may contribute to wider *Desulfovibrio* research due to it being a novel technique not previously applied to biological samples from this genus. Only a single example exists in literature of *Desulfovibrio* proteomics data acquired using 2D-GE, which gives a proteome overview of the model sulphate reducing bacteria *Desulfovibrio Vulgaris* Hildenborough (M. Fournier *et al*., 2006).

Although the preparation, running and imaging of the 2D-DIGE gels was outsourced, all down-stream analysis and protein identification was performed "in house", to take a more hands on and tailored approach to the proteomics rather than relying on a standardised methodology provided by Applied Biomics. This was a risk and was invariably more time consuming, but was deemed necessary to give integrity to the data interpretation.

Several immediate observations were made from the raw 2D-DIGE gel images of the *Desulfovibrio* cell lysate fractions obtained from Applied Biomics (Figures 28-31). Firstly, a clear difference was seen in the general protein profile of alkane producing strains compared to the negative control *Dsp* 496. Although the close phylogenetic relationship of the positive strains may go some way to explain the similarity in observed protein profile between these strains and the marked difference compared to the observed protein profile of the non-alkane producing strain, different gels run on separate days are not directly comparable and many conserved proteins are likely to be present on all gels even if this is not visually apparent.

To gain further data regarding which protein spots correspond to proteins only found in the alkane-containing cell lysate fractions (50% AS), images were analysed using ImageJ software. ImageJ software was used to definitively identify proteins unique to the alkane containing cell lysate fractions by using the Image calculator tool to subtract the gel images corresponding to non-alkane containing fractions from the gel image

corresponding to the alkane containing fraction for each strain (Figures 28-30). This resulted in images containing protein spots present in the alkane containing fractions but not present or present at lower intensity (depending on the intensity of the spot remaining) in the non alkane containing fractions that had been subtracted. These images were coloured using the 16-colour lookup table which enabled protein spots remaining at high intensity following this subtraction to be easily recognised from corresponding yellow/red (warm) colours indicating high intensity. These yellow/red spots were deemed to represent the most likely proteins to be associated with alkanes in the alkane containing cell lysate fractions, and therefore proteins which may have a role in *Desulfovibri*o alkane synthesis.

From this ImageJ analysis only 2 or 3 protein spots were identified as being unique to, and abundant in, the alkane containing cell lysate fraction of each alkane producing strain studied. However, there are likely additional protein spots that were unique to alkane containing cell fractions that were not identified here as their observed intensity was low, making it less certain that they were not present in the non-alkane containing fractions. In future work, more sophisticated analysis to identify all proteins unique to alkane containing fractions would provide a more comprehensive data set.

From analysis using the synchronization tool in ImageJ, there was no overlap between protein spots of interest identified in each alkane producing *Desulfovibrio* strain. This reduces the probability the proteins identified may have integral roles in alkane synthesis as they would be highly conserved in all alkane producing strains. However, it is difficult to accurately compare protein spots analysed on different gels due to variance in preparation or run conditions potentially effecting how the proteins migrate through the gel. In future work it would be important to run samples from each alkane producing strain on a single 2D-DIGE to accurately identify any overlap between proteins unique to alkane containing cell lysate fractions. Furthermore, for the same reasons it is difficult to accurately subtract proteins present in the the 50% AS fraction of the negative control strain *Dsp* 496 from the alkane containing fractions in the positive species.

Once protein spots of interest had been identified it was planned to excise these spots and prepare them (by tryptic digest and peptide extraction) for MALDI-TOF and MALDI-TOF/TOF mass spectrometry analysis to obtain predicted peptide sequences that would allow protein identification. Conservation between protein spots of interest across the

positive strains and subtractive analysis of proteins from the negative control strain could then be accurately performed by comparing peptide sequences.

Unfortunately, there was insufficient time to perform this work in the current study, although this work will be completed in the future and is hoped to complement and inform a colleague's work, where a subtractive genomic approach has been taken to gain insight into *Desulfovibrio* alkane production. Even prior to identifying the relevant peptide sequences, useful information can be obtained from the 2D-DIGE gel images pertaining to the approximate molecular mass and iso-electric point of proteins identified as being unique to alkane containing cell lysate fractions (Table 2). This data may be used to calculate approximate nucleotide lengths required to generate proteins of the molecular masses identified which would enable genes with a potential role in *Desulfovibrio* alkane synthesis to be narrowed down.

Conclusion

Twenty-one *Desulfovibrio* strains were screened for alkane production using stable isotope labelled media components so metabolically produced alkanes could be definitively distinguished from potential contamination with 'white oil'. Six alkane producing strains were identified: *D. gabonesis* 10636 (*Dg* 10636), *D. desulfuricans desulfuricans* 8326 (*Dd* 8326), *D. desulfuricans desulfuricans* 8338 (*Dd* 8338), *D. marinus* 18311 (*Dm* 18311), *D. Paquesii* 16681 (*Dp* 16681) and *D. gigas* 9332 (*Dg* 9332). The main alkanes produced by these strains were *n*-octadecane and *n*-eicosane which lead to the hypothesis that *Desulfovibrio spp.* produce alkanes from fatty acid precursors of the same carbon chain length, via a reductive pathway. The caveat to this hypothesis is that all free fatty acids in *Desulfovibrio* are of an even carbon chain length as seen in other micro-organisms, however the fatty acid profile of *Desulfovibrio spp*. has yet to be confirmed.

Time-course analysis of *Dd* 8338 identified acetic acid and protein production peaked at approximately 5 days post inoculation, whereas alkane production continued to increase steadily upto the final 11 day time-point, with octadecane being produced at a significantly faster rate than eicosane. This observation indicates alkanes are produced from a precursor that remains abundant long after the main carbon source is utilised.

Nine hydrocarbons (including fatty alcohols and ketones) and nine fully deuterated hydrocarbons (including alkane and fatty alcohols) were supplied exogenously to *Dd* 8338 cultures with the aim of identifying a competitive inhibitor or substrate to alkane synthesis. Tetradecanol, hexadecanol, hexadecanone, octadecanol, tridecane d28, tetradecane d30, hexadecane d34, octadecanol d37 and tridecanol d27 were all identified as having an inhibitory effect on alkane synthesis in pilot screens, however in repeat experiments results were inconsistent leading to this line of experimentation being terminated.

Identification of a clear deuterated alkane signal in cell lysate of *Dd* 8338 lead to several protein fractionation methods being employed alongside GC/MSD analysis to narrow down which proteins present in the cell lysate may be associated to alkanes. The cell lysate fractionation method chosen for further experiments was ammonium sulphate saturation which produced distinct protein fractions with clear alkane presence or absence. Three alkane producing strains, *Dd* 8338, *Dm* 18311 and *Dg* 9332, were then analysed alongside one non-alkane producing strain, *Dsp* 496. Three cell lysate fractions were obtained for each strain one of which contained a clear alkane signal (in the alkane producing strains) and two with very little or no alkane presence.

All three cell lysate fractions from each *Desulfovibri*o strain were analysed on a single 2D-DIGE gel, allowing proteins unique to the alkane containing fractions to be identified. ImageJ software was used to subtract gel images from each other to identify protein spots unique to the alkane containing fractions. In *Dd* 8338 two unique proteins were identified, with molecular masses (MMs) of 10-18 kDa, and 25-30 kD and iso-electric points (IEPs) of pH 4 and pH 7 respectively. In Dm 18311 three proteins unique to the alkane containing cell lysate fraction were identified with MMs of 25-28 kDa, 33-38 kDa and 50-66 kDa and IEPs of pH 6.5, pH 5.5 and pH 5 respectively. *Dg* 10636 didn't have as intense unique protein spots as found in the other two strains, however two unique proteins spots were identified corresponding to proteins with MMs of 35-40 kDa and 40-50 kDa and IEPs of pH 4 and pH 5 respectively. All proteins identified fall with a relatively narrow molecular mass range increasing the likelihood of protein conservation between strains.

In future work these protein spots would be excised and subject to mass spectrometry analysis to identify peptide sequences and enable further characterisation and analysis. Peptide sequence data would also allow proteins from different strains to be compared and conserved proteins identified, something which cannot be done by comparing the location of protein spots from samples analysed on different gels. Definitively identifying

proteins present in the alkane containing cell lysate fractions of all alkane producing *Desulfovibrio* strains and not present in non-alkane producing strains would provide valuable insight into possible alkane synthesis enzymes. However, this analysis was not possible in the current study due to time constraints.

This project has refined several methods of *Desulfovibri*o alkane and protein analysis which may be integral to discovering enzymes involved in *Desulfovibrio* alkane synthesis. If carbon is fully conserved throughout the *Desulfovibrio* alkane synthesis pathway, as hypothesized here, the enzymes that facilitate this pathway may be integral to future synthetic biofuel production where the carbon conservation would be critical to economic viability and sustainability.

References

Anderson, J.E., Hardigan, P.J., Ginder, J.M., Wallington, T.J. and Baker, R.E. (2009). *Implications of the energy independence and security act of 2007 for the US light-duty vehicle fleet* (No. 2009-01-2770). SAE Technical Paper.

Andrietta, M.G.S., Andrietta, S.R., Steckelberg, C. and Stupiello, E.N.A. (2007) Bioethanol—Brazil, 30 years of Proalcool. *Int. Sugar J* 109: 195–200.

Bagaeva, T.V. and Chernova, T.G. (1994). Comparative characteristics of extracellular and intracellular hydrocarbons of Desulfovibrio desulfuricans. *Biochemistry* (Moscow), *59*, pp. 31–33 [translated from Biokhimiya].

Bagaeva, T.V. (1998). Sulphate-reducing bacteria, hydrocarbon producers. Thesis Doctoral (Biol) Dissertation. Russia: Kazan State University [in Russian].

Bernard, A., Domergue, F., Pascal, S., Jetter, R., Renne, C., Faure, J.D., Haslam, R.P., Napier, J.A., Lessire, R. and Joubès, J. (2012). Reconstitution of plant alkane biosynthesis in yeast demonstrates that Arabidopsis ECERIFERUM1 and ECERIFERUM3 are core components of a very-long-chain alkane synthesis complex. *The Plant Cell*, *24*(7), pp.3106-3118

Biester, E. M., Hellenbrand, J., Gruber, J., Hamberg, M. and Frentzen, M. (2012). Identification of avian wax synthases. *BMC biochemistry*, *13*(1), 4.

Bird, C. W. and Lynch, J. M. (1974). Formation of hydrocarbons by micro-organisms. *Chem. Soc. Rev.*, *3*(3), 309-328.

Blomquist, G. J. and Bagnères, A. G. (Eds.). (2010). Insect hydrocarbons: biology, biochemistry, and chemical ecology. *Cambridge University Press*.

Bonaventure, G., Salas, J.J., Pollard, M.R. and Ohlrogge, J.B. (2003). Disruption of the FATB gene in Arabidopsis demonstrates an essential role of saturated fatty acids in plant growth. *The Plant Cell*, *15*(4), pp.1020-1033.

Brennan, L. and Owende, P. (2010). Biofuels from microalgae—a review of technologies for production, processing, and extractions of biofuels and co-products. *Renewable and sustainable energy reviews*, *14*(2), pp.557-577.

Collins, K. J. (2008). The role of biofuels and other factors in increasing farm and food prices: a review of recent developments with a focus on feed grain markets and market prospects.

European Commission. (2016). Biofuels. Available at: http://ec.europa.eu/energy/en/topics/renewable-energy/biofuels. Accessed on 9th February 2016.

De Almeida, P. and Silva, P.D. (2009). The peak of oil production—timings and market recognition. *Energy Policy*, *37*(4), pp.1267-1276.

Dennis, M. and Kolattukudy, P.E. (1992). A cobalt-porphyrin enzyme converts a fatty aldehyde to a hydrocarbon and CO. *Proceedings of the National Academy of Sciences*, *89*(12), pp.5306-5310.

Doney, S.C., Fabry, V.J., Feely, R.A. and Kleypas, J.A. (2009). Ocean acidification: the other CO2 problem. *Marine Science*, *1*.

Fangrui, M. and Hanna, M.A. (1999) Biodiesel production: a review. *Bioresour. Technol.* 70(1), pp.1-15.

Frazão, C., Silva, G., Gomes, C.M., Matias, P., Coelho, R., Sieker, L., ... and Le Gall, J. (2000). Structure of a dioxygen reduction enzyme from Desulfovibrio gigas. *Nature Structural & Molecular Biology*, *7*(11), 1041-1045.

Garland, P., Raftery, A.E., Ševčíková, H., Li, N., Gu, D., Spoorenberg, T., Alkema, L., Fosdick B.K., Chunn, J., Lalic, N., Bay, G., Buettner, T., Heilig, G.K., and Wilmoth, J. (2014) World population stabilization unlikely this century. *Science 346* (6206), pp.234-237.

Gerpen, J.V. (2005). Biodiesel processing and production. *Fuel processing technology* 86(10), pp.1097-1107.

Graham-Rowe, D. (2011). Agriculture: Beyond food versus fuel. *Nature*,*474*(7352), S6-S8.

Greer, S., Wen, M., Bird, D., Wu, X., Samuels, L., Kunst, L. and Jetter, R. (2007). The cytochrome P450 enzyme CYP96A15 is the midchain alkane hydroxylase responsible for formation of secondary alcohols and ketones in stem cuticular wax of Arabidopsis. *Plant Physiology*, *145*(3), pp.653-667.

Goldberg, A.L. and St. John, A.C., 1976. Intracellular protein degradation in mammalian and bacterial cells: Part 2. *Annual review of biochemistry*, *45*(1), pp.747-804.

Gilmour, C.C., Elias, D.A., Kucken, A.M., Brown, S.D., Palumbo, A.V., Schadt, C.W. and Wall, J.D. (2011). Sulfate-reducing bacterium Desulfovibrio desulfuricans ND132 as a model for understanding bacterial mercury methylation. *Applied and environmental microbiology*, *77*(12), pp.3938-3951.

Heidelberg, J.F., Seshadri, R., Haveman, S.A., Hemme, C.L., Paulsen, I.T., Kolonay, J.F., ... and Fraser, C.M. (2004). The genome sequence of the anaerobic, sulphate-reducing bacterium *Desulfovibrio* vulgaris Hildenborough. *Nature biotechnology*, *22*(5), pp.554-559.

Howard, R.W., and Blomquist, G.J. (2005). Ecological, behavioral and biochemical aspects of insect hydrocarbons. *Annu. Rev. Entomol.*, *50*, pp. 371-393.

Howard, T.P., Middelhaufe, S., Moore, K., Edner, C., Kolak, D.M., Taylor, G.N., Parker, D.A., Lee, R., Smirnoff, N., Aves, S.J. and Love, J. (2013). Synthesis of customized petroleum-replica fuel molecules by targeted modification of free fatty acid pools in Escherichia coli. *Proceedings of the National Academy of Sciences*, *110*(19), pp.7636-7641.

Humud, C.E., Pirog, R. and Rosen, L. (2015). Islamic State Financing and US Policy Approaches. *International Journal of Terrorism & Political Hot Spots*, *10*(2).

International Energy Agency. (2008). World Energy Outlook 2008. Available at: https://www.iea.org/publications/freepublications/publication/weo-2008.html. Accessed on 9th February 2016.

IPCC. (2007). Climate Change 2007: The Physical Science Basis. available at: http://www.ipcc.ch/SPM2feb07.pdf . Accessed on 12th January 2016.

IPCC. (2013). Climate Change 2013: The Physical Science Basis. Contribution of Working Group I to the Fifth Assessment Report of the Intergovernmental Panel on Climate Change [Stocker, T.F., D. Qin, G.-K. Plattner, M. Tignor, S.K. Allen, J. Boschung, A. Nauels, Y. Xia, V. Bex and P.M. Midgley (eds.)]. *Cambridge University Press*, 1535 pp.

Keller, K.L., Bender, K.S. and Wall, J.D. (2009). Development of a markerless genetic exchange system for Desulfovibrio vulgaris Hildenborough and its use in generating a strain with increased transformation efficiency. *Applied and environmental microbiology*, *75*(24), pp.7682-7691.

Kumar, P., Barrett, D.M., Delwiche, M.J. and Stroeve, P. (2009). Methods for pretreatment of lignocellulosic biomass for efficient hydrolysis and biofuel production. *Industrial & Engineering Chemistry Research*, *48*(8), pp.3713-3729.

Kunst, L. and Samuels, L., 2009. Plant cuticles shine: advances in wax biosynthesis and export. *Current opinion in plant biology*, *12*(6), pp.721-727.

Kreith, F. and Krumdieck, S. (2014) Principles of Sustainable Energy Systems, Second Edition. pp 202.

Lam, M.K. and Lee, K.T. (2012). Microalgae biofuels: a critical review of issues, problems and the way forward. *Biotechnology advances*, *30*(3), pp.673-690.

Lee, S.B. and Suh, M.C. (2015). Advances in the understanding of cuticular waxes in Arabidopsis thaliana and crop species. *Plant cell reports*, *34*(4), pp.557-572.

Li-Beisson, Y., Shorrosh, B., Beisson, F., Andersson, M.X., Arondel, V., Bates, P.D., Baud, S., Bird, D., DeBono, A., Durrett, T.P. and Franke, R.B. (2013). Acyl-lipid metabolism. *The Arabidopsis Book*, *11*, p.e0161.

Matias, P.M., Pereira, I.A., Soares, C.M. and Carrondo, M.A. (2005). Sulphate respiration from hydrogen in Desulfovibrio bacteria: a structural biology overview. *Progress in biophysics and molecular biology*, *89*(3), pp.292-329.

Matthews, H., Gillett, N., Stott, P. and Zickfeld, K. (2009). The proportionality of global warming to cumulative carbon emissions. *Nature 459*, pp.829–832.

Mendez-Perez, D., Begemann, M.B. and Pfleger, B.F., 2011. Modular synthase-encoding gene involved in α-olefin biosynthesis in Synechococcus sp. strain PCC 7002. *Applied and environmental microbiology*, *77*(12), pp.4264-4267.

Meyer, B., Kuehl, J., Deutschbauer, A.M., Price, M.N., Arkin, A.P. and Stahl, D.A. (2013). Variation among Desulfovibrio species in electron transfer systems used for syntrophic growth. *Journal of bacteriology*, *195*(5), pp.990-1004.

Mitchell, D. (2008). A note on rising food prices. *World Bank Policy Working Research Paper No. 4682.*

Millar, A.A., Clemens, S., Zachgo, S., Giblin, E.M., Taylor, D.C. and Kunst, L. (1999). *CUT1*, an Arabidopsis Gene Required for Cuticular Wax Biosynthesis and Pollen Fertility, Encodes a Very-Long-Chain Fatty Acid Condensing Enzyme. *Plant Cell*,*11*, pp.825-838.

Moore, A. (2008). Biofuels are dead: long live biofuels (?)–Part one. *New Biotechnology*, *25*(1), pp.6-12.

Naik, S.N., Goud, V.V., Rout, P.K. and Dalai, A.K. (2010). Production of first and second generation biofuels: a comprehensive review. *Renewable and Sustainable Energy Reviews*, *14*(2), pp.578-597.

Natale Netto, J. (2005). A Saga do Álcool. *Novo Século Editora*, Osasco.

Pfennig, N. (1975). The phototrophic bacteria and their role in the sulfur cycle. *Plant and Soil*, *43*(1-3), pp.1-16.

Postgate, J.R. (1979). The sulphate-reducing bacteria. *CUP Archive*.

Postgate, J.R., Kent, H.M., Robson, R.L. and Chesshyre, J.A. (1984). The genomes of *Desulfovibrio gigas* and *D. vulgaris*. *Journal of general microbiology*, *130*(7), pp.1597-1601.

Price, M.N., Ray, J., Wetmore, K.M., Kuehl, J.V., Bauer, S., Deutschbauer, A.M. and Arkin, A.P. (2014) The genetic basis of energy conservation in the sulphate-reducing bacterium *Desulfovibrio alaskensis* G20. *bioRxiv*, p.005694.

Qiu, C., Colson, G. and Wetzstein, M. (2014). An ethanol blend wall shift is prone to increase petroleum gasoline demand. *Energy Economics*, *44*, pp.160-165.

Ravallion, M. (2010). The developing world's bulging (but vulnerable) middle class. *World Development*, *38*(4), pp.445-454.

Rosenzweig, C., Iglesias, A., Yang, X.B., Epstein, P.R. and Chivian, E. (2001). Climate change and extreme weather events; implications for food production, plant diseases, and pests. *Global change & human health*, *2*(2), pp.90-104.

Sander, K., Murthy, G.S. (2010) Life cycle analysis of algae biodiesel. *Int J Life Cycle Assess*, *15*, pp.704–714.

Schirmer, A., Rude, M.A., Li, X., Popova, E. and Del Cardayre, S.B. (2010). Microbial biosynthesis of alkanes. *Science*, *329*(5991), pp.559-562.

Schmidhuber, J., and Tubiello, F.N. (2007). Global food security under climate change. *Proceedings of the National Academy of Sciences, 104*(50), pp.19703-19708.

Schnurr, J. and Shockey, J. (2004). The acyl-CoA synthetase encoded by LACS2 is essential for normal cuticle development in Arabidopsis. *The Plant Cell*, *16*(3), pp.629-642.

Sims, R.E., Mabee, W., Saddler, J.N. and Taylor, M. (2010). An overview of second generation biofuel technologies. *Bioresource technology*, *101*(6), pp.1570-1580.

Tan, X., Yao, L., Gao, Q., Wang, W., Qi, F. and Lu, X. (2011). Photosynthesis driven conversion of carbon dioxide to fatty alcohols and hydrocarbons in cyanobacteria. *Metabolic engineering*, *13*(2), pp.169-176.

Thomas, C.D., Cameron, A., Green, R.E., Bakkenes, M., Beaumont, L.J., Collingham, Y.C., ... and Williams, S.E. (2004). Extinction risk from climate change. *Nature*, *427*(6970), pp.145-148.

Tillman, J.A., Seybold, S.J., Jurenka, R.A., and Blomquist, G. J. (1999). Insect pheromones—an overview of biosynthesis and endocrine regulation. *Insect biochemistry and molecular biology*, *29*(6), pp.481-514.

Voordouw, G. (1995). The genus Desulfovibrio: the centennial. *Applied and environmental microbiology*, *61*(8), p.2813.

United Nations. (1992). United Nations Framework Convention on Climate Change. Available at: http://unfccc.int/resource/docs/convkp/conveng.pdf. Accessed on 10th January 2016.

U.S. Environmental Protection Agency. (2016). DRAFT Inventory of U.S. Greenhouse Gas Emissions and Sinks:1990 – 2014. Available at: https://www3.epa.gov/climatechange/ghgemissions/usinventoryreport.html. Accessed on 26th February 2016.

World Energy Council. (2011). Global Transport Scenarios 2050. Project Partners IBM Corporation and Paul Scherrer Institute.

Zhu, P. (2014). Effects of E85 Fueling Stations And State Incentives On Private Flex Fuel Vehicle Demand.